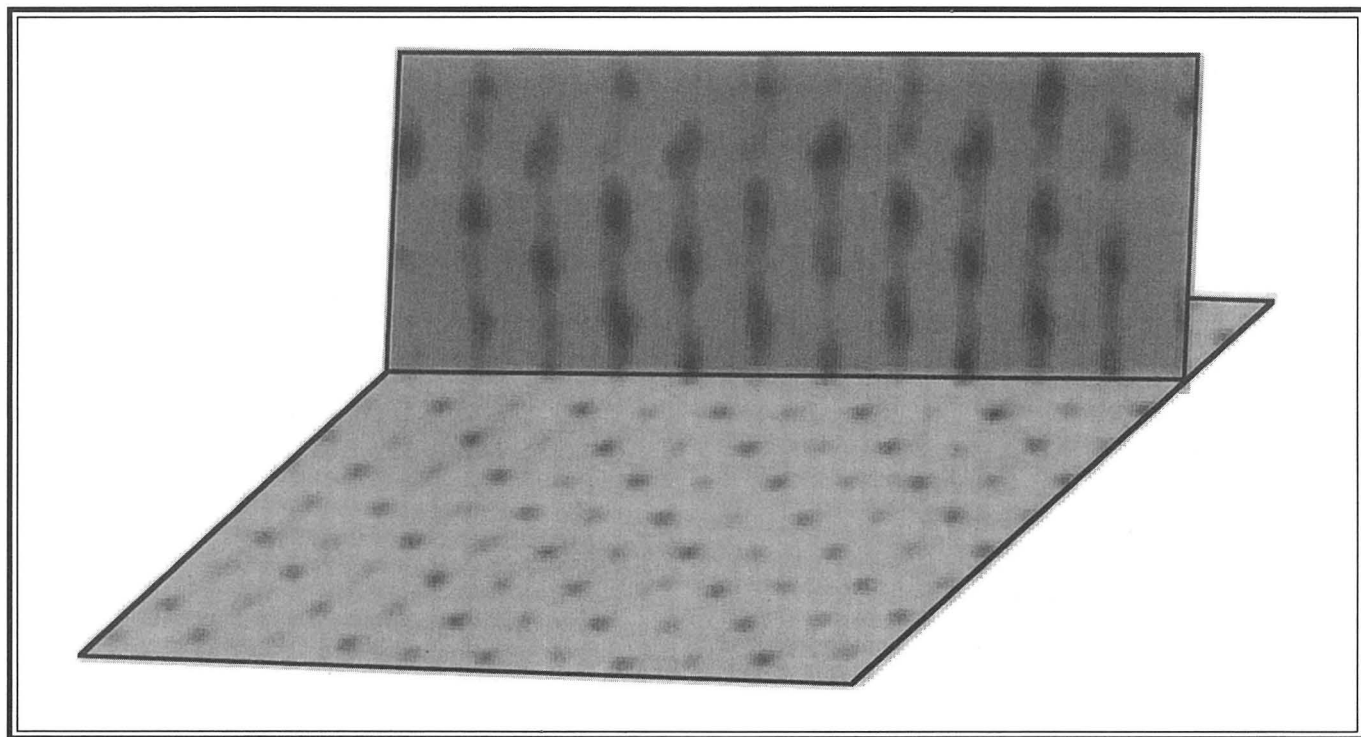


BULLETIN

OF THE AMERICAN PHYSICAL SOCIETY



**1995 Program of the 48th Annual
Gaseous Electronics Conference
October 9-13, 1995
Berkeley, California**

**October 1995
Volume 40, No. 9**

BULLETIN

OF THE AMERICAN PHYSICAL SOCIETY

Coden BAPSA6
Series II, Vol. 40, No. 9

ISSN: 0003-0503
October 1995

APS COUNCIL 1995

President

C. Kumar N. Patel, *University of California-Los Angeles*

President-Elect

Robert Schrieffer, *Florida State University*

Vice-President

D. Allan Bromley, *Yale University*

Executive Officer

Judy R. Franz, *University of Alabama, Huntsville*

Treasurer

Harry Lustig, *City College of the City University of New York*

Editor-in-Chief

Benjamin Bederson, *New York University*

Past-President

Burton Richter, *Stanford Linear Accelerator Center*

General Councillors

Kevin Aylesworth, Arthur Bienenstock, Virginia R. Brown, Jolie A. Cizewski, Jennifer Cohen, Charles Duke, Elsa Garmire, Jerry Gollub, Laura H. Greene, William Happer, Wick C. Haxton, Anthony M. Johnson, Miles V. Klein, Zachary Levine, Barbara Wilson

Chair, Nominating Committee

James Langer

Chair, Panel on Public Affairs

David Bodansky

Division and Forum Councillors

Frank C. Jones (*Astrophysics*), Joseph Dehmer, Gordon Dunn (*Atomic, Molecular, and Optical*), W. Webb (*Biological*), R. Stephen Berry (*Chemical*), Joe D. Thompson, Shirley Jackson, Lu J. Sham, Allen Goldman (*Condensed Matter*), David Anderson (*Computational*), Guenter Ahlers (*Fluid Dynamics*), James J. Wynne (*Forum on Education*), Albert Wattenberg (*Forum on History of Physics*), Ernest Henley (*Forum on International Physics*), Barbara Levi (*Forum on Physics and Society*), Andrew Lovinger (*High Polymer*), William R. Appleton (*Materials*), Steve Koonin, Peter Paul (*Nuclear*), Henry Frisch, Anne Kernan (*Particles and Fields*), Andrew Sessler (*Physics of Beams*), Roy Gould (*Plasma*)

COUNCIL ADVISORS

Sectional Representatives

John Pribram, *New England*; Allen Goland, *New York*; Bunny C. Clark, *Ohio*; Joseph Hamilton, *Southeastern*; Stephen Baker, *Texas*

Representatives from Other Societies

Howard Voss, *AAPT*; Marc Brodsky, *AIP*

Staff Representatives

Stanley Brown, *Administrative Editor*; Irving Lerch, *Director of International Scientific Affairs*; Barrett Ripin, *Associate Executive Officer*; Robert L. Park, *Director, Public Information*; Cindy Rice, *Director of Editorial Office Services*; Michael Lubell, *Director Public Affairs*; Michael Stephens, *Assistant Treasurer and Controller*

Editor: Barrett H. Ripin

Coordinator: Tammany Buckwalter

APS MEETINGS DEPARTMENT

One Physics Ellipse

College Park, MD 20740-3844

Telephone: (301) 209-3200

FAX: (301) 209-0866

Michael Scanlan, *Meetings Manager*

Tammany Buckwalter, *Assistant Meetings Manager*

Lauri A. Nichols, *Meetings Coordinator*

Desiree Atherly, *Secretary*

The *Bulletin of The American Physical Society* is published 14X in 1995: March, April, May (2X), June, July, August, September, October (3X), November (2X), and December, by The American Physical Society, through the American Institute of Physics. It contains advance information about meetings of the Society, including abstracts of papers to be presented, as well as transactions of past meetings. Reprints of papers can only be obtained by writing directly to the authors.

The *Bulletin* is delivered, on subscription, by 2nd Class Mail. Complete volumes are also available on microfilm. **APS Members** may subscribe to individual issues, or for the entire year. **Nonmembers** may subscribe to the *Bulletin* at the following rates: Domestic \$350; Foreign Surface \$360; Air Freight \$375. Information on prices, as well as subscription orders, renewals, and address changes, should be addressed as follows: **For APS Members**—Membership Department, The American Physical Society, One Physics Ellipse, College Park, MD 20740-3844. **For Nonmembers**—Circulation and Fulfillment Division, The American Institute of Physics, 500 Sunnyside Blvd., Woodbury, NY 11797. Allow at least 6 weeks advance notice. For address changes, please send both the old and new addresses, and, if possible, include a mailing label from a recent issue. Requests from subscribers for missing issues will be honored without charge only if received within 6 months of the issue's actual date of publication.

Second-class postage paid at Woodbury, NY and additional mailing offices. Postmaster: Send address changes to *Bulletin of The American Physical Society*, Membership Department, The American Physical Society, One Physics Ellipse, College Park, MD 20740-3844.

ON THE COVER: 3-D image of a crystallized dusty plasma. Charged 9- μm microspheres are levitated above an rf electrode and arranged in a bcc crystal. The particle separation is 194 μm . Gravity, ion flow and electric field are all downward. *Image courtesy of John Pieper and John Goree, The University of Iowa.*

**1995 PROGRAM OF THE 48th ANNUAL
GASEOUS ELECTRONICS CONFERENCE**
9-13 October 1995; Berkeley, California

TABLE OF CONTENTS

General Information	iii
Executive Committee	iii
Epitome	iv
Main Text	1543
Author Index	1589
Five-Year Calendar	Cover 3

1995 PROGRAM OF THE 48th ANNUAL GASEOUS ELECTRONICS CONFERENCE

9-13 October 1995; Berkeley, California

GENERAL INFORMATION

The Gaseous Electronics Conference (GEC) is an annual topical conference of the American Physical Society, sponsored by the Division of Atomic, Molecular and Optical Physics. The focus of the conference is on basic phenomena and plasma processes in ionized gases and on the relevant theory and measurement of basic atomic and molecular collision processes. The 48th Annual GEC will be held 9-13 October, 1995, at the Berkeley Marina Marriott in Berkeley, California. Support for this conference is anticipated from the National Science Foundation, ASTEX, Lam Research, Intel, OSRAM Sylvania, General Electric, Tegal, and Lawrence Livermore National Laboratories. An updated list of sponsors will be distributed to participants.

Special topics to be highlighted at the 1995 GEC include a special Monday workshop on performance and scalability of high density plasma reactors for semiconductor and flat panel manufacturing, plasma-surface phenomena, lighting and lamps, flat panel displays, plasma immersion ion implantation, data needs in plasma mod-

eling, electron hydrocarbon collisions, ion-molecule processes, collisional phenomena between electrons and excited state species, electric probe diagnostics in discharges, and the GEC reference cell. The conference also will include a GEC Reference Cell Users Group meeting.

EXECUTIVE COMMITTEE

The members of the Executive Committee for the 48th GEC are:

J. Norman Bardsley, Chairman, *Lawrence Livermore National Laboratory*; **David B. Graves**, Secretary, *University of California at Berkeley*; **Harold M. Anderson**, Treasurer, *University of New Mexico*; **James T. Dakin**, Past Chairman, *GE Lighting*; **Michael A. Dillon**, Secretary-Elect, *Argonne National Laboratory*; **Richard J. Van Brunt**, *NIST*; **Michael Barnes**, *Lam Research*; **Paul D. Burrow**, *University of Nebraska*; **Toshiaki Makabe**, *Keio University*; **Robert B. Piejak**, *OSRAM Sylvania*.

The local committee included: **D. B. Graves**, **V. Vahedi**, **J. N. Bardsley**, and **K. PoECKert**

EPITOME OF THE 48TH ANNUAL GASEOUS ELECTRONICS CONFERENCE

9-13 October 1995; Berkeley, California

All functions and sessions at the Berkeley Marina Marriott.

EB Measurements and Transport in Discharges

MONDAY, 9 OCTOBER 1995

- Workshop on Performance and Scalability of High Density Plasma Reactors for Semiconductor and Flat Panel Manufacturing
- 8:00-9:00** Workshop Registration
- 9:00-12:00** Morning Workshop Sessions
- 14:00-18:00** Afternoon Workshop Sessions
- 14:00-22:00** GEC Registration
- 18:00** Reception

TUESDAY, 10 OCTOBER 1995

- 8:00 AA** Uniformity and Scaling of Etching Reactors. Chair: *L. Jerde*
- 8:00 AB** Lighting and Lamps. Chair: *R. B. Piejak*
- 10:15 BA** Plasma Etching. Chair: *N. Benjamin*
- 10:15 BB** Collisional Phenomena Between Electrons and Excited State Species. Chair: *T. Walker*
- 13:30 CA** Optical Diagnostics. Chair: *G. Hebner*
- 13:30 CB** Electron and Ion Transport. Chair: *J. de Urquillo*
- 15:45** Posters. Chair: *U. Schmidt*
- DA** Lighting Discharges
- DB** Electron and Photon Collisions
- DC** Materials Processing and Phenomena
- DD** Helical Resonators and Microwave Plasmas
- 19:45** Posters. Chair: *P. Egan*
- EA** Diagnostics and Optical Methods

WEDNESDAY, 11 OCTOBER 1995

- 8:00 FA** Glows and Inductively Coupled Plasmas. Chair: *A. Wendt*
- 8:00 FB** Ion-Molecule Collisions. Chair: *M. Kushner*
- 10:15 GA** Innovative Lighting. Chair: *J. Lapatovich*
- 10:15 GB** Electron-Hydrocarbon Collisions. Chair: *J. Olthoff*
- 13:30 HA** Plasma-Surface Interactions. Chair: *R. Champion*
- 13:30 HB** Data Needs in Plasma Modeling. Chair: *T. Rescigno*
- 16:15** Posters. Chair: *J. Jeffries*
- IA** Plasma-Surface Interactions
- IB** Inductively Coupled Plasmas
- IC** GEC Reference Cell
- ID** Glow Discharge Modeling
- IE** Fundamental Processes in Discharges

THURSDAY, 12 OCTOBER 1995

- 8:00 KA** GEC Reference Cell. Chair: *B. Graham*
- 8:00 KB** Electron Collisions. Chair: *I. Fabrikant*
- 10:15 LA** Dusty Plasmas. Chair: *C. Cui*
- 10:15 LB** Flat Panel Displays. Chair: *R. McGrath*
- 13:30 MA** Deposition. Chair: *K. Stalder*
- 13:30 MB** Diagnostics: Electrical Methods. Chair: *B. Ellingboe*
- 15:45** Posters. Chair: *J. Shon*
- NA** Deposition

NB Magnetically Enhanced Plasmas
NC Diagnostics: Electrical Methods
ND Plasma Displays

Chair: *M. Lampe*

8:00 PB Kinetic Effects and RF Glows.
Chair: *M. Surendra*

10:15 QA Plasma Immersion Ion
Implantation. Chair:
M. Lieberman

FRIDAY, 13 OCTOBER 1995

8:00 PA Magnetically Enhanced Plasmas.

10:15 QB Environmental Applications,
Chair: *A. Gentile*

MAIN TEXT

SESSION AA: UNIFORMITY AND SCALING OF ETCHING REACTORS

Tuesday morning, 10 October 1995

Berkeley Marina Marriott

Yerba Buena/Treasure Rooms, 8:00-10:00

L. Jerde, presiding

8:00

AA 1 Experimental Results from the LLNL Large Area ICP.*
R.D. BENJAMIN, P.O. EGAN, C.S. MULLIN and R.A. RICHARDSON, LLNL.—We describe experiments to explore the issues associated with large-area inductively coupled plasma (ICP) sources for producing high density plasmas with potential use for processing 300 mm semiconductor wafers or even larger FPD substrates. Our initial source design experiments are done in a large (76-cm diameter) plasma source chamber and typically use planar ICP coils with diameters from 30 to 64 cm, driven at 13.56 MHz and coupled to the plasma through a 5-cm thick dielectric window. Plasma and system data are obtained for both Ar and N₂ over the pressure range 3-50 mtorr. RF inductive power was typically varied from 100-1200 W, but the system is capable of 5000 W. Diagnostics include Langmuir probes, B-dot probes, electrical circuit measurements and optical emission spectroscopy. Measurements will be compared with LLNL INDUCT94 plasma modeling codes described in the abstract of P. Vitello, et al. (this conference) and with commercial EM modeling codes. For proper choice of operating conditions, excellent plasma uniformity over 400 mm diameter can be obtained. Effects of pressure, power, RF coupling, and coil geometry on plasma density and uniformity will be presented.

*Work performed under the auspices of Department of Energy at Lawrence Livermore National Laboratory under contract W-7405-ENG-48

8:15

AA 2 A Novel Slab Geometry Helicon Plasma Source for Large Area Plasma Etch Applications, R.F. JEWETT, H.M. ANDERSON, University of New Mexico, A.J. PERRY, R.W. BOSWELL, Australian National University, N.M. BENJAMIN, S. MANGANO, Lam Research Corporation. Future plasma processing will require tools to handle wafer substrates as large as 300-400 mm and flat panels as large as 600 x 600 mm. This work describes a novel slab geometry, 0.5 x 1.2 m plasma reactor with an extended helicon antenna source suitable for such applications. The extended source uses 13.56 MHz rf power to generate helicon waves along a 1.0 m length of one side of the slab geometry processing chamber. The extended plasma source produces uniformly high plasma densities ($> 10^{12}$ cm⁻³ in Ar) over large areas in the processing chamber for certain types of weak (<200 G) confining magnetic field arrangements. Cusped static fields are shown to result in poor helicon wave propagation out of the source and a resultant poor plasma uniformity. Magnetic beach or mirror static field arrangements on the other hand allow significant helicon wave propagation out of the source and produce uniform dense plasmas over a large area in the substrate processing chamber. The characteristics of Ar plasmas produced in this new helicon plasma reactor are discussed, along with potential implications for large area plasma processing.

8:30

AA 3

Optimization of the Plasma Characteristics of a Planar Inductively Coupled Plasma Source, John Holland, Frank L. n, Michael Barnes, Lam Research Corporation, Fremont, CA—

The performance of planar inductively coupled plasma sources used in the plasma processing of 200 mm wafer substrates can be greatly improved by optimizing the geometry of the source. Planar ICP sources have often been represented as simple spirals or concentric rings. However, in actual operation, these designs may produce spatially nonuniform plasmas. Optimization of the RF current distribution in a planar source coil has been used to produce a more

uniform plasma density profile across a 200 mm diameter. The source design was examined in terms of the performance in both radial and angular directions. Performance of the ICP source was monitored by both the measurement of ion density uniformity and the etching of 200 mm wafer substrates.

8:45

AA 4 A numerical and experimental study of plasma process uniformity in rf capacitive systems: Electrode assembly effects, M. Surendra, C. R. Guarnieri, M. Dalvie, IBM Res. Ctr. Yorktown Hts. NY, and P. A. Vitello, LLNL, Livermore, CA. — Experimental measurements of SiO₂ etching in CF₄/Ar discharges, and fluid simulations of capacitive rf discharges in two spatial dimensions have been performed. Experimental results show a strong dependence of wafer-edge etch rate on the geometry of the electrode assembly at the wafer periphery. The height of a dielectric collar around the wafer edge is varied to demonstrate the geometry effect. When the top of the dielectric collar is higher than the wafer, the wafer-edge etch rate drops significantly, whereas the converse is observed when the dielectric collar is below the wafer. These effects are altered by operating pressure. The model predicts across-wafer ion flux uniformity, which is a convenient measure of oxide etch rate. Results are in reasonable agreement with the experiments, indicating that the model is a useful development tool for optimal electrode assembly design.

9:00

AA 5 An Integrated Equipment Model for Inductively Coupled Plasma Etching Reactors: Electrical Circuit to Etching Profiles* ROBERT J. HOEKSTRA, MICHAEL J. GRAPPERHAUS, WENLI Z. COLLISION, and MARK J. KUSHNER University of Illinois, Dept. of Elect. and Comp. Engr., Urbana, IL 61801 USA - A comprehensive Hybrid Plasma Equipment Model (HPEM) for inductively coupled plasma (ICP) etching has been developed to investigate issues related to wafer scaling and substrate topography. The HPEM consists of circuit, electromagnetic, electron Monte Carlo simulation (MCS), sheath and fluid modules. Source functions from the HPEM are used in a plasma chemistry Monte Carlo Simulation which produces ion and radical energy and angle distributions to the wafer. These fluxes are used as input to a profile simulator (PS). The PS uses Monte Carlo techniques to follow the evolution of surface features incorporating user defined chemistry. Results will be presented for plasma properties and etch features in p-Si for 20-30 cm wafers using chlorine chemistry. We demonstrate the effects of substrate topography (wafer clamps, gas cooling channels) on etch profiles.

* Work supported by SRC, Sandia National Lab/Sematech, NSF and the Univ. of Wisconsin ERC for Plasma Aided Manufacturing.

9:15

AA 6

Simulations of schemes for feedback and optimal control of etch rate and uniformity in inductively coupled plasma sources* N. YAMADA, P.L.G. VENTZEK, Y. SAKAI, H. TAGASHIRA, Dept. of Electrical Eng., Hokkaido University, Sapporo, Japan, and K. KITAMORI, Dept. of Industrial Eng., Hokkaido Institute of Technology, Sapporo, Japan. - Plasma process control is important because of stringent quality control requirements as larger areas are processed for both etching and flat panel display applications. Among other factors, coil configuration strongly affects plasma and etch uniformity. In this presentation, control of a density

TUESDAY MORNING

measurement based plasma uniformity using two independently powered and controlled sets of coils will be simulated using different control strategies: feedback and optimal control. Both 2-dimensional and well-stirred models will be used to investigate the impact of fluid flow through the chamber, diagnostic and actuator response times, and the behavior of the coils. Most importantly, observability will be investigated. The simulation will be used to investigate the utility of different diagnostics for control and the correlation between measurable quantities and the quantities that are to be controlled.

*Grant-in-Aid of Scientific Research, Min. of Education, Japan.

9:30

AA 7 The Uniformity of Ion Fluxes at Low Pressures in Inductively Coupled Plasmas¹ WENLI Z. COLLISON, MICHAEL J. GRAPPERHAUS, and MARK J. KUSHNER University of Illinois, Dept. of Elect. and Comp. Engr., Urbana, IL 61801 USA - Inductively coupled plasmas (ICPs) are currently being investigated as high plasma density ($> 10^{11}$ - 10^{12} cm⁻³), low gas pressure (< 10-20 mTorr) sources for semiconductor etching and deposition. A previously developed 2-dimensional (r,z) hybrid model for ICP sources² has been improved to better address low pressures by including momentum equations for all neutral and ion species, and an integrated sheath model. The fluid portion of the hybrid includes slip boundary collisions and inter-species momentum transport. The sheath model computes the sheath potential and thickness at all locations around the reactor. If the sheath is thinner than a single cell, it is included as a jump boundary condition in potential. We will present results for ion and radical flux uniformity, and compare those values obtained using drift-diffusion algorithms.

¹ Work supported by SRC, Sandia National Laboratory/Sematech, NSF, and U of Wisconsin ERC for Plasma Manufacturing.

² P. Ventzek, M. Grapperhaus and M. J. Kushner *J. Vac. Sci. Technol. B*, 12(6), 3118-3137(1994)

9:45

AA 8 Predictive Modeling of Rate Constants and Uniformity for Large Area Chemical Plasma Etching DANIEL L. FLAMM and JOHN VERBONCOEUR, University of California Berkeley and SHIMAO YONEYAMA, MC Electronics-Japan This paper addresses two problems: 1) predicting uniformity in chemical plasma etching as a function of processing parameters, and 2) measuring absolute gas-surface reaction rates in commercial processing equipment without the benefit of sophisticated diagnostic equipment. First, a model for commercial wafer and flat panel resist strippers is described. The peak etching rate is determined by the supply of etchant from a remote plasma and consumption of etchant by the substrates being etched. The effective area for global loading effect depends parametrically on uniformity. At constant temperature, it is shown that uniformity of etching, $u(x,y,k_0/D)$, (dimensions) is set by the ratio of etchant diffusion to the chemical reaction rate plus geometrical parameters which depend on substrate shape and spacings. Peak etching rate, on the other hand, is determined by source etchant production and global loading effects. Analytical relations are developed for rectangular and round substrates and applied to extract basic gas-surface rate constants, $k_{01}(T)$, from ashing uniformity data and predict uniformity (u) and the atomic oxygen concentration profile (n_0) along the surface of a substrate as a function of temperature, pressure and geometrical spacing.

SESSION AB: LIGHTING AND LAMPS

Tuesday morning, 10 October 1995

Berkeley Marina Marriott

Belvedere Room, 8:00-10:00

R. Piejak, presiding

Invited Papers

8:00

AB 1 Positive column discharge models for lighting* TIMOTHY J. SOMMERER *Corporate Research and Development, General Electric Company, P. O. Box 8, Schenectady, New York 12301*—A properly optimized low pressure positive column (LPPC) can efficiently convert input electrical power into atomic resonance radiation. As such, LPPCs form the heart of both rare-gas/mercury fluorescent lamps and low pressure sodium lamps. We have also recently investigated argon/xenon LPPCs for use in mercury-free fluorescent lamps. A portion of this talk will be of a tutorial nature and will highlight key differences between models used for lighting applications and those used for materials processing plasmas, the latter being perhaps more familiar to this audience. The remainder of the talk will focus on a hybrid model presently under development for LPPCs. The model is based on fluid equations to determine species densities and obtains electron-impact rates from the zero-dimensional Boltzmann equation. Predictions will be shown for both rare-gas/mercury and argon/xenon LPPCs.

*A portion of this work has been supported under the NIST Advanced Technology Program.

8:30

AB 2 Electron Energy Distribution in the Ambipolar Positive Column. J. H. INGOLD, GE Lighting, Cleveland, OH 44112—The traditional view of the ambipolar positive column—namely, Maxwellian EEDF with or without tail depletion due to inelastic collisions, and radially invariant average energy, or nearly so—is examined within the framework of the Boltzmann equation and the two-term Legendre expansion. It is concluded that the traditional view is consistent with the scalar equation for f_0 whenever the dimensionless ratios $E^2\Lambda^2/\theta^2$, Λ^2/λ_T^2 , and μ_i/μ_e , are significantly less than unity, where E is axial electric field, Λ is characteristic diffusion length, θ is characteristic energy of electrons, λ_T is elastic energy relaxation length, and $\mu_{e,i}$ is electron/ion mobility. Based on published data for E and θ versus pressure for positive columns in atomic gases, it is concluded that the traditional view is valid in the free-fall range of pressure times radius pR for all atomic gases, and is approximately valid well into the mobility-limited range of pR for some atomic gases.

The traditional view is contrasted with the nonlocal electron kinetics view. It is suggested that the latter view may be useful for estimation of radially averaged measurable quantities, but may not be useful for estimation of their radial variation.

9:00

AB 3 Compact Electrodeless High Intensity Discharge Lamps. W. P. LAPATOVICH, OSRAM SYLVANIA INC., 71 Cherry Hill Drive, Beverly, MA 01915 - The operation of compact electrodeless high intensity discharge lamps is described.^{1, 2} These lamps are energized by microwaves in the ISM bands centered around 915 and 2450 MHz. The fill chemistries reported are conventional metal halide lamp fills exhibiting very good efficacy, high color rendering, and excellent lifetime. The lamps are small cylinders typically 2 mm I.D., 4 mm O.D. and less than 10 mm long. The discharges are capacitively coupled and are sustained with power densities on the

order of 1.2 kW/cm^3 . The temporal evolution of the discharge from glow to thermal arc phase is correlated with the spectral emission evolving from the ignition of the low pressure (15 torr) Hg/Ar cold fill to the dense (30 atm) plasma in the fully developed arc. High lamp luminance, approaching 100 candela/mm^2 was recorded over approximately 80% of the arc length. The small source size and uniform luminance make these compact arcs effective sources for a number of optical applications with restrictive etendue.

¹W. P. Lapatovich and S. J. Butler, Bull. Am. Phys. Soc. 38 (13), 56 (1993).

²S. J. Butler, H. H. Goss, and W. P. Lapatovich, IEEE Conf. on Plasma Sci., Madison, WI, Paper No. 4D02, 5-8 June 1995.

9:30

AB 4 Miniature High Intensity Discharge Lamps Fabricated by Micro machining Techniques, BABAR A. KHAN, DAVID A. CAMMACK and RONALD D. PINKER, Philips Laboratories, Briarcliff Manor, NY 10510, Philips Electronics North America Corporation - Miniaturization of electronic components has laid the foundations of the new information age. This miniaturization was made possible by the development of integrated circuit (IC) technology. In this work, we demonstrate the application of IC technology toward miniaturization of high intensity gas discharge light sources. We have fabricated electrodeless lamps in quartz substrates using IC and micro machining techniques, such as photolithography, etching and wafer bonding. These lamps were dosed with mercury and argon and excited by a microwave source operating at 2.45 GHz. Lamps containing varying amounts of mercury were fabricated to obtain high pressure discharges in the range of 10 - 175 atmospheres. The light output and efficacy increased with increasing gas pressure. Lamp efficacies over 40 lumens per watt were obtained. We have also fabricated high pressure mercury discharge lamps with conventional electrodes using IC fabrication and obtained lamp efficacies over 50 lumen/watt. These results illustrate the potential of this technology for lighting, as well as for other applications.

SESSION BA: PLASMA ETCHING

Tuesday morning, 10 October 1995

Berkeley Marina Marriott

Yerba Buena/Treasure Rooms, 10:15-12:15

N. Benjamin, presiding

10:15

BA 1 Plasma Diagnostics and Sensors for Process Control Development, M.P. SPLICHAL and H.M. ANDERSON, Univer Shrinking IC linewidths implies even tougher tolerances for plas equipment, particularly for the parameters of uniformity and line control. Nonintrusive, optical and laser plasma diagnostics are increasingly important to both optimizing these parameters during development and detecting drift in the factors which affect these parameters during etching. This talk reports on recent work in the SEMATECH J-88 program for Advanced Process Control and F /Classification (FDC/APC) and the use of spatially resolved optical emission spectroscopy as a plasma process sensor. The technique to be a sensitive indicator of plasma nonuniformity and resultant width losses in the etching of stacked metal gate structures. Such information is being applied along with other electrical (RF current voltage) probes and machine state probes to develop a virtual sensor model for run-to-run process control of a Lam 9600 TCP. The work, done in collaboration with Texas Instruments, Lam Research Berkeley, Neurodyne, Inc. and SEMATECH, is being performed. Instruments Semiconductor Process and Device Center.

10:30

BA 2 Impact of x-ray photoelectron spectroscopy on process control polysilicon gate patterning

F. H. Bell, O. Joubert, France Télécom, CNET BP 98, 38243 Meylan cedex LPCM UMR 110 IMN, 44072 Nantes Cedex 03 France

The characteristics of poly-Si trench etching in high density plasmas have studied by x-ray photoelectron spectroscopy (XPS). Special emphasis is placed on a new approach, using XPS, to monitor gate oxide thicknesses remaining open and patterned areas after wafer processing. Poly-Si films on SiO₂-co-

Si (100) substrates were masked whether with photoresist (1 μm thick) or SiO₂ (0.2 μm thick). Two hundred mm wafers are processed in a high density plasma helicon source using chlorine-based or HBr/Cl₂/O₂-based chemistries. After etching, samples are transferred under ultrahigh vacuum to a surface analysis chamber equipped with an x-ray photoelectron spectrometer. The ratio between the SiO₂ peak area and the elemental Si 2p peak area of blanket oxide films of different thicknesses on silicon substrate has been calculated using XPS. The SiO₂/Si ratios are then plotted as a function of the oxide thicknesses as measured by spectroscopic ellipsometry. Using this calibration the gate oxide thickness can be easily determined by XPS. Furthermore, a calibration curve can be employed to determine the gate oxide thickness in patterned areas from the measured SiO₂/Si ratio, where other techniques cannot operate. Consequently, gate oxide thicknesses were measured after etching using different etch chemistries, a photoresist mask and an oxide hard mask in features of different aspect ratios. It is found, that the gate oxide consumption is enhanced in high aspect ratio features masked with photoresist whereas no difference is observed when the hard mask is used. This result is correlated with a higher carbon coverage (as measured by XPS) on the oxide at the bottom of high aspect ratio features.

10:45

BA 3 The Role of Ions in the Chemistry of SiO₂/Si Selectivity in High Density Fluorocarbon Discharges*, A. E. WENDT, K. H. R. KIRMSE, R. A. STEWART, R. A. BREUN, J. Z. WU, I. C. ABRAHAM, S. B. DISCH, J. A. MEYER, R. C. WOODS, Engineering Research Center for Plasma-Aided Manufacturing, U. of Wisconsin-Madison - Mechanisms of SiO₂/Si selectivity in ECR fluorocarbon discharges (CHF₃, C₂H₂F₄, CF₄) have been investigated over a wide range of conditions. Although ion concentrations are much lower than neutral radical concentrations, their fluxes to the substrate are comparable and they are likely to play an important role in surface chemistry. Etch rate measurements of Si and SiO₂ have been combined with chemical characterization of the discharge using optical diagnostics and an in-line quadrupole mass spectrometer. These measurements include both absolute and relative measurements of gas phase species concentrations as well as fluxes of ionic radicals. We find that the conventional theory that selectivity is governed by the relative content of fluorine vs. carbon in the fluorine and fluorocarbon radicals incident on the substrate appears consistent with our results when oxygen is added to a fluorocarbon discharge. However, for the case of hydrogen addition to the fluorocarbon discharges studied, the conventional theory appears to work only when contributions of fluorocarbon ions, CF_x⁺, are considered.

* Work supported in part by NSF Grant # ECD-8721545.

11:00

BA 4 Gas Composition Measurements Downstream of CF₄/O₂ Microwave Discharge, C. A. Fox*, B. Swansiger, W.L. Hsu, D. Buchenauer, J. Shon, E. Meeks - Sandia National Laboratories, Livermore Ca - Modulated molecular beam mass spectroscopy and threshold ionization techniques were used to understand the factors which effect the gas composition downstream of pure CF₄ and CF₄/O₂ microwave discharges. The discharges were ignited in quartz and alumina tubing in order to elucidate the effects of wall chemistry on the downstream species' composition. The etching of the quartz tube surrounding the microwave discharge was monitored by measuring the SiF₄ concentration. The SiF₄ signal intensity was relatively invariant with discharge position, over the range of 2" to 30"; this indicates that etching reactions which occur in discharge region are primarily responsible for SiF₄ production, while reactions downstream are negligible. The conditions which minimize quartz tube etching are also addressed. Similarly, the conditions which maximize the atomic fluorine concentration will also be addressed. For the pure CF₄ microwave discharge, maximization of the downstream fluorine atom concentration was achieved at high gas flow rates, minimum distance from the discharge to the sampling orifice, and maximum microwave power.

TUESDAY MORNING

11:15

BA 5 Modeling of CF₄/O₂ Chemical Downstream Etch Systems and Comparisons with Gas Composition Measurements* - J. W. Shon, R. S. Larson, E. Meeks, S. R. Vosen, C. A. Fox, Sandia National Laboratories, Livermore CA - Chemical downstream etch processes using CF₄/O₂ are investigated. Modeling includes the generation of the charged species and radicals in a microwave-excited CF₄/O₂ plasma source, etching of the quartz tube, and transport through a flow tube and a process chamber. The CF₄ dissociation depends mainly on power deposition, residence time, and an oxygen mole fraction. 50% dissociation of CF₄ is obtained for 30W of microwave power, a flow rate of 18 sccm, and an oxygen mole fraction of 0.2 to 0.6. The maximum fluorine concentration at the tube exit is obtained for oxygen mole fraction of 0.3 to 0.4 and compares well with the experimental results¹ of the outlet gas composition at the downstream end.

*Work supported by SEMATECH and U.S. Department of Energy

¹C. A. Fox, B. Swansiger, W. L. Hsu, D. Buchenauer, J. Shon, E. Meeks, will be presented at 48th Gaseous Electronics Conference.

11:30

BA 6

Development of 0.18 μm Polysilicon Gate Patterning in High De Plasmas: Influence of the nature of the mask on process robustness: O. Joubert and F.H. Bell, France Télécom, CNET BP 98, 38243 M. cedex and LPCM UMR 110 IMN, 44072 Nantes cedex 03, France Processes currently developed using a high density Helicon source 0.25 μm polysilicon patterning generally combine the use of a resist and polymerising chemistry such as HBr/Cl₂/O₂. Severe damage induced at the edges of the features when using similar process pattern 0.18 μm polysilicon gates (holes are observed in the active after removing the 45Å gate oxide). In this study, we demonstrate that damage is due to microtrenching, occurring at the edges of the feature and transferred into the gate oxide during the main etch of the polysilicon. Consequently, damage can be observed even if the overetch step is highly selective. Robust processes can be designed by suppressing the main induced microtrenching and improving the selectivity of the etch. This is achieved by replacing the resist mask by an oxide hard mask. Using this mask, we observe that:

- the selectivity of both etching steps (main etch and overetch) of the process is strongly improved.
- using identical chemistries and plasma operating conditions, microtrenching is reduced.
- a non polymerising process can be developed based on an HBr chemistry which also reduces the microtrenching induced effect chlorine.

11:45

BA 7 Investigating the Role of Localized Charging on Profile Evolution in Oxide Etching V. VAHEDI¹, M. DALVIE², S. HAMAGUCHI³, and D. HEWETT¹, ¹Lawrence Livermore National Lab., ²Sematech, Austin, and ³IBM T. J. Watson - Results from recent experiments by G. Oehrlein et al. (1994) suggest that in an oxide etching environment, high energy ions may be responsible for oxide and polymer etching while the low energy ions may only contribute to polymer deposition. In this work we intend to investigate the role of localized charging of features on local etch rates obtained from a model based on Oehrlein's data. We use a particle-in-cell/Monte Carlo code to obtain the ion and electron fluxes arriving at a wafer through an RF sheath. A 2D micron-scale particle code which includes surface charging effects then uses these fluxes to obtain the localized ion energy and angular flux arriving at a feature during plasma etching. A local etch rate is then calculated based on the ion flux. This etch rate will then be used to evolve the feature using a profile evolution code. Once the profile is evolved, the charging of the new feature is recalculated using the 2D particle code to obtain a new localized ion energy flux. This iterative process is repeated to investigate the role of localized charging on local etch rates and profile evolution. We intend to study the role of localized charging on etching of oxide features with insulating polymer resist masks.

12:00

BA 8 Modeling of Localized Charging Effects during Plasma Etching, L. VALLIER and P. CZUPRYNSKI, FranceTelecom/CNET Grenoble and LPCM/U. of Nantes - Localized charging effects that occur during the etching of sub-micron trenches in high density plasmas have been simulated. Silicon wafers patterned with a perfect insulating mask are exposed to an idealized plasma while RF power is capacitatively coupled to the wafer. The isotropic electron flux and the accelerated (100 eV) anisotropic ion flux coming from the plasma are simulated to provide a zero net charge flux on insulating surfaces such as the sidewalls of the mask. Calculations are made using a PC based software to solve the Laplace equation and particle trajectories. The self-bias potential distribution in the submicron structure is derived; typical differences of 20 V are observed between the top and the bottom. Simulations are performed for trenches having different aspect-ratios and for isolated lines. Ion fluxes and their energies are estimated in the etched areas. Correlation with aspect-ratio dependent etching and trenching effects are made for poly-Si and oxide etching.

SESSION BB: COLLISIONAL PHENOMENA BETWEEN ELECTRONS AND EXCITED STATE SPECIES

Tuesday morning, 10 October 1995

Berkeley Marina Marriott

Belvedere Room, 10:15-12:00

T. Walker, presiding

Invited Papers

10:15

BB 1 Electron Impact Ionization of Metastable Neon, M. JOHNSTON^{**}, K. FUJII, S. TRAJMAR, AND J. NICKEL, U. of California, Riverside. - The cross section for electron impact ionization of metastable neon has been measured in the energy range from threshold to 200 eV. The crossed-beam experiment used a fast neutral target (both ground state and ground state plus metastable) formed by charge transfer between an 800 eV neon ion beam and neon gas or sodium vapor. The ionization cross section for the ³P₂ and ³P₀ metastable components, assumed to be equal, was placed on an absolute scale by utilizing the known ground state cross section and assuming that the beam fractions of the mixed state were statistically distributed. The high perveance metastable beam source is discussed and the results are compared with the preliminary experimental work of Dixon *et al.*¹ and available theoretical results.

* Research supported by the joint Los Alamos - University of California, Riverside Laboratory Collaboration, (CALCOR)

** Permanent Address: University of St. Thomas, St. Paul, MN 55105

¹ A. J. Dixon, M. F. A. Harrison and A. C. H. Smith **VIII ICPEAC Abstracts of Papers (Belgrade)** ed. B. C. Cobic and M. V. Kurepa pp 405-6 (1973)

10:45

BB 2 Electron Impact Excitation and Ionization of Metastable Rare Gas Atoms and Laser-Excited Barium, G. CSANAK, D.C. CARTWRIGHT, R.E.H. CLARK, AND J. ABDALLAH, JR. Los Alamos National Laboratory. The role of differential, magnetic sub-level and integral cross sections for electron collisions with atoms and ions in excited states in plasma environments will be discussed. Methods for obtaining these cross sections will be summarized and recent theoretical results for electron impact excitation of metastable Helium; metastable Neon; and laser-excited

Barium, will be compared to the available experimental data and to results from other calculations. Some recent efforts for obtaining cross sections for excitation from excited state Chlorine will also be discussed.

The connection between the various excitation cross sections and the polarization properties of the plasma will be summarized in the context of Plasma Polarization Spectroscopy as a tool for determining the electron/ion distribution functions in the plasma. Results from model kinetic calculations will also be discussed to demonstrate the importance of electron collisions with excited states for certain plasma environments.

Contributed Papers

11:15

BB 3 Electron-Excitation out of the 2³S Metastable Level of Helium,* GARRETT A. PIECH, MARK E. LAGUS, JOHN B. BOFFARD, L.W. ANDERSON, and CHUN C. LIN. *Univ. of Wisconsin-Madison.* - We have performed two independent experiments measuring the electron-excitation cross sections out of the 2³S level of He into higher triplet levels. The first uses a hollow cathode discharge as a source of metastable atoms, and with it we have obtained excitation functions and cross sections into the n = 2, 3, 4 and 5 triplet levels. While the hollow cathode produces a metastable density of 10⁹ atoms/cm³, the experiment is limited to energies below 20eV due to overwhelming ground state densities. The second experiment uses charge exchange of He⁺ with cesium to produce a primarily metastable He beam, with a target density of 10⁶ atoms/cm³. We use this apparatus to measure the absolute cross sections for selected triplet levels for electron energies from threshold to 500eV. We will compare the two experimental results with each other and with various theoretical calculations.

*Work supported by National Science Foundation.

11:30

BB 4 Azimuthal Asymmetry in Elastic Electron Scattering by Polarized 3P Sodium Atoms,* Z. SHI, H. WEI, C. H. YING, L. VUŠKOVIC, Old Dominion U.---Azimuthal asymmetry of the differential cross sections between two polarized states has been measured in elastic electron scattering by laser-excited sodium atoms prepared in the 3²P_{3/2}, F=3 (M_F=+3 or M_F=-3) polarized states. These results are the first observation of the orbital effect in the elastic electron collision due to M_L atomic state perpendicular to the scattering plane. Data will be reported for electron energies in the range of 1 eV to 10 eV, comparable with the kinetic energy of the atomic valence electron. At polar scattering angle 135° we found the asymmetry to be more significant when the incident electron energy is lower. Measurements at 45° are in progress and will be presented at the conference, as well. Differential cross sections for 3²P_{3/2}, M_L=±1 as a function of energy are also obtained. The experimental results are compared with R-matrix based close-coupling¹, and the convergent close-coupling calculations².

*Research supported by Physics Department at Old Dominion U., and partially by U.S. National Science Foundation.

¹H.L. Zhou, D.W. Norcross, and B.L. Whitten, IOP Conf. Proc. No. 122, pp.39-48 (1992); private communication (1994).

²I. Bray, D.V. Fursa, and I.E. McCarthy, Phys.Rev.A 49, 2667 (1994).

11:45

BB 5 Dissociative Attachment and Vibrational Excitation in e-Na₂ Collisions,* I.I. FABRIKANT, Univ. of Nebraska-Lincoln—Recent experimental observations¹ indicate very strong enhancement of the electron attachment rate in e-Na₂ collisions, when the vibrational quantum number *v* of the initial state varies from 0 to about 10. In this work we have performed semiempirical calculations of dissociative attachment and vibrational excita-

tion of Na₂ molecules using the semiclassical resonance R-matrix theory.² Overall, the *v*-dependence of the dissociative attachment cross section agrees quite well with the experiment,¹ but its energy dependence is strongly affected by very sharp drops at the vibrational excitation thresholds. The vibrational excitation out of the ground to the first excited vibrational state can be fitted to the Breit-Wigner cross section with the peak value 22 Å² and the total width 0.1 eV. Cross section for excitation of the *v*=2 state is lower by a factor of 2.34.

*Supported by the National Science Foundation.

¹ M. Kütz, A. Kortyna, M. Keil, B. Schellhaab, and K. Bergmann, Phys. Rev. A 48, R4015 (1993).

² I.I. Fabrikant, J. Phys. B 24, 2213 (1991).

SESSION CA: OPTICAL DIAGNOSTICS

Tuesday afternoon, 10 October 1995

Berkeley Marina Marriott

Yerba Buena/Treasure Rooms, 13:30-15:30

G. Hebner, presiding

13:30

CA 1 2-D Measurements of CF₂ Density in CF₄/O₂/Ar rf Plasmas by Laser-Induced Fluorescence Imaging, B. K. McMILLIN and M. R. ZACHARIAH, *National Institute of Standards and Technology, Gaithersburg, MD* - Spatially resolved 2-D measurements of the relative CF₂ density in low-pressure rf CF₄/O₂/Ar discharges have been obtained using planar laser-induced fluorescence imaging. The plasmas examined were generated in a parallel-plate GEC cell and cover a wide range of conditions (13.3-133.3 Pa, 1-100%CF₄, 0-10%O₂, 3-35 W, 5-100 sccm). In general, varying the pressure led to significant changes in both the magnitude and spatial distribution of CF₂ density, while varying the composition, flowrate, and power primarily only affected its magnitude. In all cases, significant radial variations were observed (up to 300%) with the peak density occurring near the edge of the discharge, while the centerline axial distribution was symmetric and peaked near the center of the gap. Based on analyzing the image-averaged CF₂ concentration, for the conditions examined here the CF₂ density increased linearly with power and CF₄ mole fraction in Ar/CF₄ discharges; the dissociation fraction in mildly diluted CF₄ discharges was less than a few percent; and the CF₂ density decreased substantially with the addition of O₂. In addition, the CF₂ density changed non-monotonically with flowrate, which we attribute to a tradeoff in CF₂ convection and diffusion losses.

13:45

CA 2 2D-Space and Time Optical Emission Spectroscopy

T.KITAJIMA, T.MAKABE and M.IZAWA

Keio Univ.

The aim in this work is the investigation of a temporal radial profile of the net production rate of active species as well as an axial distribution in an radiofrequency CCP reactor. Attention will be paid to the phenomena in the edge of electrodes (or substrates). Our previous experimental system of the spatiotemporal optical emission spectroscopy¹ is developed in order to measure a 2D-distribution by changing the detector of an emission in an rf glow discharge from the focused lens system to a line integral one. The temporally resolved net excitation rate $\Lambda(r, z, t)$ is numerically obtained from a series of a line integrated signals $\Phi(z, t)$ by Abel inversion and deconvolution procedure. In this talk, 2D-profile of the net production rate of Ar(3p₂) in parallel plates with 2 cm spacing at 2 Torr in Ar is mainly discussed. The result will give an important information on the design of a plasma reactor, and will serve as complementary one to a 2D-modeling.

1.F.Tochikubo and T.Makabe; Meas.Sci. and Technol.2 1133(1991).

Toshiaki Makabe

3-14-1 Hiyoshi, Yokohama 223 Japan

045-563-1141(ex.3358)

makabe@mkbe.elec.keio.ac.jp

TUESDAY AFTERNOON

14:00

CA 3 **Practical Applications for Optical Emission Spectroscopy in a Microwave Plasma**, U.M. KELKAR and M.H. GORDON, High Density Electronics Center, University of Arkansas at Fayetteville - The use of optical emission spectroscopy (OES) in a microwave plasma is limited by the non-Maxwellian EEDF. However, for a CH_4/H_2 microwave plasma used for diamond deposition, the authors have previously shown that accurate EEDF predictions were possible if two-step ionization were self-consistently modeled. By carefully comparing both experimental measurements and numerical predictions of atomic hydrogen bound-excited and free electron number densities, important non-equilibrium mechanisms have been identified and accounted for enabling correlations between OES and fundamental plasma parameters such as electron number density, gas temperature, atomic hydrogen mol fraction, etc. For example, results indicate, due to low electron densities (near $5 \times 10^{18} \text{ m}^{-3}$) and low electron-atom collision frequencies, that the relative distribution of the atomic hydrogen excited states is governed by the gas temperature.

14:15

CA 4 **Optical Emission Spectroscopy as a Baseline Uniformity Sensor**, M. J. BUIE, J. LEWIS, L. POSLAVSKY, and M. WELCH, Applied Materials; Dielectric Etch Division; Santa Clara, CA - The idea of using optical emission spectroscopy (OES) as a baseline uniformity sensor is to enable prediction of the etch uniformity without the substantial investment of time, effort and fiscal resources needed for traditional baselining experiments. Traditionally, baselining involves a series of tests under certain process variable conditions in order to verify chamber operation before the experimentation which leads to the selection of an optimum process window. These baseline tests are conducted using test wafers -- requiring investment for no scientific return. Establishing a diagnostic which would eliminate part of this process would cut down on wafer resources as well as money. Initial experiments were conducted using Applied Materials optical emission endpoint system and indicate the existence of a relationship between the film / etch uniformity and the endpoint OES intensity signal modulations.

14:30

CA 5 **A Computer Simulation of Optogalvanic Signals in Neon Gas Discharges**, S.Uchida, H. Sugawara, P.L.G. Ventzek, Y. Sakai, and H. Tagashira, Hokkaido University, Sapporo 060 Japan - When a self-sustained gaseous discharge is illuminated by radiation resonant with an atomic transition of the gas, a change in the electrical conductivity occurs. It is known as "the optogalvanic (OG) effect". We simulate OG signals in steady-state neon discharges for $14 < E/N < 28 \text{ Td}$ and $10^9 < n_e < 10^{12} \text{ cm}^{-3}$ using a propagator method¹. It is shown that the electron energy distributions consistent with the OG signals can be obtained for various discharge conditions and transition wavelength lines. The transient behavior of the discharge after the light illumination is discussed.

¹ H.Sugawara, et al, J.Phys.D27,90-94(1994)

14:45

CA 6 **Optogalvanic and Laser Induced Fluorescence: Experiment and Theory**, R. S. STEWART, I. S. BORTHWICK AND A. M. PATERSON, Dept. of Physics and Appl. Phys., Strathclyde University, Glasgow, G4 0NG, UK - We have developed complementary rate equation modelling to describe the optogalvanic (OG) and laser induced fluorescence (LIF) spectra produced when the long-lived species of a noble gas are perturbed by slowly chopped ($\sim 90 \text{ Hz}$) CW tunable laser radiation. Our model, developed from a basic set of rate equations, accurately describes both the OG and LIF spectra as well as the excited atom populations and their emission and absorption spectra. A proper description of population mixing and redistribution is vital in both OG and LIF spectroscopy. We believe that the model constitutes a fundamental advance when applied to LIF because it accurately describes both the primary and secondary (i.e. collisionally coupled) signals, including the positive and negative signs of the latter observed under certain conditions - a rigorous test of the model. We will discuss comprehensive experimental results for positive column discharges in neon for pressure ranging from 1 to 10 Torr and currents from 1 to 10mA, and will also present results for helium and krypton.

15:00

CA 7 **Time-Dependent Optogalvanic Effects in Neon Discharge Plasma***. X.L.Han†, N.J.Perry, R.C. Duckworth, S.R. Brown, Dept. of Phys. and Astron.; and M.C.Su†, Dept. of Chemistry, Butler University. — In the previous study of neon optogalvanic effects (OGE) involving only two optically allowed states, we have developed a simple theoretical model that gave an excellent agreement with the experimental results. The study has been extended to include neon transitions that involve more than two optically connected states in this work. It was found that most of these transitions give OGE signals consisting of two dominant exponential profiles. Theoretical modeling suggests the existence of possible final state selectivity after electron-neon collisions. The identification of dominant states and collisional ionization dynamics will also be discussed.

* Supported by the Holcomb Research Institute, Butler University; Laser Science Topic Group, American Physical Society; and Research Corporation.

† Also with the Holcomb Research Institute, Laboratory for Quantum Physics, Butler University.

15:15

CA 8 **Production and destruction of CF_x radicals in radio-frequency fluorocarbon plasmas**, M. Haverlag, W.W. Stoffels, E. Stoffels, G.M.W. Kroesen, F.J. de Hoog, Dept. of Physics, University of Technology, P.O. Box 513, 5600 MB Eindhoven. Densities of CF , CF_2 and CF_3 radicals have been determined by means of infrared absorption spectroscopy employing a tunable diode laser spectrometer in rf discharges of CF_4 and CHF_3 . Measurements were performed as a function of the axial position both during plasma operation and after extinction of the plasma to study the kinetics of CF , CF_2 and CF_3 . It was found that the CF_2 density decays much faster in the afterglow of a CF_4 plasma as compared to the afterglow of a CHF_3 plasma. This indicates that the surface is more important in the former case. Moreover, it has been established that the stationary CF_2 density in CF_4 plasmas depends strongly on the electrode material, suggesting catalytic destruction of CF_2 on the surface. All densities of the radicals studied increase near the electrodes, leading to the conclusion that production of CF_x radicals takes place in the sheath region. It is proposed that collisions between ions and the source gas results in production of CF_x radicals in the sheath. In the absence of strong destruction processes in the sheath this results in the observed increase of CF_x densities near the electrodes.

SESSION CB: ELECTRON AND ION TRANSPORT

Tuesday afternoon, 10 October 1995

Berkeley Marina Marriott

Belvedere Room, 13:30-15:30

J. de Urquillo, presiding

13:30

CB 1 **Electron Excitation of 2p levels of Ne** - J. BOŽIN, Z. VELIKIĆ, Z. Lj. PETROVIĆ and B. M. JELENKOVIĆ, Institute of Physics, University of Belgrade - Excitation coefficients for ten 2p levels of Ne have been measured using a drift tube and measuring absolute intensities of 2p-1s transitions. The data are corrected for collisional quenching¹. The range of E/N was from 20 Td to 3 kTd, while pressure range was 20 - 0.45 Torr. The excitation coefficients for 2p₁ level, which is the least affected by collisional mixing is $3.7 \times 10^{-22} \text{ m}^2$ at 100 Td, in good agreement with previous work². Excitation coefficients for most of the 2p levels have a similar variation vs E/N with a maxima around 500 Td. Ionization coefficients were determined from the exponential slope of spatial scans. At 100 Td the value is $1.2 \times 10^{-21} \text{ m}^2$ in agreement with previous data³, at 2 kTd, where no data is available, we obtained $1.1 \times 10^{-20} \text{ m}^2$.

¹ T. Fujimoto, C. Goto, and K. Fukuda, *Opt. Commun.* **40**, 23 (1981).

² K. Tachibana, H. Harima and Y. Urano, *J. Phys. B* **17**, 879 (1984).

³ K. Tachibana and A. V. Phelps, *Phys. Rev. A* **36**, 999 (1987).

13:45

CB 2 **Effects of the Time Evolution of the Electron Distribution Function on the Pulse Radiolysis of Rare Gases.** R. Cooper, M. Burgers, Melbourne University, Australia, M. A. Dillon, M. Kimura, Argonne National Laboratory.

Pulse radiolysis of the rare gases and the time-dependent detection of initial products may be used to test the predictions of the Boltzmann equation. A fast emission spectroscopy technique was employed to monitor the production of both optically forbidden levels (the 2p₁ levels) and some optically allowed levels (excited ionic species). The observed time-dependent yields of these states in neon and argon are in good agreement with those derived from numerical calculations.

Supported by the U.S. Department of Energy, Office of Energy Research, under contract No. W-31-109-Eng-38.

14:00

CB 3 **The Effect of Vibrational Excitation on Electron Thermalization in an Ar-CH₄ Mixture.** M. KIMURA, Argonne National Laboratory, and I. KRAJČAR-BRONIĆ, Ruder Bošković Inst., Croatia--The effect of vibrational excitation on electron thermalization was studied for an Ar-CH₄ mixture for electron energy below 1 eV, on the basis of the Boltzmann equation. Methane has two vibrational excitations, for the $\nu = 1 \rightarrow 3$ and $\nu = \rightarrow 4$ transitions, with thresholds of 0.361 and 0.162 eV, respectively. The magnitude of cross sections is comparable to that for momentum transfer, except in the region of the Ramsauer-Townsend minimum. When vibrational excitation was included in the calculation, the energy relaxation proceeded much faster (by a factor of 5000) than without the vibrational excitation.

*Supported in part by the U.S. Department of Energy, Office of Energy Research, Office of Health and Environmental Research, under Contract W-31-109-ENG-38 (MK).

14:15

CB 4 **Electron Thermalization and Attachment in CCl₄ and Ar Mixtures.** K. KOWARI and B. D. SHIZGAL, Department of Chemistry, U. of British Columbia - The time dependent electron distribution function of energetic electrons in CCl₄ and Ar mixtures is determined with a numerical solution of the Boltzmann equation. Thermalization by elastic and vibrationally inelastic collisions is considered as are superelastic collisions which are found

to be important. Electron attachment to CCl₄ is also included and the coupling of thermalization and attachment is studied in detail. The methodology used is similar to that employed in the study of pure systems without attachment¹ and in systems with attachment without account taken of molecular vibrational states.²

* Work supported by a grant from the Natural Sciences and Engineering Research Council of Canada.

¹ K. Kowari and B. D. Shizgal, *Chem. Phys.* **185**, 1-11 (1994).

² B. Shizgal, *J. Phys. B: At. Mol. Opt. Phys.* **24**, 2909-2903 (1991).

14:30

CB 5 **Electron Dynamics in Time-Varying Electric Fields in Gases,** H. DATE†, P. L. G. VENTZEK, M. SHIMOZUMA, H. TAGASHIRA and *D. B. GRAVES, Hokkaido Univ. JAPAN and *UC Berkeley - The behavior of electron swarms in time-varying electric fields is investigated using a Monte Carlo simulation. In particular, the case of swarms in Cl₂ gas under linearly increasing or decreasing electric fields E/N with a variety of $|dE/dt|$ from 5×10^9 to 40×10^9 Td/sec is considered for the quantitative specification of RF plasmas. The swarm parameters as a function of instantaneous E/N and the power into the discharge volume at every moment are deduced, and compared to the steady-state case. At higher $|dE/dt|$, the parameters and the power deposition are shifted to later times, following those of the steady-state case at the same E/N. The drift velocity curve as a function of E/N is characterized by evolution of a peak at a low E/N. Validity of the use of the steady-state parameters in analyzing dynamic plasmas is also discussed.

†Currently, Univ. of Calif. at Berkeley

14:45

CB 6 **Electron Diffusion Peculiar to Radiofrequency Fields**
K. MAEDA and T. MAKABE,
Keio Univ.

Basic knowledge of electron transport in space and time is of key importance to understanding modern low temperature radiofrequency plasmas for material processes. The phase space transport of electrons is essential since electrons are primarily responsible for the maintenance of an rf discharge and the production of active species. In these circumstances, we address our attention to the electron transport in gases under rf fields from the phase space Boltzmann equation. Especially, the diffusion tensor of electrons is theoretically obtained from a direct numerical procedure of the Boltzmann equation. We focus our attention here on the temporal characteristics of the diffusion tensor unique to rf fields¹. Unusual increase in longitudinal diffusion coefficient just before and after the zero crossing time of the applied high frequency field is completely opposite to the characteristics in low frequency.

1. K. Maeda, J. Matsui, T. Makabe; *Proc. of 12 Symp. on Plasma Processing* (Jan. 1995).

Toshiaki Makabe
3-14-1 Hiyoshi, Yokohama 223 Japan
045-563-1141 (ex. 3358)
makabe@mkbe.elec.keio.ac.jp

15:00

CB 7 **Kinetic energy distributions of He⁺ in He and Ne⁺ and Ne²⁺ in Ne at high E/N produced in Townsend discharges,** M. V. V. S. RAO, R. J. VAN BRUNT AND J. K. OLTHOFF, NIST - Measurements have been made of the translational kinetic energy distributions for He⁺ ions in He at electric field-to-gas density ratios (E/N) in the range of 0.6×10^{-18} to $10 \times 10^{-18} \text{ Vm}^2$ and for Ne⁺ and Ne²⁺ ions in Ne at E/N from 0.8×10^{-18} to $20 \times 10^{-18} \text{ Vm}^2$. The gas of interest (He or Ne) was introduced into the discharge cell consisting of two circular stainless-steel parallel-plane electrodes, with interelectrode spacing

TUESDAY AFTERNOON

that could be varied from 1 to 4 cm, between which a diffuse, low-density (Townsend) discharge is generated that can be characterized by a constant uniform electric field, i.e., a constant E/N . The pressure times electrode spacing values for this discharge lie on the "left-hand" side of the Paschen curve. The ions were sampled through a 0.1 mm orifice in the center of the cathode and were simultaneously energy and mass analyzed using a cylindrical-mirror electrostatic energy selector coupled to a quadrupole mass filter. The results are interpreted using a model for ion transport in a uniform field which assumes that symmetric charge transfer is the dominant ion collision process. Deviations from the predictions based on this model are observed for both neon and helium ions as E/N is increased that have implications about the validity of the charge-transfer model at high E/N .

15:15

CB8 Role of H^+ , H_2^+ and H_3^+ Ions in the Secondary Emission. G.GOUSSET, J.BRETAGNE and T.ŠIMKO, LPGP UPS Orsay, France — The coupled transport of H^+ , H_2^+ and H_3^+ ions in H_2 has been studied with the aid of the Convective Scheme method¹. Following a suggestion of Phelps² the code was used to study the relative contribution of these ions to the secondary emission from the cathode in the Townsend discharge for E/N values ranging from 50 to 1000 Td. Referencing the statement of Fletcher and Blevin³ that only H^+ contribute to the secondary emission, we found similar trends for the secondary yield per ion, but our values were by far too low. Thus we introduced the effect of H_2^+ and H_3^+ (the dominant species). Not sufficient, two arguments must further be considered: (i) energetic H atoms formed in collisions of ions with H_2 can participate to secondary emission² and (ii) recent experimental results of NIST group⁴ indicate that H_3^+ to H^+ conversion is probably more efficient than assumed in our model.

¹J.Bretagne, G.Gousset and T.Šimko, J.Phys.D27, 1866 (1994).

²A.V.Phelps, private communication.

³J.Fletcher and H.A.Blevin, J.Phys.D14, 27 (1981).

⁴R.J.Van Brunt, private communication.

POSTER SESSION DA: LIGHTING DISCHARGES

Tuesday afternoon, 10 October 1995

Berkeley Marina Marriott

Angel/Quarterdeck Rooms, 15:45–17:15

U. Schmidt, presiding

DA 1 Radiometric and Electrical Characteristics of Low Pressure Sulfur Discharges* N. D. GIBSON, U. KORTSHAGEN and J. E. LAWLER, Physics Department, University of Wisconsin, Madison, WI 53706 - Sulfur (S) and S-Ar discharges have been studied over a wide range of operating conditions. Both DC positive column discharges and inductively coupled 13.56 MHz discharges have been studied. Even though the equilibrium partial pressure of S_2 is extremely low in the 50 C - 200°C temperature range investigated here, the primary radiating molecule in these discharges is S_2 . About 80 % of the spectral emission occurs in the 2800 Å - 3500 Å range. The spectrum observed from the 13.56 MHz discharge corresponds nicely to that obtained from DC discharges at much higher temperatures¹. The ultraviolet radiation output has been studied as a function of discharge temperature, cold spot temperature, input power, buffer gas species and pressure, discharge radius, and discharge current. The absolute efficiency of the discharge in generating near uv radiation has been measured and results are presented for many areas of the multidimensional parameter space.

*This work was supported by the General Electric Company and the NIST under the Advanced Technology Program (#70NANB3H1372).

¹Peterson, D. A., and Schlie, L. A., J. Chem. Phys. 73(4), 15Aug1980.

DA 2 Study of Transient Mercury Distribution Along the Axis of a Low Pressure Hg-Ar Discharge. M.W. GROSSMAN, OSRAM SYLVANIA INC. - A quasi-steady state Hg vapor pressure difference results in the transfer of the mercury condensate across a long discharge tube. The transfer process is characterized by an initially increasing, then quasi-stationary, and finally, a decaying axially varying mercury density profile, $n(x,t)$. If certain factors are taken into account $n(x,t)$ is described by the familiar diffusion equation:

$$\frac{\partial n}{\partial t} = D \frac{\partial^2 n}{\partial x^2} \quad (1)$$

where D is the Hg-Ar diffusion coefficient. The factors are discharge heating of Argon, mercury source characteristics, and discharge impedance. In addition to discussing the transfer characteristics, equation (1) together with the discharge model GLOW¹ are used to predict the variation of important parameters versus the condensate temperature during the initial transfer phase. These parameters are wall power deposition, axial electric field, and radiation emission profiles. The computational results are compared with recent experimental data.

¹R. Lagushenko and J. Maya, J. IES, 306 (1984)

DA 3 Time-dependent Modelling of C.W.-pulsed High pressure rare gas Plasmas,

T. THRUM and M. NEIGER, LTI/Univ. of Karlsruhe - In this paper we present the time-dependent modeling of a cylindrical wall-stabilized long arc rare gas plasma column in local thermal equilibrium. The model is based on the conservation law of energy, including heat conduction, convection and radiation, the conservation law of mass and Ohm's law. The calculated variables of this model are the time-dependent temperature profiles $T(r_i, t_k)$, the plasma velocity profiles $v_r(r_i, t_k)$ and the time-dependent axial electrical field strength $E(t_k)$. With the help of this model a rare gas plasma column in pulsed mode with pulses in the range of 1 μ s up to 10 ms, variable pulse form and amplitude, superimposed to different simmer currents can be analyzed. The nonlinear model equations are solved by a general implicit finite difference algorithm based on the Crank-Nicholson method. The model is used to investigate rare gas long arc plasmas operated with different pulse modes and base loads and to determine the transient thermal behaviour.

DA 4 New Broadband VUV-Light-Source,* J.WIESER, D.E.MURNICK, and A.ULRICH, Rutgers Univ. and TU-Munich - A novel low power broadband VUV light source has been developed. The well known rare gas excimer continua of the heavy rare gases argon, krypton and xenon in the wavelength region between 110nm and 200nm are used to generate the VUV light. The gases, or gas mixtures, are at atmospheric pressure. A low energy electron beam of typically 20keV is used for excimer excitation. Thin ceramic windows, such as 200nm to 400nm thick Si_3N_4 foils, are used to separate the vacuum in the electron source from the gas-filled volume. Electron energy loss in these foils is only a few percent. Preliminary experiments showed that current densities up to 10 μ A/cm² could be used without damage over several hours, thus a spectral radiance in the order of mW/(cm² nm sr) can be reached. This provides a small, easy to use rare gas excimer lamp working at moderate dc-voltage without hard x-ray or microwave background. Emission spectra and operating parameters are presented.

* Work supported by the NSF (CTS 94-19440) and the Humboldt Foundation

DA 5 On the transition limits between laminar and turbulent flow in high pressure Hg discharge plasmas. K. CHARRADA, G. ZISSIS, C.P.A. Toulouse.— In the case of an atmospheric pressure discharge, the mass flow is largely dependent of total mercury amount and current as well as arc tube dimensions. In this work the simulation of arc properties is performed with a two-dimensional fluid code based on a finite element semi-implicit scheme. Transition from laminar to turbulent flow is usually characterised by a critical value of 1400 for the Reynold's number. Extrapolating our calculation results by simple analytical formulas we are able to calculate the limits of turbulence in the plasma. We found that the flow become turbulent for a mercury amount greater than 150 mg/cm, or/and a tube diameter larger than 7 cm. However, the flow is found to be laminar for any value of electric current .

DA 6 Barium Transport in Fluorescent Lamp Negative Glow Plasma, Y. M. LI, OSRAM SYLVANIA INC., 71 Cherry Hill Drive, Beverly, MA.—The fluorescent lamp life is mainly controlled by the loss of barium oxide from the electrodes. In our previous analysis, the spatial distributions of neutral barium in the negative glow were determined with varying argon pressure. A one-dimensional ionization-diffusion transport model for neutral barium was used to describe the measured profiles¹. To determine the overall barium loss, the transport equations for neutral and ion were solved numerically in the negative glow region. The plasma and electric field distributions were derived from the planar analytic negative glow model as given by Ingold². The neutral and ion spatial distributions, net barium atom and ion losses, and their dependence on argon pressure were computed. Some preliminary conclusions are drawn. First, the Ba is lost mostly in form of ion even at pressures down to 0.2 Torr. Second, the ion spatial profile is roughly exponential at low pressures.

¹Y. M. Li, P. Moskowitz, Conf. Rec. IEEE ICOPS, p.209 (1994)

²J. H. Ingold, Phys. Rev. , vol. 43, p. 3093 (1991)

POSTER SESSION DB: ELECTRON AND PHOTON COLLISIONS

Tuesday afternoon, 10 October 1995

Berkeley Marina Marriott

Angel/Quarterdeck Rooms, 15:45–17:30

DB 1 Photoionization of K near the 3p Threshold: Coupling and Correlation Effects.* Z. FELFLI, A.Z. MSEZANE, *CTSPS, Clark Atlanta U.* — Channel-coupling, spin exchange interactions and (CI) effects in the initial and final states in the photoionization of the ground state of K have been investigated using the R-matrix method¹. Two through five lowest extensive CI target states are coupled and results obtained in the length and velocity forms for photon energies from near the 3p inner-shell thresholds to about 70 eV. We find that the inclusion of configurations 3p⁴3d² in the initial and final states improves the agreement between the length and velocity forms of the cross section. Channel-coupling, spin-exchange interactions and the addition of more states generally attenuate the individual and uncoupled cross sections near the 3p threshold. Results will be presented and compared with those of Be² and Na³ where the triplet state cross section dominates and spin-exchange interactions and coupling enhance the cross section near the inner-shell thresholds.

*Research supported by AFOSR and DoE office of Basic Energy Sciences, Division of Chemical Sciences.

¹ K.A. Berrington *et. al.*, *Comput. Phys. Commun.* **14**, 367 (1978)

² M.O. Krause and C.D. Caldwell, *Phys. Rev. Lett.* **59**, 2736 (1987)

³ A.Z. Msezane, F. Nyandeh and J. Niles, *J. Phys. B* **23**, L691 (1990)

DB 2 Universal Representation of Cross-Sections from First Principles Dispersion Relations.* D. BESSIS, A. HAFFAD, Z. FELFLI, A.Z. MSEZANE, *CTSPS, Clark Atlanta U.* — A dispersion relation is derived at fixed energy, in K^2 , for the electro-production of resonances in electron-atom collisions. This dispersion relation leads to a representation of the differential cross-sections by a diffraction peak which automatically embeds the "hump". A global optimal parametrization of this diffraction peak, which has large scattering angle measurements embedded into it, is presented. This is one of the crucial features of this approach since experimental errors increase when approaching the interesting limit $K^2 = 0$, and a method able to embed correctly large scattering angles, where the errors are small, will allow a more reliable $K^2 = 0$ limit. Therefore, any analysis able to integrate them will improve the reliability and the accuracy of the extrapolation of the generalized optical oscillator strength (GOS) down to zero K^2 to obtain the optical oscillator strength (OOS). The method is applied to electron-scattering from Xe, Ar, Kr and Ne atoms at energies from 100 eV to 500 eV, and compared with measurements.

*Work Supported by NSF, AFOSR and DoE, Office of Basic Energy Sciences, Division of Chemical Sciences.

DB 3 Atomic Transition Probabilities for Rare Earths,* H. M. ANDERSON, E. A. DEN HARTOG, M. E. WICKLIFFE, and J. E. LAWLER *Univ. of Wisconsin-Madison*—Accurate absolute atomic transition probabilities for selected neutral and singly ionized rare earth elements including Tm, Dy, and Ho are being measured. The increasing use of rare earths in high intensity discharge lamps provides motivation; the data are needed for diagnosing and modeling the lamps. The basic approach used in earlier work on Sc and Hg is used.¹ Radiative lifetimes, measured using time resolved laser induced fluorescence (LIF), are combined with branching fractions, measured using a large Fourier transform spectrometer. More than 6000 LIF decay curves from Tm atoms and ions in a slow beam have been recorded and analyzed to determine radiative lifetimes for more than 250 levels of TmI and TmII. Representative lifetime results will be presented and discussed. These provide the absolute normalization needed to determine transition probabilities of most (>1000) of the strongest lines in TmI and TmII. ¹ Marsden *et al.*, *J. Opt. Soc. Am. B* **5**, 606 (1988); Lawler & Dakin, *J. Opt. Soc. Am. B* **8**, 1457 (1989); Benck *et al.*, *J. Opt. Soc. Am. B* **6**, 11 (1989).

*Supported by Osram Sylvania Inc. and by the NSF.

DB 4 Spatially Resolved Measurements of Electron-Ion Recombination Products in Flowing Afterglow Plasmas*. T. GOUGOUSI, M.F. GOLDE, and R. JOHNSEN, *U. of Pittsburgh* —We have developed a technique in which the products of dissociative recombination are detected by position-sensitive Laser induced fluorescence at different points in the recombining plasma. Radiating products can also be observed by spatially resolved emission spectroscopy. We will present examples of LIF data on OH production from H₃O⁺ recombination, OH emission spectra obtained from H₂O⁺ recombination, CO emissions from recombination of CO₂⁺ ions with electrons, and CH emissions from CH₃⁺ recombination. We find that position-sensitive detection provides a valuable tool in separating recombination products and emission features from those arising from extraneous reactions. The technique also allows a far more sensitive comparison between model calculations and experimental observations than can be made by observations at fixed locations.

*This work was, in part, supported by NASA

DB 5 Mechanisms for Producing an Intense Metastable Calcium Beam, J.V.B. GOMIDE, G.A. GARCIA, D. PEREIRA and SCALABRIN, Instituto de Física, Unicamp- Intense metastable calcium beam is produced by means of an electron bombarder. The light from the arc discharge region is sent to a double grating spectrometer while the density of metastable atoms is monitored by laser absorption. Almost all singlet transitions are observed in the pre-breakdown regime. In the sustained regime there appears intense triplet and Ca II transitions, a more than 20% of the atoms is in the metastable triplet. The formation population in this level, as observed, is due to direct excitation from the fundamental state or by cascade decay from the higher lying triplet level. The role of each one of these processes depends on the discharge working point. In a previous paper with Mg^I, only direct excitation from the fundamental state was taken into account in the theoretical calculation. These results will be useful to improve the design of the discharge.

¹ G Giusfredi et al, J. Appl. Phys. 63, 1279 (1988)

DB 6 Modeling the Electron Energy-Loss Spectrum of N₂ H. Helm, Universität Freiburg and D. L. HUESTIS, SRI International. —We have modeled the electron impact cross sections of Geiger and Schroeder¹ and Chan et al.² with the objective of deriving improved values of the transition moments for the lowest Rydberg states: b - X, c - X, o - X, b' - X, c' - X, and e' - X. Our spectroscopy model³ has a total of 71 mixed vibronic levels, resulting in about 5300 rotational transitions from the ground state, each with a transition strength of the form:

$$I_i = (C_i^b \mu_{bx} + C_i^c \mu_{cx} + C_i^o \mu_{ox} + C_i^{b'} \mu_{b'x} + C_i^{c'} \mu_{c'x} + C_i^{e'} \mu_{e'x})^2$$

These lines are broadened and summed for direct comparison with the experimental data. The transition moments are determined by least-squares minimization. Our modeling of the data of Geiger and Schroeder¹ is consistent with the simpler analysis of Stahl et al.⁴ Modeling of the data of Chan et al.² suggests a transition moment for $o^1\Pi_u - X^1\Sigma_g^+$ that is three times smaller than that inferred from the Geiger and Schroeder data.¹

¹ Geiger and Schroeder, J. Chem. Phys. 50, 7-11 (1969).

² Chan et al., Chem. Phys. 170, 81-97 (1992).

³ Helm Phys. Rev. A 48, 2762 (1993).

⁴ Stahl et al., J. Chem. Phys. 79, 2541-2558 (1980).

DB 7 Analysis of Optical Emissions Produced by Electron Impact on Sulfur-Containing Molecules*. P. KURUNCZI, J.P. MICHEL, N. ABRAMZON, K. BECKER, City College of C.U.N.Y. and K.A. Blanks, ALCOA Technical Center --- The sulfur-containing molecules SO₂, COS, CS₂, and H₂S are trace constituents of the gaseous emissions produced in the aluminum refining process. Optical emission spectra in the 200 - 500 nm region produced by electron impact were analyzed in terms of emitting species and their appearance energy in an effort to explore the possibility of using electron-impact induced optical emissions to monitor the concentrations of these molecules. While SO₂ has been studied before in some detail [1,2], no comprehensive data base is available for the other three molecules. A complete account of all observed emissions in terms of identification of emitting species, absolute emission cross section as a function of impact energy and appearance energy will be presented at the Conference and the possibility of using these emissions for pollutant monitoring will be discussed.

1. K. Miller Jr. and K. Becker, Can. J. Phys. 65, 530 (1987)

2. J.M. Ajello, private communication (1992)

*Work supported in part by ALCOA Technical Center and by the U.S. National Science Foundation (NSF).

DB 8 Electron Impact Excitation of Clusters*, L.A. PASTORIUS and J.W. McCONKEY, University of Windsor, Ontario, Canada N9B 3P4—A pulsed electron beam crossed with a pulsed cluster beam has been used to study the excitation of Ar and other clusters. Time of flight techniques have enabled prompt photon decay, coincident with the exciting electron beam pulses, to be separated from energetic metastable fragments arriving at a channeltron detector. Various filters have been used to isolate different spectral regions in the V.U.V. A number of excitation processes have been identified from a study of the excitation functions.

* Research supported by the Natural Sciences and Engineering Research Council of Canada.

DB 9 Elastic DCS and Differential Vibrational Excitation Cross Sections for the Series CH₄, CH₃F, CH₂F₂, CHF₃, and CF₄, T. MASAI, L. BOESTEN, H. TANAKA, M.YURI, Sophia U. Tokyo, and M. A. DILLON, Argonne National Laboratory - We have measured the elastic and some vibrational differential excitation cross sections of the fluorinated series from CH₄ to CF₄ in the energy range from 1.5-100 eV over scattering angles from 15° -130°. Excitation functions were recorded at the two characteristic stretching and bending vibrational modes. All these molecules show a single broad vibrational peak near an impact energy of 7.5 eV. Similar to the constant C-H and C-F bond lengths, the C-H or C-F stretching/bending modes -whenever they can be identified as such - seem to inherit the characteristics of their "parent" molecule CH₄ and CF₄; the C-F vibration excitation peaks are larger (0.1Å²/sr) and narrower (5 eV), and the C-H peaks are smaller (0.04 Å²/sr) and wider (7-8 eV). The elastic DCS of the polar molecules of this series are larger than those of the non-polar molecules over an unusually wide angular range, and there may be stronger direct scattering at energies below 2 eV. Only CF₄ shows the small peak at 21 eV reported previously.

*Supported by the U.S. Dpt. of Energy, Office of Energy Research, Office of Health and Environmental Research, under Contract W-31-ENG-38 and by Grant in Aid from the Ministry of Education, Science, and Culture, Japan.

DB 10 Characteristic Energy of Electrons in Carbon Monoxide at Elevated E/N. W.ROZ- NERSKI, J. MECHLIŃSKA-DREWKO, Faculty of Physics and Mathematics, Technical University of Gdańsk, 80-952 Gdańsk, Poland, and Z.Lj. PETROVIĆ, Institute of Physics, 11001 Belgrade, Yugoslavia - By means of experimental method and numerical procedure described earlier¹ the characteristic energy (D/A) over the reduced electric field E/N: 50 ≤ E/N ≤ 1000Td has been determined. The present results are within the combined errors of this work and those by Petrović and Crompton.² These results also agree fairly well with those by Kontoleon et al.³ and by Al-Amin et al.⁴ up to 500Td but for E/N=1000Td they are about 25 percent lower than the results of Kontoleon et al.³ and about 40 percent lower than those by Al-Amin et al.⁴

¹ W. Roznerski et al., J. Phys. D 27, 1862 (1994)

² Z. Lj. Petrović et al., Aust. J. Phys. 42, 609 (1989)

³ C. S. Lakshminarasimha et al., J. Phys. D 7, 2545 (1974)

⁴ S. A. Al-Amin et al., J. Phys. D 18, 2007 (1985)

DB 11 The Covariance Mass Spectrum of the Polar Dissociation (ion pair production) States of CF₄ in the 20-40 eV Electron Impact Energy Range. L. M. C. R. SPORLEDER, and R. A. BONHAM, Department of Chemistry, Indiana University, Bloomington, IN 47405 - The time of flight of both ions formed from the excitation of polar dissociative states by electrons, with energies from 20 to 40 eV, have been recorded for the molecule CF₄. At 20 eV the only observed reaction is CF₄⁺ → F⁻ + CF₃⁺, while at 25 eV the additional, and much stronger reaction, CF₄⁺ → F⁻ + CF₂⁺ + 2F or F₂ also occurs. At 40 eV impact energy these two reactions are joined by the reactions CF₄⁺ → F⁻ + C⁺ + 3F or F + F₂ and CF₄⁺ → F⁻ +

$F^+ + CF_2$ or $CF + F$ or $C + 2F$ or $C + F_2$ where the reaction forming C^+ is the dominant one of the four. The total absolute F^- cross section at 40 eV electron impact energy is about 10^{-19} cm², which is in agreement with the observations of Iga et al. [I. Iga, M.V.V.S. Rao, S.K. Srivastava, and J.C. Nogueira, Z. Phys. D 24, 111 (1992)]. Absolute cross sections for all observed dissociation channels as a function of electron impact energy will be reported.

* Work supported by grant NSF-PHY 9214126.

POSTER SESSION DC: MATERIALS PROCESSING AND PHENOMENA

Tuesday afternoon, 10 October 1995

Berkeley Marina Marriott

Angel/Quarterdeck Rooms 15:45-17:30

DC 1 Simulations of Laser Ablation of Cl₂ (solid) as a Possible Neutral Beam Source for Etching* M. SUZUKI, H. DATE, P.L.G. VENTZEK, Y. SAKAI, H. TAGASHIRA, Dept. of Electrical Eng., Hokkaido University, Sapporo, Japan, and K. KITAMORI, Dept. of Industrial Eng., Hokkaido Institute of Technology, Sapporo, Japan. - Recently, charge damage considerations in high density plasma processing reactors have prompted the development of neutral beam sources for etching. Anisotropic etching of Si has already been demonstrated¹ using vibrationally excited Cl₂ and, recently, a back-illuminated laser ablation Cl₂ source has been developed.² Here, we investigate a neutral beam source in which a pulsed laser beam is incident off the normal of the frozen Cl₂ target (from the front). In particular, using a 2-dimensional fluid-Monte Carlo simulation, we are studying the degree of controllability of the composition and energetics of the source. The influence of variations in the initial electron temperature, dissociation fraction and on magnitude of the applied electric fields will be presented.

1. A. Szabo and T. Engel, J. Vac. Sci. Technol., A12, 648 (1994)

2. S.R. Leone, Dry Process Symposium, p. 85 Tokyo, 1994.

*Grant-in-Aid of Scientific Research, Min. of Education, Japan.

DC 2 Neutral Shadowing in Plasma Etching of Circular Trench Holes. B. ABRAHAM-SHRAUNER, Washington University - The flux of neutral molecules created by a glow discharge is determined analytically in a circular cylindrical trench hole etched on a semiconductor wafer patterned with a photoresist mask. The neutral distribution function is Maxwellian where directed neutrals created by charge-exchange collisions with ions are neglected. Straight line trajectories of the neutrals in the trench are assumed and the surface sticking coefficient of the neutrals is 1. Dependence of the shadowing on the aspect ratio (depth/width) is shown and compared to that for the directed ions in plasma-assisted etching. Etch profiles of the trench for etch rates proportional to the neutral flux are plotted. The profiles are calculated by trajectory equations found by the method of characteristics from the surface evolution equation. The neutral flux and the etch profiles are compared to those for a rectangular trench whose length is large compared to its width and depth.¹

* Supported by the National Science Foundation under grant ECS-9310408.

1. B. Abraham-Shrauner and C. D. Wang, IEEE ICOPS, 42, June, 1995, Madison WI.

DC 3 Neutral Beam Studies : Etching of Si and SiO₂ with Fluorocarbon / Ar Gas Mixtures. G.P.KOTA, J.W.COBURN, and D.B.GRAVES, U. of California at Berkeley, and L.CHEN, Sematech - An inductively coupled plasma¹ has been used to generate a beam of mixed ions, effusive neutrals and fast, directed neutrals. We have characterized the composition and

energy distribution of the effluent beam, in addition to conducting extensive measurements of Si and SiO₂ etch rates. We have made measurements using CF₄/Ar, CHF₃/Ar and C₂F₆/Ar mixtures, varying gas composition, pressure and applied rf power in each case.

¹L.Chen, Proceedings of the SPIE, 2091, 136 (1994)

DC 4 Model of Oxide Etching in High Density Plasmas. D. B. GRAVES, MING LI, R. A. STEWART and J. D. BUKOWSKI, U.C. Berkeley - Fluorocarbon-containing plasmas are used extensively for etching silicon dioxide in the semiconductor manufacturing industry. We have modeled an inductively coupled plasma reactor using CF₄, etching a blanket silicon dioxide substrate. Etch products have been included in the model. In addition to etching, we have developed rate expressions for the deposition of polymeric films on surfaces from both neutral and ionic precursors, based on reports of these processes in the literature. Using the model, we examine several issues related to the operation of fluorocarbon plasmas under high plasma density conditions, including the effects of gas flow and residence time, applied power, gas pressure and surface temperature on the operation of the plasma. These effects included the neutral and ionic composition of plasma. Uniformity of etching on the substrate is also examined.

DC 5 Diamond Film Formation by RF Plasma CVD with Radical Source Employing H₂ and H₂O gases. E. MIZUNO, K. YAMADA, S. KATO, M. HIRAMATSU, M. NAWATA, M. IKEDA*, M. HORI* and T. GOTO*, Meijo Univ. and Nagoya Univ.*, Japan - It has been reported that CH₃ and H radicals are important species for the formation of diamond in hydrocarbon-hydrogen plasmas. Although CH₃ radicals exist enough in a capacitively-coupled RF CH₃OH plasma, the formation of diamond has been never synthesized because of a lack of H radicals. We designed a new system to supply RF CH₃OH plasma with H radicals activated by microwave H₂/H₂O plasma. In this system the amount of H radical could be varied independently. Films were deposited with varying mixture ratio between H₂ and H₂O at the total pressure of 13.3Pa, CH₃OH pressure of 0.67Pa, RF power of 100W, microwave power of 100W, substrate temperature of 600 °C. It was found that the diamond was successfully formed with a supply of H radicals and H radical played a role of removing non-diamond phase. Furthermore, H₂O addition enhanced the removal process and grain size of diamond became large with increase in H₂O fraction .

DC 6 Observation and Analysis of Coulomb Liquid-to-Solid Phase Transition in a Dusty Plasma.

Y. HAYASHI and K. TACHIBANA, Kyoto Inst. Tech. and Kyoto Univ. - The liquid-to-solid phase transition for bound dust particles by Coulomb force in plasma was observed by scattered light using a CCD video camera and analyzed by Mie-scattering ellipsometry¹. Carbon particles were grown and a Coulomb solid was formed under the same conditions as published before² except for the gas of ethylene. When particles grew to 1100 nm in diameter by coating, those around the lower sheath-plasma boundary were observed to become spotty from halo-patterned. At the time, the decreasing rate of particle density around the upper boundary changed higher, while the density around the lower boundary once increased but soon decreased with the lower rate. This suggests that the density decreased by the rather repulsive force between particles in the liquid phase while they were bound by the attractive force after the phase transition. The density decrease is considered to be due to the escape of particles through the electrode gap, because the decreasing rate was lower when particles were confined laterally in a potential bucket.

¹Y. Hayashi & K. Tachibana, Jpn. J. Appl. Phys. 33, L476 (1994)

²Y. Hayashi & K. Tachibana, Jpn. J. Appl. Phys. 33, L804 (1994)

DC 7 Contribution of Electron Inertia to Two-Dimensional Solitons in a Weakly Relativistic Plasma, H.K. MALIK and R.P. DAHIYA of CES, IIT Delhi, India - Propagation characteristics of two-dimensional ion acoustic solitons in a plasma with finite temperature ions drifting relativistically are investigated. The basic fluid equations for weakly relativistically drifting ions are presented. With relativistically drifting ions the electron inertia is important and therefore the finite electron mass is included in the fluid equations instead of the usual Boltzmann distribution for obtaining the Kadomtsev-Petviashvili (KP) equation. Effect of the electron inertia and finite ion temperature is analysed on the soliton characteristics. It is found that the peak soliton amplitude decreases as ion drift velocity is increased because of the electron inertia effect but it increases as the ion temperature is raised.

POSTER SESSION DD: HELICAL RESONATORS AND MICROWAVE PLASMAS

Tuesday afternoon, 10 October 1995

Berkeley Marina Marriott

Angel/Quarterdeck Rooms, 15:45-17:30

DD 1 Plasma production by large amplitude plasma surface waves, $\omega < \omega_{pe}$. D. J. COOPERBERG AND C. K. BIRDSALL, *University of California at Berkeley**—Surface waves in a warm, unmagnetized, bounded plasma have been investigated via electrostatic 2½d particle simulation. Our study focuses on a slab configuration in which the y direction is periodic and the x direction is bounded by grounded, absorbing conducting walls. Our prior simulation has produced dispersion relations and eigenfunctions for surface waves analogous to the Gould-Trivelpiece¹ waves in cylindrical systems for which the $k_y = 0$ cut-off of the asymmetric mode defines the series resonance and secondary branches whose cutoffs represent Tonks-Dattner resonances.² The current work demonstrates progress made in studying 2 species, low voltage, collisional systems sustained both by uniform ionization for which the randomly excited surface wave modes remain in a linear regime and also by resonant interaction with surface waves which are excited beyond the linear regime. Surface wave sustained plasmas have been studied extensively by Moisan et al. in cylindrical devices and this work hopes to extend such studies to planar configurations more suitable for large area plasma processing.

¹A. W. Trivelpiece and R. W. Gould, J. Appl. Phys. 30, 1784 (1959)

²D. J. Cooperberg and C. K. Birdsall, Bull. APS II, 39, 7, 1552 (1994)

*This work supported by Office of Naval Research contract N00014-90-J-1198.

DD2 ATOM DENSITY MEASUREMENT IN A MOLECULAR GAS MIXTURE MICROWAVE DISCHARGE, P. BLETZINGER and B. N. GANGULY, Wright Laboratory, WPAFB, OH—The H₂ dissociation efficiency in a microwave (2.45 GHz) excited H₂ - N₂ gas mixture discharge has been measured from 0.5 Torr up to 4 Torr pressure with 20 to 30 watt input power. The H atom density as a function of %H₂ - %N₂ gas mixture at a given pressure, flow rate and input power has been measured downstream from the microwave discharge region by two-photon laser induced fluorescence. At pressures 1 Torr and below, H atom density decreased monotonically with increased N₂ dilution, whereas for pressures 2 Torr and above the H atom density initially increased with N₂ dilution

and remained nearly constant over a wide range of %H₂ - %N₂ gas mixtures. The H atom density has also been measured with H₂ added to the N₂ discharge afterglow region. The pressure and the flow rate dependent measurements show evidence of H₂ dissociation by N₂.

DD 3

Measurements of the Populations of the n=3,4 and 5 Excited States of Atomic Hydrogen in a Microwave Discharge in Hydrogen, M.J. WOUTERS, I.S. FALCONER, B. W. JAMES and J.

KHACHAN, U. of Sydney - Absolute line intensity measurements of the H_α, H_β and H_γ lines have been used to calculate the corresponding excited state populations in a microwave discharge in H₂. The discharge is in tube reactor of the kind commonly used for diamond deposition. In the pressure range 2 to 55 torr, the populations range from 2 x 10¹⁴ - 2 x 10¹³ m⁻³ for n=3, 8 x 10¹³ - 8 x 10¹² m⁻³ for n=4, and 3 x 10¹³ - 3 x 10¹² m⁻³ for n=5. A spectroscopic model incorporating a kinetic calculation of the relevant rate coefficients has also been used to estimate the average electron energy from the excited state populations. At 20 torr, the average electron energy is calculated to be 3 to 4 eV, compared with a theoretical estimate of 3 eV. The present limitation to this method is poor knowledge of the density of atomic hydrogen.

DD 4 Ion Energy Distributions from a Helical Resonator Discharge*, B. SMITH and L. OVERZET, U. of Texas at Dallas

- Helical resonator discharge reactors are high density, low pressure, plasma sources commonly used for semiconductor etching. Just as in other high density sources, the ions should have relatively low energy directed at the substrate and should permit energy control with an applied rf bias at the substrate. In this investigation I will examine ion energy distributions at an electrode in contact with the plasma, near the helical resonator coils. The ions are brought into a quadrupole mass spectrometer equipped with a Bessel box energy analyzer through pinholes of various aspect ratios, simulating surface features of an actual etch. Variations in the IED's with pressure and power should indicate how to improve the development of etch processes in similar tools, while differences in the ion flux due to different pinholes may help determine aspect-ratio-dependent etch properties.

*This work is supported in part by the National Science Foundation and the State of Texas Advanced Research Program.

DD 5

Modeling the Capacitive to Inductive Mode Transition in the Helical Resonator Discharge, K. Niazi, Applied Materials--The helical resonator can be operated in a capacitive mode, in which the discharge is created between the maximum rf potential on the coil and any part of the chamber near ground, as well as in an inductive mode in which the sustaining field is the induced azimuthal electric field. A numerical global model used previously to study the helical resonator discharge in the capacitive mode[1], is extended to include operation in the inductive mode. Predicted values for density, sheath thickness, and coil voltage are presented, and compared to values for a purely capacitive discharge.

[1] K. Niazi, A. J. Lichtenberg, M. A. Lieberman, and D. L. Flamm, Plasma Sources Sci. and Technol., 3, 3482 (1994).

POSTER SESSION EA: DIAGNOSTICS-OPTICAL METHODS
 Tuesday evening, 10 October 1995
 Berkeley Marina Marriott
 Belvedere Room, 19:45-21:30

EA 1 Degenerate Four Wave Mixing Measurements in a Helium Radio-Frequency Discharge, M.D. BOWDEN, H. TAGAWA, D.W. GAO, K. UCHINO, K. MURAOKA and M. MAEDA, Kyushu U.-

Degenerate-four-wave-mixing (DFWM) has recently been applied to make measurements in microwave discharges and flow reactors. In this paper, we report measurements made in a medium pressure (~ 1 Torr) helium RF discharge. The main transition which was studied was the $1s2s\ ^1S - 1s3p\ ^1P$ transition at 501.56 nm. The other transitions studied also originated in the metastable $1s2s\ ^1S$ energy level. The aim of the study was to examine plasma effects which determine the applicability of DFWM as a diagnostic technique in these kinds of discharges. Measurements were made for different discharge conditions and for several different optical arrangements. These measurements clearly showed the effect that the diffusion of excited atoms had on the DFWM process in the plasma. A model for the diffusion process was constructed and the results of the model were compared to the dependences which were observed in the experiment.

¹D.S Green and J.W. Hudgens, 47th GEC Meeting, Gaithersburg, October 1994.

EA 2 Thomson Scattering Measurements of T_e and N_e in Low Pressure Discharges, M.D. BOWDEN, N. AOKI, K. UCHINO, K. MURAOKA and M. MAEDA, Kyushu University - We have

previously reported incoherent Thomson scattering measurements of electron temperature T_e and density N_e in ECR and RFI discharges operated in argon^{1,2}. In this paper, we report measurements in an ECR discharge operated in a variety of different gas mixtures, using gases such as Ar, He, Ne, Kr, O₂ and N₂. The measurements were made in the source region of an ECR discharge at gas pressures of a few millitorr. The detection limits for measurements in each gas are presented and the limits of applicability of Thomson scattering as a processing plasma diagnostic technique are discussed.

¹M.D. Bowden *et. al.*, *J. Appl. Phys.* **73**, 2732 (1993)

²M.D. Bowden *et. al.*, 47th GEC Meeting, Gaithersburg, October 1994.

EA 3 Application of Rayleigh Scattering to Measure the Neutral Density in Low Pressure Discharges, M.D. BOWDEN,

W. CRONRATH, T. HORI, K. UCHINO, K. MURAOKA, M. MAEDA, Kyushu University - Recently, incoherent Thomson scattering of a high power laser has been used to measure electron properties in ECR and RFI discharges^{1,2}. In this paper, we report laser scattering measurements of the neutral gas density in these plasmas. In this technique, the complete scattered spectrum containing both Thomson and Rayleigh components is measured. The different spectral widths of the two components allows them to be readily separated. The Rayleigh signal can then be used to determine the neutral density in the plasma. The size of the Rayleigh scattered signal is very sensitive to the number of metastable atoms in the discharge, and this dependence is discussed in detail. Measurements in both ECR and RFI argon discharges showed strong depletion of the neutral gas atoms in the centre of the discharge. This depletion was attributed to the combined effects of ion-neutral charge exchange collisions and heating of the neutral atoms by electron-neutral collisions.

¹M.D. Bowden *et. al.*, *J. Appl. Phys.* **73**, 2732 (1993)

²M.D. Bowden *et. al.*, 47th GEC Meeting, Gaithersburg, October 1994.

EA 4 Actinometry Measurements of Atomic Oxygen Densities in a Downstream Microwave Plasma Source *,

ALEXANDER ERSHOV and JACEK BORYSOW, Physics Department, Michigan Tech. University - We have verified the validity of actinometry to measure oxygen atom densities in O₂/Ar

microwave flow discharge. The measurements were done at flow rates up to 100 sccm. We have shown that emission ratio from $3p^3P$ state of oxygen atom at 844.6 nm and from $3p^54p$ of argon atom at 750.4 nm is well correlated with oxygen atom concentrations. Absolute flow rate of oxygen atoms was up to 70 sccm and was determined by titration with NO₂.

* Supported by Photran Corporation

EA 5 LIF Detection of CF and CF₂ radicals during Treatment of Polymer Surfaces in Fluorocarbon Plasmas, A.

TSEREPI, T. GLASSON, J-P. BOOTH, J. DEROUARD and N. SADEGHI, Labo. de Spectrométrie Physique, Université J. Fourier Grenoble I, France - In order to elucidate the role of fluorocarbon radicals on the surface modification of polymers, the evolution of CF and CF₂ close to the polymer surface was monitored in real-time by LIF. In a pure CF₄ discharge, we found that these radicals are consumed mainly through gas-phase recombination reactions with F atoms, monitored by optical emission measurements, which are primarily responsible for the polymer surface modification. However, a drastic change of the kinetics of the radicals can be induced by varying the concentration of F atoms in the feed gas (CF₄/H₂, He/F₂). In particular, the addition of 15% H₂ in the feed, as a F reducing agent, resulted in a consumption of CF₂ primarily on the polymer surface. Finally, the temporal evolution of CF, CF₂ and F was correlated to the modification of the surface properties, during comparable time scales, detected by *ex-situ* surface analysis (XPS, surface energy measurements).

EA 6 Laser-Induced Fluorescence Measurements of Metastable Fluorine in a SF₆ Discharge, E. BENCK, T. WEBER*

and J. ROBERTS, NIST - Spatially-resolved, laser-induced fluorescence measurements have been made utilizing the $3s\ ^4P_{3/2}$ metastable level of fluorine in a SF₆ discharge. Atomic fluorine, important in the semiconductor industry, is created by the dissociation of SF₆. The measurements were made utilizing a rf (13.56 MHz) discharge created in a GEC Reference Cell. The relative metastable densities were measured under a variety of different plasma conditions in pure SF₆ and also in mixtures with N₂ or Ar. In addition, the results are compared with spatially resolved, optical emission measurements of fluorine, which originate from higher lying excited states. The fluorine spectra dominates the weak optical emissions in the visible from these discharges.

* Summer Undergraduate Research Fellow, Bryn Mawr College, Bryn Mawr, PA.

EA 7 Experimental evidence of formation of NH₃ in N₂-H₂ discharge and post-discharge by Induced Fluorescence Laser on the H atom, G. SULTAN, G. BARAVIAN, P. STRATIL

and J. AMORIM*, LPGP, CNRS, U. of Paris-Sud - Two-photon absorption laser-induced fluorescence technique (TALIF) has been utilized to determine the H atom spectral profile in N₂-H₂ dc microwave discharges and in flowing afterglow post-discharges. It appears that the experimental LIF profile results of the addition of two gaussian shape profiles with same center and different heights and widths. The narrow one is related to the H atoms present in the medium and is similar to that obtained in pure hydrogen or in H₂-Ar mixtures. From its Doppler width, we deduced the H atoms kinetic temperature which is in the range 500K-1000K depending on the experimental conditions. The widest one would result from the photolysis of NH₃ molecules by the laser photons at 205 nm where the H resulting atom from the dissociation process is then

detected by LIF during the same laser pulse. From the maximum kinetic energy of the H atoms contributing to the wide wing of the Doppler profile we determine the dissociation energy of NH_3 .

* Present address Inst. Estud. Avanc., Sao Jose dos Campos, Brasil

EA 8 Diode Laser Measurement of Cl Atoms in an Inductively Coupled GEC Reference Cell Cl_2 Discharge. R.M. FORRISTER and H.M. ANDERSON, University of New Mexico. Single-pass, FM diode laser absorption spectroscopy has been used to study dissociation of Cl_2 to Cl atoms in the inductively coupled GEC Reference Cell. The measurements were made utilizing the spin-orbit transitions in the ground state of atomic chlorine near 882 cm^{-1} . The Cl_2 discharge exhibited two characteristic modes. At 20 mTorr and low power (less than $\sim 65\text{ W}$ calculated power) the discharge was in a "dim" mode (probably capacitive), whereas for powers greater than 65 W , the discharge exhibited a "bright" inductive mode. A weak 882 cm^{-1} absorption signal was observed in the dim mode which tended to increase linearly with power. At the transition from the dim to bright mode, the strength of the absorption feature made a discontinuous jump on the order of 3-4 times that of the dim mode value. The absorption signal peaked just beyond this transition to the inductive mode at $\sim 80\text{ W}$. Further power increases cause the absorption signal to decrease by as much as a factor of 2. This decrease in signal strength at higher powers is thought to be due to electron excitation of the Cl atom to its upper spin orbit state, and not a decrease in Cl atom concentration. The magnitude of the jump in absorption signal at the transition between the dim and bright modes indicates substantial dissociation ($>75\%$) of Cl_2 at even the lowest sustaining power of the inductive mode.

EA 9 Atomic Hydrogen Concentration Determined From LIF Temperature in a Dc-Arcjet.* ELIZABETH A. BRINKMAN and JAY B. JEFFRIES, SRI International—The gas temperature distribution is determined by laser-induced fluorescence of NO in the plume of reacting gas in a dc arcjet reactor which is used for chemical vapor deposition of diamond thin-film. In an arcjet reactor, the feedstock gases are activated by electron impact in the arc and evolve by chemical reaction in the gas plume between the nozzle and the substrate. In the short transit time, the gas composition in the plume has not reached chemical equilibrium and is determined by the gas kinetics. Gas temperature coupled with calorimetry of the dc-arc water cooling is used to determine the fraction of the feedstock hydrogen which has been dissociated by the dc-arc into atomic hydrogen.

* Sponsored by ARPA via the Naval Research Laboratory and the Army Research Office

EA 10 Correlation of TALIF with Fülcher Band and H_α Emission in H_2 Discharges* B. N. GANGÜLY, P. BLETZINGER, and A. GARSCADDEN, Wright Laboratory, Wright Patterson AFB, OH 45433- Simultaneous measurements of H_2 Fülcher band (612.2 nm) and H_α emission along with two photon allowed laser induced fluorescence (TALIF) of the H atom have been performed in the positive column of a dc discharge to determine the correlation of plasma induced emission (PIE) with the H atom density¹. These measurements have been performed from 0.5 Torr up to 2 Torr pressures, current densities from 4 mA/cm^2 to 40 mA/cm^2 and $E/p < 50\text{ Vcm}^{-1}\text{ Torr}^{-1}$ (E measured by probe). Under the measured discharge conditions, the TALIF and Fülcher band emission show a proportional increase in signal indicating a strong correlation of H atom density with Fülcher band intensity. The H_α PIE also shows a positive correlation with the TALIF signal. The measured data indicate that Fülcher band and H_α emission may be used to monitor the H atom density changes under low H_2 dissociation because all of the processes are dominated by the forward rate constants¹.

¹R. Nagpal and A. Garscadden (this conference).

EA 11 Calibration of H_2 Dissociation in Glow Discharges* R. NAGPAL and A. GARSCADDEN, WL/POOC-3, Wright Patterson AFB, OH 45433- Results from self-consistent solutions of Boltzmann transport equation in H_2-H mixtures over wide ranges of E/N (10-100 Td) and fractional dissociation (0-50%) are reported. The results show that since the dissociation of H_2 in glow discharge conditions occurs exclusively by electron impact, changes in the electron energy distributions in H_2-H mixtures can be used to provide direct estimates of fractional H_2 dissociation. Molecular H_2 Fülcher band and H_α excitations are used as calibration parameters in the calculations. The calculated excitation rates-% dissociation- E/N surfaces show that there is a dynamic range of ≈ 2 orders of magnitude in the Fülcher band and H_α excitations as the fractional dissociation is increased from 0 - 100%. The corresponding dynamic range versus E/N (10-100 Td) is ≈ 4 orders of magnitude. The calculated surfaces have been calibrated to the corresponding TALIF measurements in H_2 discharges which are reported in a companion paper.

*Work Supported by Air Force Office of Scientific Research.

EA 12 Optical and Electrical Investigations on DC-Excited C_2H_2 Plasmas used in Polymerization Processes M. A. ALGATTI, J. M. BARTELEGA, J. C. TEIXEIRA, R. P. MOTA, M.E. KAYAMA and R. Y. HONDA; Unesp-Campus de Guaratinguetá, Depto de Física e Química, 12500-000 Guaratinguetá, SP, Brazil

Plasma Polymerization Processes, obtained from glow discharges in hydrocarbons and organic vapours are extremely important for many current day technological applications. The understanding of the kinetics of these discharges are in the early stage. In fact, much of the experimental and theoretical efforts all around the world are directed to the solutions of the problems related to the controlling of all the relevant parameters of such discharges. We realized the optical and electrical characterization of DC discharges in acetylene using the actinometric optical emission spectroscopy (AOES) and pulsed Langmuir probe technique. The AOES was used to follow the trends of CH and H species in the reactive C_2H_2 -plasma environment for different gas pressures and electrical power coupled to the plasma reactor. Electrical single probe was biased by a pulsed ramp varying from -150 to +150 volts in 1 ms. The results obtained indicated electronic temperatures around 2 eV and densities of the order of 10^8 cm^{-3} . The effects of probe's tip contamination by film deposition was investigated using Ar and N_2 as reference gases. The results indicated a reliable application of the probe during few cycles of the probe's biasing ramp.

EA 13 Interrogation of Surfaces and Films by Resonant Laser Ablation. N. S. Nogar¹, C. G. Gill¹, T. M. Allen², P. B. Kelly², P. H. Hemberger¹ and A. W. Garrett¹, ¹CST1, J565, LANL, ²Dept. of Chem, U. Cal., Davis. We report on the resonant laser ablation (RLA) of copper at low laser fluences ($<100\text{ mJ/cm}^2$). Resonant ablation occurs when the laser is tuned to an n-photon ($1 \leq n \leq 3$) transition for a gas phase atom or molecule.¹ This leads to preferential and increased ionization of the resonant component in the plume. We present an analysis of: bulk copper and copper films; spot size effects; results dependent on surface sample preparation; the effects of beam polarization; and, an accurate measurement of material removal rates. Removal rates range from 10^{-3} to 10^{-2} Å/shot .² Prospects for interrogation of dopants and impurities are evaluated. In addition, we discuss the production of diffraction-like surface features, and the possible participation of non-thermal mechanisms.

1. G. C. Eiden and N. S. Nogar, Chem. Phys. Lett, **226**, 509 (1994)
2. T. M. Allen, P. B. Kelly, J. E. Anderson, T. N. Taylor and N. S. Nogar, Appl. Phys. A, in press.

EA 14 Ultra-Sensitive Absorption Spectroscopy on Ions using UV/VUV Synchrotron Radiation*, K. L. MULLMAN, S. D. BERGESON, & J. E. LAWLER *Univ. of Wisconsin-Madison* - A new absorption experiment utilizing continuum radiation from the Alladin electron storage ring, a 3 m focal length vacuum echelle spectrometer, and a CCD detector array is reported. The extremely high spectral radiance of the storage ring in the UV and VUV provides unique capabilities for both basic atomic spectroscopy and for plasma diagnostic work. The thinned, back illuminated, boron doped (VUV sensitive) CCD array extends the usual signal to noise advantage of a detector array in an absorption experiment to short wavelengths. This experiment achieves both spectroscopic resolving powers of 350,000 and sensitivities to fractional absorptions much smaller than 1% at deep UV and VUV wavelengths. Absorption spectra of Fe^+ in a high current hollow cathode discharge are presented. For a strong line (oscillator strength = 1) an absolute column densities of ions as small as $3 \times 10^8 \text{ cm}^{-2}$ can be measured. This experiment is applicable to many atomic ions in a variety of discharge plasmas.

*Supported by N.A.S.A. & N.S.F.

EA 15 Studies of a Discharge Plasma for Excimer Laser Pumping Using Thomson Scattering Diagnostics and a Computer Simulation, K. UCHINO, H. YAMAKOSHI, K. MURAOKA, M. MAEDA, A. TAKAHASHI and M. KATO, *Kyushu U., Mitsubishi Heavy Industries, Ltd. and Fukuoka U.* - Thomson scattering from plasmas in high-pressure discharges for rare-gas halide excimer laser pumping¹ was observed using a frequency-doubled 300 ps Nd:YAG laser. Detailed temporal changes of the electron density and temperature were measured in Kr/Ne and Kr/F₂/Ne plasmas, and the results were compared with those calculated by a computer simulation,² showing good agreement between them. In particular, electron velocity distribution functions were discussed based on the experimental observations and the simulations.

1 K. Uchino et al., *J. Appl. Phys.* 70, 41 (1991).

2 M. Maeda et al., *Jpn. J. Appl. Phys.* 21, 1161 (1982).

POSTER SESSION EB: MEASUREMENT AND TRANSPORT IN DISCHARGES

Tuesday evening, 10 October 1995

Berkeley Marina Marriott

Belvedere Room, 19:30-21:45

EB 1 Mass Spectrometric Investigation of Positive Ions and Neutrals in SF₆-Ar RF Discharges, R. FOEST, *INP Greifswald, Germany*, J. K. OLTHOFF and R. J. VAN BRUNT, *NIST* - We report experimental results obtained in a GEC Reference cell for rf discharges generated in 1% and 5% mixtures of SF₆ in argon at pressures from 1.3 to 33 Pa and applied rf voltages from 100 to 300 V. Ions and neutrals are sampled from the plasma through a 0.1 mm diameter orifice in the grounded electrode, and are analyzed by mass and energy filters. Relative intensities of neutral species are presented along with the degree of dissociation of SF₆, which is about 0.1 at low power and increases to nearly 0.8 at higher powers. Kinetic energy distributions of ions produced in the plasma are measured at the grounded electrode. Relative ion intensities are obtained by integration of the kinetic energy distribution functions over the energy range. While at low pressures, Ar⁺ is the most abundant positive ion, the ion flux is dominated by SF₂⁺ and SF⁺ at higher pressures. Other significant ions include SF_x⁺ ions (x = 0, 1, 2, 4), F⁺, HF⁺, and oxygen-containing ions, such as SOF⁺ and SOF₃. Preliminary data from discharges in SF₆-O₂ and SF₆-N₂ are also presented.

EB 2 Cross Section for Destruction of H₃⁺ by Collision with H₂ and Ion Kinetics in Hydrogen at High E/N, M.V.V.S. RAO, R.J. VAN BRUNT AND J.K. OLTHOFF, *NIST*, Y. WANG, *Notre Dame Radiation Lab.*, R. L. CHAMPION, *Coll. of William and Mary* - The translational kinetic energy distributions and relative fluxes of H⁺, H₂⁺ and H₃⁺ ions have been measured in a diffuse Townsend discharge characterized by a well defined electric field-to-gas density ratio (E/N) in the range from 0.7×10^{-18} to $20 \times 10^{-18} \text{ Vm}^2$. The results are consistent with theoretical predictions,¹ with the exception that the H₃⁺ energy distributions do not exhibit the predicted high-energy tail, thus suggesting that the cross sections for destruction of H₃⁺ at energies above about 50 eV are higher than assumed in the model.² Measurements of total cross sections for destruction of H₃⁺ in collisions with H₂ were made using an ion-beam apparatus. These results show that in the laboratory energy range from 25 to 300 eV, the H₃⁺ destruction cross section is nearly constant (varying from 2.9×10^{-20} to $3.6 \times 10^{-20} \text{ m}^2$) and more than an order-of-magnitude greater than the total H₃⁺ destruction cross sections² assumed in the model.

¹J. Bretagne, G. Gousset and T. Simko, *J. Phys. D: Appl. Phys.* 27 1866 (1994).

²A.V. Phelps, *J. Phys. Chem. Ref. Data*, 19, 653 (1990)

EB 3 Self Consistent Modeling of pure H₂ Surface-wave discharges, G. Gousset, A. Rousseau, J. Bretagne, *LPGP UPS Orsay, France* - The electron kinetics, described by homogeneous Boltzmann equation, is self-consistently coupled to the kinetics of molecules, H atoms and positive ions. The kinetics of the three types of ions H⁺, H₂⁺ and H₃⁺, is described, in a quasi-neutral theory, by the radial continuity and transport equations. The last problem can be regarded as a transcendental equation for the maintenance hf reduced electric field versus the product of the total neutral concentration times the discharge radius. It is pointed out that the atom and ion kinetics are strongly coupled. Finally, it is also demonstrated that H₃⁺ ions remain the dominant ion species under our experimental pressure conditions (up to 10 torr) however large molecular dissociation degree may be (up to 60% as experimentally observed¹). It is due to the associative ionization² of H(2s) by collision with molecules giving H₃⁺. Consequently, the reduced electric field is predicted decreasing when the dissociation increases, in good agreement with experiments.

¹M Glass-Maujean, *Phys. Rev. Lett.* 62 (1989) 144

²A Rousseau & al. *Phys D: Appl. Phys.* 27 (1994) 2449

EB 4 Ion Energy Distributions in Capacitively Coupled RF Plasma Reactors*, E. KAWAMURA, V. VAHEDI[†], M.A. LIEBERMAN, and C.K. BIRDSALL, *U. C. Berkeley and [†]LLNL* - Drawing on a review of previous works on ion energy distributions (IED) arriving at the target in the collisionless regime, we determine what factors influence the shape of the IEDs. This regime is of great interest to experimentalists and modelers studying the new generation of high density sources in which the sheath is much thinner than in the conventional RIE systems. Having determined the important parameters, we will show some particle-in-cell simulation results of a current driven rf plasma sheath. The results show that for $\tau_{ion}/\tau_{rf} \ll 1$; the sheath is resistive and the IEDs are broad and bimodal with a dominant low energy peak. Here, τ_{ion} is the ion transit-time across the sheath, and τ_{rf} is rf period. As τ_{ion}/τ_{rf} increases, the sheath becomes capacitive, the IED narrows, and the two peaks become more equal in height.

* Work supported by LLNL under U.S. D.O.E. Contract W-7405-ENG-48, U.S. D.O.E. Contract DE-FG03-90ER54079, and in Berkeley, O.N.R. Contract FD-N00014-90-J-1198.

EB 5 Negative Ion Density in Inductively Coupled Chlorine Plasmas,* G. A. HEBNER, Sandia National Laboratories, Albuquerque NM - The negative ion density in radio-frequency (rf) inductively-coupled chlorine discharges has been inferred using laser photodetachment spectroscopy. A Gaseous Electronics Conference (GEC) rf Reference Cell with an inductively coupled plasma source was used to produce the plasma. The chlorine pressure was between 20 and 50 mTorr and the rf power into the plasma was 150 to 250 Watts at 13.56 MHz. Light from a frequency quadrupled Nd:YAG laser was used to photodetach electrons from Cl⁻. The time dependent excess electron density was then detected by a microwave interferometer operating at 80 GHz. Based upon the cross section for photodetachment and the measurement geometry, negative ion densities can be calculated. The inferred negative ion densities are comparable to the steady state electron density over the parameter space investigated. The dependence of the negative ion density on rf power, gas pressure, flow rate and rf phase will be presented.

* This work was supported by the United States Department of Energy and SEMATECH.

EB 6 Effect of Ion-Molecule Reactions on the Measurement of Drift Velocities and Longitudinal Diffusion Coefficients,* J. DE URQUIJO, I. ALVAREZ, C. CISNEROS and H. MARTINEZ, Instituto de Fisica, UNAM, Mexico - We present a method for obtaining the ion drift velocity and the longitudinal diffusion coefficient from the first two moments of the ion flux at the exit of a drift tube¹. Besides drift and diffusion, the presence of primary ion conversion processes is considered. Full expressions for the mean and the variance of the ion arrival-time spectra are obtained. From these, under special experimental conditions, simpler expressions are obtained, from which the determination of the above transport coefficients is straightforward. However, large errors affect these transport coefficients when ion-molecule reactions are important.

* Work supported by DGAPA and Conacyt

¹ E.A. Mason and E.W. McDaniel, "Transport Properties of Ions in Gases", Wiley, N.Y., 1988

EB 7 Ion Energy and Angular Distribution Spectra in Argon Discharges: J. R. WOODWORTH and D. MEISTER, Sandia National Laboratories - In support of the SEMATECH plasma modeling program, we are measuring the energy and angular distribution spectra of ions in argon discharges in a GEC reference cell. Our cell has been modified to produce inductively-coupled discharges at 13.56 MHz. The ion detector, which is based on work at MIT¹, is a gridded energy analyzer and is located below a pinhole in the grounded lower electrode. The ion analyzer can detect both the energy and the angular distribution of the positive ions passing through the pinhole. Initial ion spectra of these discharges show ion energy distributions with a single, relatively narrow peak (FWHM ≤ 4 eV). In 150-watt RF discharges, the peak of the ion distribution moves from 13 to 32 eV as the pressure is reduced from 50 to 2.4 millitorr. Details of the spectra and apparatus will be presented.

This work was supported by the U. S. Department of Energy under contract DE-AC04-94AL85000.

1. Liu et. al., J. Appl. Phys. 68 (8), p. 3916, (1990)

EB 8 Ion Distribution Functions in an Inductively Coupled Plasma*, E.R. KEITER, DAN BEALE, V.L. KOLOBOV, K.M. KRAMER, AND W.N.G. HITCHON, University of Wisconsin Madison. In developing plasma processes, it is important to understand the effect of different process parameters on the distribution functions of ions which are incident on a wafer surface. In this work, two dimensional ion distribution functions are calculated using a kinetic model based on the method described in Hitchon et. al.¹ For lower pressure regimes, fluid techniques become inadequate for tracking ions, making a kinetic technique necessary. This kinetic module is but one component of a multi module hybrid, which also includes modules for calculating electric fields, the electrostatic potential, and the electron energy distribution function (EEDF). The EEDF calculation is based on a non-local approach. A comparison of ion distributions, distributions and how they vary with process parameters such as system geometry, pressure, and coil placement will be presented.

* This work was supported by NSF Grant ECD-8721545.

¹ W. N. G. Hitchon, D. J. Koch and J. B. Adams, J. Comp. Phys., 83, 79 (1989).

EB 9 Ion Flux Measurements in Fluorocarbon Plasmas N. ST.J. BRAITHWAITE* J. P. BOOTH AND G. CUNGE Laboratoire de Spectrométrie Physique, Université de Grenoble I, France - Absolute electrostatic measurements have been made of the ion flux towards both earthed and driven electrodes in an RIE type CF₄ plasma (50-200 mtorr, 30-200W). These results complement earlier LIF studies in which CF and CF₂ concentration profiles were mapped, leading to estimates of the fluxes of these radicals. The ion flux to the powered electrode is a little larger than that to the earthed counter electrode. The flux to the relatively remote sidewalls is considerably less. It is found that ion fluxes decrease as the pressure is raised, particularly at higher power. This is attributed to the influence of negative ions on the boundary physics which influences the rate at which positive ions are ejected from the plasma. Quantitative measurements are consistent with the positive ions being both neutralised and subsequently dislodged from the powered electrode surface which then forms a net source of neutral radicals. Under the conditions prevailing at the earthed surfaces it appears that there is a net accumulation of incident species.

*The Open University, UK.

EB 10 Ion Energy Distributions in Argon and Chlorine ECR Discharges, * S.B. RADOVANOV, G.J. MELDEN, and R.M. FORRISTER, University of New Mexico, Measurements of the energy distributions of ions using the MIT designed¹ retarding grid analyzer have been carried out in pure argon and chlorine ECR discharges, for the range of pressures from 0.13 to 2.6 PA and applied source power from 300 to 1000 W. Downstream measurements were done with and without applied rf-bias power. Significant modulation of the plasma potential is observed in chlorine with applied rf-bias power of 100 W. With increasing source power in argon, broadening of the beam-like ion energy distribution was observed. High resolution and reproducibility was obtained in both gases.

¹ G.W. Gibson, H.H. Sawain, I. Tepermeister, D.E. Ibbotson, and J.T.C. Lee, J. Vac. Sci. Tech. B12(4), 1994.

* Authors wish to acknowledge discussions with K.E. Greenberg

EB 11 Effect of Added H₂ on the Loss Processes of N₂(A³Σ_g⁻).

S. SUZUKI, H. OKUTSUNO, H. ITOH, H. SEKIZAWA and N. IKUTA, Chiba Inst. Tech., Japan. ---The loss processes of N₂(A³Σ_g⁻) were studied from the observation of effective lifetime^{1), 2)} in Townsend discharge. In this study, we investigate the relationship between the second ionization coefficient γ_m by N₂(A³Σ_g⁻) and the starting voltage of self-sustaining discharge V_s of N₂/H₂ mixture gases. The values of V_s were measured in various contents of H₂ in N₂. We presumed that the values of V_s of N₂/H₂ mixture gas would be higher than that of pure N₂ gas, because of the quenching effect of N₂(A³Σ_g⁻) by H₂. The obtained value of the quenching rate coefficient is 2.6×10^{-18} cm³/s. However, the curves of V_s of N₂/H₂ mixture gases decreased lower than that of pure N₂, and shifted to the low pressure side with an increase of H₂ mixture up to 10% H₂. This decrease of V_s by H₂ admixture is not explain only α processes. We measured the value of the current ratio I_m/I¹⁾ meaning the effective coefficient γ_m , and confirmed that the values of I_m/I of N₂/H₂ mixture gas were larger than that of pure N₂. The existence of H₂ seems to be the effect to increase the probability for electron release from the cathode by N₂(A³Σ_g⁻).

¹S. Suzuki, H. Itoh, H. Sekizawa and N. Ikuta: J. Phys. Soc. Jpn., **62**, 2694, 1993.

²S. Suzuki, H. Itoh, N. Ikuta and H. Sekizawa: J. Phys. D (Appl. Phys.), **25**, 1568, 1992.

EB 12 Determination for zero field mobility of O₂⁻ at

atmospheric pressure. K. NORIMOTO, T. HAYASHI and H. ITOH, Chiba Inst. Tech., Japan. ---The negative ion mobilities in O₂ are measured at atmospheric pressure, that is, extremely low E/p₀ condition.

A cascaded gap, which consists of an ion drift gap and an ion detecting gap, is used for this experiment¹⁾. The electrons are emitted from the electrode which is irradiated by pulsed UV light, and that collide with O₂ molecules. Then, negative ions are produced near the electrode. These ion traverse in the uniform electric field. After the flight across the drift space, ions enter the ion detecting gap which is formed with positive point plane electrode, so-called Geiger Counter. The electrons are detached from the negative ions and formed electron avalanche rapidly. Then we can observe burst pulses by oscilloscope and estimate the mobility of negative ions. The reduced zero field mobility of O₂⁻ is 1.99 ± 0.07 (cm²/V·s). This value agreed well with the Snuggs et al²⁾, however that is slightly smaller than the Voshall et al³⁾. While another ion mobility was detected for $1 \leq E/p_0 \leq 4$ (V/cm·Torr) region, that seems O₂⁻.

¹Y. Gosho and A. Harada: J. Phys. D: Appl. Phys., **16**, 1159, 1983.

²R. M. Snuggs et al: Phys. Rev. A, **3**, 477, 1971.

³R. E. Voshall, J. L. Pack and A. V. Phelps: J. Chem. Phys., **43**, 1990, 1965.

WEDNESDAY MORNING

SESSION FA: INDUCTIVELY COUPLED PLASMAS

Wednesday morning, 11 October 1995

Berkeley Marina Marriott

Yerba Buena/Treasure Rooms, 8:00-10:00

Amy Wendt, presiding

8:00

FA 1 Simulation of Chlorine Plasma Flow in a GEC/ICP Source and Comparison with Experiments,* D. ECONOMOU, R. WISE, D. LYMBEROPOULOS, T. BARTEL, and J. JOHANNES, University of Houston and Sandia National Labs - We have performed simulations of chlorine plasma flow in a Gaseous Electronics Conference/Inductively Coupled Plasma (GEC/ICP) source. The simulator is Plasma-DSMC which consists of a fluid description of electrons and particle description of ions and neutrals which are followed by a Direct Simulation Monte Carlo (DSMC) method. Simulations have been performed for 20 mtorr pure chlorine and for different power levels to cover the range of experimental conditions used in a GEC/ICP cell at SNLA¹. Simulation results of electron density as a function of power agree well with the experimental data. Also, a negative ion density comparable to the electron density is predicted, again in agreement with the data. However, the negative ion density is predicted to decrease with increasing power, in contrast to the data. The influence of the wall recombination probability of Cl atoms, the only adjustable parameter in the model, is being examined in an effort to resolve this issue.

* Work supported by NSF and Sandia National Labs under a CRADA with SEMATECH.

¹G. Hebner, private communication.

8:15

FA 2 RF B-Field Effects in ICP's: An Update.* R. H. COHEN AND T. D. ROGNLIEN, *Lawrence Livermore National Laboratory*—We have shown previously¹ that, in an inductively coupled plasma, RF magnetic fields have several significant effects: they change the direction of heating from that of \mathbf{E} to that of $\mathbf{E} \times \mathbf{B}$; they reduce the electron density in the region of the electromagnetic skin fields; and they reduce the heating by the induced electric field. Here we report two new developments: (1) analytic calculation of the electron density reduction (neglecting electrostatic fields) which agrees well (with no adjustable parameters) with orbit-code calculations, and (2), the magnitude and consequences of self-consistent electrostatic potential. On the RF time scale, a fluctuating electrostatic potential sets up to compensate for the aforementioned electron density reduction, maintaining quasineutrality; on a longer timescale, the average of the potential reduces the ion density in the skin region, and from this we obtain the criterion by which we calculate the steady-state quasineutral density profile. We discuss the consequences of these effects for the heating rate, the overall plasma potential and bulk plasma uniformity.

*Performed at LLNL for USDOE under Contract W7405-ENG-48.

¹T.D. Rognlien, R.H. Cohen, et al., *Bull. Am. Phys. Soc.* 39, 1444 (1994).

8:30

FA 3 Comparison of Measured and Simulated Electron Energy Distribution Functions in a Low Pressure Inductively Excited rf Discharge, B. A. COONAN, M. B. HOPKINS and M. M. TURNER, *Dublin City University, Ireland* - We present comparisons between data obtained from a Langmuir probe in a low-pressure inductively coupled rf discharge excited at 13.56 MHz and simulations carried out using an electromagnetic particle in cell simulation with Monte Carlo collisions. Langmuir probe measurements have been made with a plane probe that allows the anisotropy of the electron energy distribution function to be determined. The data show that such anisotropy does exist at low pressure, and is in reasonably good agreement with the simulation predictions.

8:45

FA 4 On the E-H mode transition in inductively coupled RF discharges, U. KORTSHAGEN, N. D. GIBSON and J. E. LAWLER, University of Wisconsin-Madison - In inductively coupled RF plasmas a mode transition between a low power-low density (E-)mode and a high power-high density (H-)mode has been frequently observed. In present experiments on an argon ICP an abrupt increase in the luminosity of almost 2 orders of magnitude with a simultaneously decreasing RF current has been measured during the E-H transition. Furthermore, a hysteresis has been found for the reverse H to E transition. The experimental results are interpreted on the basis of a simple discharge model. The discontinuous character of the E-H transition can be related to an increasing efficiency of the inductive coupling with increasing plasma density. The observed hysteresis may be caused by multistep ionization processes.

9:00

FA 5 Electromagnetic Fields in a Planar Radio-Frequency Inductively Coupled Argon Discharge,* J. A. MEYER, R. MAU and A. E. WENDT, U. of Wisconsin - Madison. -

The results of electromagnetic field studies in a planar radio-frequency (13.56 MHz) inductively coupled plasma source will be reported. The spatial distribution of the fields in an Ar plasma was measured using inductive loop probes oriented to measure the time derivative of the axial and radial components of the magnetic field (\dot{B}_z and \dot{B}_r , respectively). The measurements of \dot{B}_z were used to calculate the azimuthal component of the rf electric field (E_ϕ) directly from Faraday's law. Simultaneous measurements of \dot{B}_r and \dot{B}_z allow estimation of the local permittivity of the plasma (ϵ). Plasma density profiles calculated using a local relation between ϵ and density compare favorably with Langmuir probe measurements of the density taken earlier in the same system. Other parameters such as azimuthal current density and drift velocity were also determined from the fields.

* Work supported by Lam Research Corporation and NSF Grant EEC-8721545.

9:15

FA 6 The Mechanism of Electron Heating and EDF Formation in ICP in a Free-Flight Regime *, V.I.KOLOBOV

G.J. PARKER and W.N.G. HITCHON, U. of Wisconsin - Madison and LLNL - In Ref.1; the mechanism of electron heating and formation of the electron distribution function (EDF) has been studied in a low-pressure inductively coupled plasma (ICP) using a "Convected Scheme" (CS) method and using a nonlocal approach in a collisional regime when Ohmic heating predominates. Here, we employ these two methods to examine a free-flight regime when noncollisional heating predominates and include the influence of the RF magnetic field on electron motion. We consider an Argon discharge in a cylindrical tube with an external coil. We will show i) heating rates P_{ohmic}/P_{total} as frequency and neutral pressure are varied, ii) the effect of the RF magnetic field on the heating rate/process, and iii) comparison between the CS and the nonlocal approach.

* Work supported in part by the Intel Corp., Plasma ERC by NSF Grant ECD-8721545, and Lawrence Livermore National Laboratory.

¹ V.I.Kolobov, G.J.Parker and W.N.G.Hitchon, submitted to *Phys. Rev. E* (1995)

9:30

FA 7 Plasma Potential in Capacitatively and Inductively Coupled Low Pressure Discharges. F. A. HAAS, S. YANG and N. St. J. BRAITHWAITE, The Open University, Oxford Research Unit, Oxford, U.K. - Plasmas generated in Argon at low pressure (100 m torr) in a glass cylinder by a concentrically wound induction coil, are investigated both experimentally and theoretically. Plasma potentials measured in the capacitive and inductive modes show a marked difference. At low powers (~100 W) the capacitive mode shows a potential which falls over 80% of the radius and then rises sharply at the wall. Increase of power up to 300 W leads to the inductive mode in which the plasma potential falls smoothly in both the radial and axial directions. A theoretical analysis based on the Maxwell and collisional two-fluid equations shows, that in the presence of a plasma source, the potential surfaces are 'ellipsoidal' with a maximum at the origin, as indicated by experiment. Using this theory to model the central regions of the capacitive mode, it is shown that in the outer regions the electrons are in equilibrium through the interaction of ponderomotive, inertial and space charges forces. At low collisionality this leads to a rising potential at the wall.

9:45

FA 8 An Experimental Study of an RFI discharge using Laser Scattering Techniques. M.D. BOWDEN, T. HORI, K. UCHINO, K. MURAOKA, M. MAEDA, Kyushu University - A combination of laser Thomson and Rayleigh scattering was used to study the electron and neutral properties of an argon radio-frequency inductively-coupled discharge. Electron temperature T_e , electron density N_e and neutral density N_0 were measured for different discharge conditions. Spatial distributions of these properties were also measured. The results indicated that T_e was spatially uniform and N_e was always peaked in the plasma center. The electron energy distribution function was measured carefully to determine any deviations from a Maxwellian distribution. In high pressure or high power discharges, the neutral density was significantly depleted in the plasma center, and this depletion can be explained to be as a result of heating of the background neutral gas atoms by electron-neutral collisions.

SESSION FB: ION MOLECULE PROCESSES

Wednesday morning, 11 October 1995

Berkeley Marina Marriott

Belvedere Room, 8:00-10:00

Mark Kushner, presiding

Invited Papers

8:00

FB 1 Ion-Molecule Reactions in Subthermal Conditions. B.R. ROWE, D. P. A. M., URA 1203 du CNRS, Université de Rennes 1, FRANCE - Much of the Universe consists of plasmas and, amongst them, those at low or ultralow temperatures (planetary ionospheres, comets, interstellar clouds) exhibit a rich ionic chemistry leading to the formation of complex (and often organic) molecules. Of particular interest is the ion-molecule chemistry of dense interstellar clouds, the cradle of stars and planets, where the temperature can be as low as 10 K. Due to the need of reliable laboratory data below 80 K several groups have developed within the last twelve years independent methods for the study of ion-molecule reactions in the 0-80 K range [1]. The aim of this lecture is to review the methods and the main results such as the important role of rotational and spin-orbit states on ion reactivity. Expansion methods are emphasized since they allow

one to work with highly condensable species at ultralow temperatures.

[1] M.A. Smith, in "Unimolecular and bimolecular ion-molecule reaction dynamics" eds L.Y. Ng, T. Baer and I. Powis, Wiley 1994, p.184.

8:30

FB 2 Investigations of Ion-Molecule Reactions in rf glow and dc Townsend Discharges. J. K. OLTHOFF, NIST - Ion bombardment of surfaces exposed to electrical discharges plays a critical role in the reactive-ion etching of semiconductor materials. A knowledge of the identities, relative intensities, and energies of the bombarding ions is essential for a fuller understanding of the etching process, and for validation of theoretical modeling results. In this talk we present mass spectrometric and ion energy data for ions sampled from rf discharges in a variety of gases and mixtures, such as Ar, O₂, H₂, SF₆, and Ar/H₂. Analysis of these data supplies, and sometimes requires, information about the transport of ions across the rf sheath, including dominant ion-molecule interactions. Often these reactions, and their role in rf plasmas, are more easily understood when investigated using simpler discharges, such as diffuse, dc Townsend discharges. Ion energy data from dc discharges in gases, such as Ar and H₂, will be shown that provide information about equilibrium conditions for ion transport and the role of charge-exchange collisions in determining ion energies.

Contributed Papers

9:00

FB 3 Nitric-Oxide Emission Spectra Arising from the Ar⁺ + NO reaction*. T. GOUGOUSI, M.F. GOLDE, and R. JOHNSEN, U. of Pittsburgh - Initially rather puzzling observations of a slow plasma decay and molecular NO emissions in recombining NO⁺ flowing afterglows motivated us to investigate the kinetic processes in some detail. On closer examination it appears that the spectra, principally the β bands, are produced by a secondary ion-molecule reaction of the NO⁺ ($a^3\Sigma^+$) metastable ion with NO, where the NO⁺(a) ion is the direct product of the Ar⁺ + NO reaction. The rather slow observed recombination of the plasma is likely to be due to the back reaction of NO⁺(a) with Ar which produces non-recombining Ar⁺ ions. The reaction scheme as such is known from earlier work¹, but it appears that both the spectral assignments and the mechanism for production of the emission in other recently published work should be revised on the basis of our measurements.

Our observations point out the subtle interactions between ion chemistry and recombination which must be understood before meaningful inferences can be drawn from afterglow measurements.

*This work was, in part, supported by NASA

9:15

FB 4 Charge Transfer and Decomposition Cross Sections for Collisions of H₃⁺ on H₂ and Rare Gas Targets.* B. L. Peko and R.L. Champion, The College of William and Mary, and Yicheng Wang, Notre Dame Radiation Lab. - Absolute total cross sections for collision-induced destruction (CID) have been measured for binary collisions of H₃⁺ with H₂ and rare gas targets for laboratory energies ranging from about 20 up to 500 eV. The cross sections which lead to fast H₂⁺ and H as products are found to be larger than the early measurements of Lange et al.¹ above 100 eV by almost one order of magnitude for H₂ targets. This destruction channel is also found to be larger than believed for Ar targets. These new results may explain the discrepancy between the measured kinetic energy distributions of H₃⁺ from a Townsend H₂ discharge² and the calculated distributions based on the early reported cross sections. They also suggest that CID of H₃⁺ is possibly a leading mechanism for fast neutral H production in Ar-H₂

WEDNESDAY MORNING

rf discharges.

*Supported in part by the U.S. DOE, Division of Chemical Sciences, Office of Basic Energy Sciences

¹ G. Lange, B. Huber, and K. Wiesmann, *Zeit. Fur Physik A281*, 21 (1977).

² M. Rao, R. Van Brunt, and J. Olthoff, 1995 Int'l. Swarm Symp.

9:30

FB 5 Electron Capture in Collisions of H⁺ Ions with C, N, and O Atoms below 100 eV. * M. KIMURA, Argonne National Laboratory, Argonne, IL 60439, J. P. GU, G. HIRSCH, and R. J. BUENKER, Universität Wuppertal, Germany--Electron capture in collisions of H⁺ with C, N, and O atoms was studied on the basis of a molecular representation below 100 eV. For all systems, the effect of metastable states of the atoms on electron capture was studied in addition to capture from the ground state. Capture cross sections were found to be large, 3×10^{-16} cm², 8×10^{-16} cm², and 5×10^{-15} cm² for C, N, and O atoms, respectively, at 80 eV.

*Supported in part by the U.S. Department of Energy, Office of Energy Research, Office of Health and Environmental Research, under Contract W-31-109-ENG-38 (MK).

9:45

FB 6 Dissociative Recombination Studies of Ar₂⁺ G. B. RAMOS, M. SCHLAMKOWITZ, J. SHELDON, K. HARDY Fla. Int'l U., J.R. PETERSON, SRI - From time-of-flight spectra of metastable Ar⁺ atoms emerging from sustained discharges in Ar, we observe discrete non-thermal peaks due to excited products of dissociative recombination (DR) of Ar₂⁺ formed by reactions in the discharge. From the peak velocities, the DR product states are uniquely determined, regardless of subsequent radiation. Most of the excited DR products are (n+1)s states, but Ar₂⁺ also yields smaller amounts of 4p and 3d states. We have also found in studies of Ne₂⁺ and Ar₂⁺ DR a substantial but undetermined fraction of reactions go to a purely ground state channel. We have found that under certain conditions in Ar discharges, the relative amount of the higher excited state products, including 4p,3d,5s and 5p can be dramatically influenced. The velocity peaks also become narrower than expected from the thermal distribution of the parent Ar₂⁺ as the energy level in the product atom increases.

Work supported in part by AFOSR grant F49620-93-1-0159DEF

SESSION GA: INNOVATIVE LIGHTING

Wednesday morning, 11 October 1995

Berkeley Marina Marriott

Yerba Buena/Treasure Rooms, 10:15-11:45

J. Lapatovich, presiding

Invited Paper

10:15

GA 1 Challenges in Increasing Efficacy of Fluorescent Lamps for Avionics

R. HALE, LCD Lighting

10:45

GA 2

Abstract not available

11:15

GA 3

Abstract not available

SESSION GB: ELECTRON-HYDROCARBON COLLISIONS

Wednesday morning, 11 October 1995

Berkeley Marina Marriott

Belvedere Room, 10:15-11:30

Jim Olthoff, presiding

Invited Paper

10:15

GB 1 The Lowest Resonance of Hydrocarbons and the Virtual π^* -Valence Orbital as seen by Electron Collisions. L. BOESTEN, H. TANAKA, M. YURI, Sophia U. Tokyo, and M. A. DILLON, Argonne National Laboratory - In the past years we have measured the elastic and vibrational differential cross sections of many hydrocarbon molecules and their isomers in the energy range from 1.5-100 eV, 15°-130°. We have obtained the lowest three virtual orbitals from a GAUSSIAN-92 calculation and determined the fundamental vibrational modes which can be enhanced by an electron trapped temporarily in these orbitals. A comparison of the observed angular behavior with predictions of angular correlation theory¹ then allows to establish the symmetry species of the temporary negative ion and thus the virtual orbital involved. A nearly unique relation was found between the presence of a low impact energy resonance near 2-3 eV and the presence

of an antibonding π^* -LUMO, not only for hydrocarbons but also for other molecules. For some molecules "pseudo π^* -orbitals" may be involved.

¹D. Andrick and F. H. Read, J. Phys. B 4 389 (1971)

*Supported by the U.S. Dpt. of Energy, Office of Energy Research, Office of Health and Environmental Research, under Contract W-31-ENG-38 and by Grant in Aid from the Ministry of Education, Science, and Culture, Japan.

Contributed Paper

10:45

GB 2 Low Energy Electron Scattering from Methyl and Ethylchloride,* P.D. BURROW, V.K. CHAN, X. SHI, and G.A. GALLUP, U. of Nebraska, Lincoln-Absolute differential cross sections for elastic scattering and vibrational excitation by electron impact are reported for scattering angles of 30° and 100°, at energies below 10 eV. Energy loss measurements are taken at several selected impact energies, and the role of temporary negative ion states on excitation of the various vibrational modes is explored. Angular distributions of the scattered electrons exciting certain of the vibrational modes at the resonance peaks are also reported. Using the mixed semi-empirical-*ab initio* model of Gallup¹, the relative strengths of the vibrational energy loss peaks in methylchloride are recomputed and compared with experiment.

*Supported by the National Science Foundation.

¹G.A. Gallup, J. Phys. B: At. Mol. Phys. 26, 759 (1993).

Invited Paper

11:00

GB 3 Theoretical Study of Low-Energy Electron-Molecule Collisions, W. M. HUO, NASA Ames Research Center - Polarized studies of electron collisions with carbon tetrafluoride and beryllium carbonyl are reported. In the e-CF₄ study, the resonance structure between 8-9 eV is shown to be a superposition of the T₂- and A₁-symmetry shape resonances. The unequivocal assignment of this feature as a double-resonance structure clarifies certain discrepancies in previous attempts to ascribe the 8-9 eV feature to a shape resonance in one or another partial channel and explains the sensitivities found in the fragment ion production in the resonance region. The Be-CO system is chosen as a prototypical example of an adsorbate-substrate interaction. To understand how bonding with the substrate affects the CO resonance, electron collision with two states of BeCO are studied, one with a very weak van der Waals bond and the other with a normal chemical bond. It is shown that the nature of the Be-CO bond has strong effects on the cross section feature.

SESSION HA: PLASMA-SURFACE INTERACTIONS

Wednesday afternoon, 11 October 1995

Berkeley Marina Marriott

Yerba Buena/Treasure, 13:30-15:30

Roy Champion, presiding

Invited Paper

13:30

HA 1 Fundamental Studies of Low Energy Sputtering*, W. G. GRAHAM, The Queen's University of Belfast, Northern Ireland. The interaction of the plasma with surrounding surfaces is important in virtually all laboratory plasmas ranging from high-temperature nuclear fusion plasmas to the low temperature plasmas used in processes such as reactive ion etching of microelectronics circuits. Identifying specific plasma-surface interactions in the

complex plasma environment is almost impossible. Here the energy distributions of sputtered atoms and ions produced by few hundred to few thousand eV ion bombardment of polycrystalline and crystalline targets have been measured. The incident ions used were chosen to be typical of those found in particular discharges and to provide a contrast between atomic and molecular and inert and chemically active species. A multiphoton ionisation technique is used in the detection of the predominant neutral species. The energy distributions of the sputtered atoms are found to be different than those of the ions. Both can be complex and sensitive to the specific bombarding species. An insight into the particular sputtering mechanisms is provided by comparing the measured energy distributions with the predictions of various theoretical models.

*Work supported by the UK Science and Engineering Research Council.

Contributed Paper

14:00

HA 2 Secondary Electron and Anion Emission from Oxidized Surfaces at Low Impact Energies* J. C. Tucek, S. G. Walton, and R. L. Champion, College of William and Mary. Absolute yields for secondary electrons and anions due to collisions of positive alkali ions with metallic surfaces having a controlled exposure to oxygen have been measured for impact energies $E < 400$ eV. Electron and anion yields, $Y_e(E)$ and $Y_i(E)$, exhibit energetic thresholds at impact energies ≈ 50 eV and behave similarly as the impact energy, the surface work function, and the oxygen coverage are varied. A model is proposed to describe the O⁻ sputtering, the dominant sputtered negative ion observed, and it is suggested that anion sputtering serves as a precursor for secondary electron emission. The possible role of surface generated secondary electrons and anions in a discharge will be discussed.

*Supported in part by the U. S. DOE, Division of Chemical Sciences, Office of Basic Energy Sciences.

Invited Paper

14:15

HA 3 Low-Energy Ar Ion-Induced and Chlorine Ion Etching of Silicon,* A. V. HAMZA, M. MOALEM, WEI-E WANG, and M. BALOOCH, UC-LLNL - A nearly monoenergetic beam of argon and chlorine ions with kinetic energy from 40 to 900 eV and intensity up to 30 $\mu\text{A}/\text{cm}^2$ is used to study the etching of Si. The etch rate and ion current density at the surface are simultaneously measured to obtain the etch yield. The ratio of atomic chlorine (Cl⁺) to molecular chlorine (Cl₂⁺) ions striking the surface is measured by a quadrupole mass spectrometer. In the absence of any chlorine, the Ar ion sputtering of silicon at 120 eV is about 0.05 silicon atoms removed per ion and monotonically increases to 1 silicon atom per ion at 800 eV. The Ar⁺-induced etch yield increases by about an order of magnitude when the surface is simultaneously exposed to a neutral molecular chlorine flux sufficient to produce saturation coverages from the effusive doser. An etch yield of 0.13 silicon atoms removed per incident Ar ion is measured at an Ar⁺ energy of 50 eV, which also monotonically increases to 4 silicon atoms removed per incident argon ion at 700 eV. The etch yield further increases, by approximately a factor of 20%, as the surface is bombarded with energetic chlorine ions. The etch yield with energetic chlorine ions increases from 0.7 to ~ 5 silicon atoms per incident ion with increasing kinetic energy from 40 to 900 eV.

*Support by USDOE at LLNL under contract No. W-7405-ENG-48.

Contributed Papers

14:45

HA 4 Molecular Dynamics Simulations of Molecular Ion-Assisted Etching M.E. Barone, and D. B. Graves, Department of Chemical Engineering, U.C. Berkeley

A key issue in plasma processing is the role played by reactive, molecular ions. We examine the dynamics of molecular

WEDNESDAY AFTERNOON

ion-surface interactions at relatively low impact energies (10 eV - 200 eV) using molecular dynamics (MD) simulations. In this talk, we summarize comparisons between molecular chlorine and atomic chlorine ions sputtering silicon. We examine etch yields (silicon removed per incident ion), dependence of etch yields on ion energy, and etch mechanisms. The fraction of molecular ions that dissociate upon impact as a function of impact energy and surface Cl content is reported. The etch yield of a molecular ion can be expressed in terms of the sputtering yields of its constituent atoms. How this expression depends on the details of dissociation upon impact of the target surface is explored. The simulation predictions are compared to experiment. Video illustrations will be presented to allow visualization of the underlying atomistic mechanisms of ion-assisted etching using molecular ions versus atomic ions.

15:00

HA 5 MODELING OF PROFILE EVOLUTION DURING ETCHING OF SILICON, G. S. Hwang and K. P. Giapis, California Institute of Technology — The Monte-Carlo method is used to model the profile evolution of trenches etched in silicon by hyperthermal neutral fluorine beams. The simulation includes a phenomenological description of the inelastic and reactive scattering dynamics of the interaction, based on detailed experimental measurements of angular and velocity distributions of the scattered products. The model captures the mechanical energy transfer in fluorine-SiF_x layer collisions as well as the competition between thermal and direct reaction mechanisms. Impulsive scattering of unreacted fluorine atoms is shown to be mainly responsible for microtrenching and inverse microloading, in addition to the substantial undercutting, all of which are seen and documented experimentally. Furthermore, the model is used to predict the effects of the incident energy and flux of the bombarding radicals; angular distributions, similar to those expected for ions leaving the plasma sheath in typical RIE conditions, are also investigated.

15:15

HA 6 Atomic Layer Etching (ALET) of Silicon, DEMETRE ECONOMOU AND SATISH ATHAVALE, University of Houston - Materials processing with atomic layer (~ 1 Å) precision is vital in a number of emerging technologies such as nanoelectronics. ALET is a cyclic process that is composed of four steps: (1) exposure of a clean crystal to a gas, so that a monolayer of the gas is chemisorbed on the surface, (2) evacuation of the excess gas, (3) exposure of the crystal to an energetic beam (electrons, ions, photons) to effect chemical reaction between the adsorbed gas and the solid, and (4) evacuation of the reaction products. Although ALET of GaAs has met with success, that of silicon is still an illusive goal. We have studied ALET of silicon using chlorine as the reactive gas in step (1) and low energy (< 50 eV) argon ions in step (3). The substrate is a short distance from a helical resonator high density plasma source. The ion energy is controlled with a RF bias applied to the substrate. Two system configurations have been examined: (a) the argon plasma is switched on continuously, but the substrate is RF biased only during step (3), and (b) the plasma and the RF bias are switched on simultaneously but only during step (3). The etch rate of silicon per ALET cycle has been studied as a function of the ion flux and energy, and the exposure time of the crystal to chlorine during step (1). Conditions for self-limiting etching with atomic layer precision will also be discussed.

SESSION HB: DATA NEEDS IN PLASMA MODELING

Wednesday afternoon, 11 October 1995

Berkeley Marina Marriott

Belvedere Room, 13:30-15:30

Tom Rescigno, presiding

Invited Papers

13:30

HB 1 Data Needs in Plasma Process Modeling: Electron Collisions, JEAN W. GALLAGHER, NIST - Electron collision cross sections are a major component of the comprehensive set of fundamental data required to model deposition and etching plasmas. Cross sections for electron collisions with plasma constituents and their products determine densities of radicals, positive and negative ions and free electrons. Specific cross sections for a number of processes including ionization to molecular parent ion, dissociative ionization, neutral dissociation, and attachment are particularly important. Internal excitation of the target may significantly affect the cross section magnitude. When considering the full chemistry of a deposition or etch plasma system, a long list of important compounds can be compiled. The definitive goal would be a database containing electron-impact cross sections for all collision channels for all compounds and potential products over an appropriate energy (temperature) range. Available data for pertinent gas-phase species are summarized. In many cases, particularly for corrosive species and radicals, data of appropriate accuracy are missing. A variety of approaches are recommended to expand the existing database.

14:00

HB 2 Ion and Neutral Chemistry Databases for Plasma Processing: Current Status and Future Needs* MARK J. KUSHNER, University of Illinois, Dept. of Elect. and Comp. Engr., Urbana, IL 61801 USA -The application of plasma equipment models for etching and deposition to industrially relevant problems is often limited by the availability of fundamental data. In this talk the current status and future needs of databases for ion and neutral chemistry will be discussed. The ion chemistry database is subdivided into: momentum transfer, ion-molecule charge exchange, ion-ion neutralization, electron-ion recombination, and ion-neutral/neutral-neutral excitation. Although measurements have been made specifically for plasma processing, the ion chemistry database was largely generated for atmospheric chemistry and lasers. The largest gaps in the database are for radical ions and branching ratios. Existing experimental techniques can address most of these needs. The neutral chemistry database is more complete for deposition compared to etching systems. The largest gaps are in hot atom chemistry and reactions for species having internal energy. Needs in the neutral chemistry database may be addressed by a combination of computations and benchmark experiments.

* Work supported by NSF, SRC, Sandia/Sematech, and the U. of Wisconsin ERC for Plasma Aided Manufacturing.

Contributed Papers

14:30

HB 3 Lifetime and excitation mechanisms of the $^2G_{9/2}$, Ar^+ metastable ions used for the ivdf measurements in plasmas, F. CHATAIN, J. DEROUARD and N. SADEGHI, Labo. de Spectrométrie Physique, Université J. Fourier Grenoble I, FRANCE--Doppler shifted laser induced fluorescence on $3d^2G_{9/2}$ argon metastable ions has been previously used to map out the 3D, ion velocity distribution function (ivdf) in ECR and Helicon reactors [1,2]. The aim of this work is to show that the observed ivdf corresponds actually to the ivdf of the ground state argon ions. The decay behaviour of n_e , $Ar^+(^3P_2)$ metastable atom and $Ar^{+*}(^2G_{9/2})$ metastable ion densities and emission intensities of Ar and Ar^+ lines in the afterglow of a high density pulsed plasma ($p \sim 1$

μbar ; $n_e \sim 10^{12} \text{ cm}^{-3}$), of a Helicon source has been analyzed. The radiative lifetime of the $\text{Ar}^{+*}(^2G_{9/2})$ was found to be $8.5 \pm 1 \mu\text{s}$. This lifetime is reduced by electron collision, $k = 2.7 \pm 0.3 \cdot 10^{-8} \text{ cm}^3 \text{ s}^{-1}$. Data shows that in the early afterglow the radiative Ar^+ levels are mainly populated by electronic excitation from the Ar^+ metastable states. The remarkably short lifetime of the $^2G_{9/2}$ state and its efficient coupling with the other short lived excited states of Ar^+ , by electron impact, suggests that over a cm scale, its vdf corresponds to that of the ground state ions.

[1] N. SADEGHI et al., J. Appl. Phys. 70, 2552 (1991).

[2] T. NAKANO et al., J. Vac. Sci. and Technol. B11, 2046 (1993).

14:45

HB 4 Role of Water in Non-thermal Plasma Destruction of Volatile Organic Compounds,* DAVID S. GREEN, L. WAYNE SIECK, JEFFREY W. HUDGENS and JOHN T. HERRON, National Institute of Standards and Technology — Chemical mechanisms governing the degradation of toluene (T) in humid air and nitrogen plasmas have been investigated both experimentally and theoretically. High-pressure pulsed electron-beam mass spectrometry confirms the role of water in ion-neutral interactions that govern the terminal ion distribution. Mass spectra reveal the rise and fall in species' concentration including those of T^+ , TH^+ , NO^+ and clusters $\text{H}_3\text{O}^+(\text{H}_2\text{O})_n$. *In situ* laser diagnostics of corona and microwave discharges have profiled the temperature and concentration of neutral radicals. These experiments probe the behavior of OH, the primary radical in toluene destruction. Experimental results validate a computational model, consisting of a select set of ion and neutral kinetics, which predicts the temporal evolution in concentration of radical and ion species.

*Work supported in part by the Strategic Environmental Research and Development Program (SERDP).

15:00

HB 5 Electron-Impact Ionization of SD_x ($x=1-3$) Free Radicals*, V. TARNOVSKY, A. LEVIN, K. BECKER, City College of C.U.N.Y., and H. DEUTSCH, Universität Greifswald, Germany — The ionization of the hydrogen-containing free radicals SiH_3 , SiH_2 , and SiH plays an important role in the silane plasma chemistry and a knowledge of the absolute partial ionization cross sections is crucial for quantitative plasma diagnostics. We used the fast-beam technique to measure absolute partial cross sections for the ionization and dissociative ionization of the SiD_x ($x=1-3$) free radicals from threshold to 200 eV. Since ionization cross sections are insensitive to isotope effects, we used the deuterated species because it allows a more complete separation of the various product ions for a given parent [1]. The partial cross sections were combined for each target to yield the total single ionization cross section which is compared to the results of calculations based on a modified additivity rule.

1. V. Tarnovsky et al., J. Phys. B, to be published

*Work supported in part by the U.S. Department of Energy (DOE) and by the National Aeronautics and Space Administration (NASA).

15:15

HB 6 Radiative Transition Probabilities for Carbon, Nitrogen and Oxygen Spectra, W. L. WIESE, T. M. DETERS, J. R. FUHR, J. MUSIELOK, and G. VERES, National Institute of Standards and Technology, Gaithersburg, MD — For the modeling and diagnostics of thermal discharges the atomic radiation data of carbon, nitrogen and oxygen are important. We have produced a new comprehensive table of radiative transition probabilities for C, N, and O, and have also carried out supporting measurements. We have critically compiled data for about 13,000 spectral lines, based on all available theoretical and experimental literature sources. All stages of ionization are covered, and the largest tables are usually those for the neutral atoms and singly charged ions. The spectral lines in the tables are arranged in multiplets. For each line the transition probability, the wavelength, statistical weights and the pertinent energy levels are given. In addition, the estimated

uncertainty and the data source are indicated. In support of this tabulation work we have measured numerous relative transition probabilities for prominent lines of selected C, N, and O spectra, using a high current wall-stabilized arc at atmospheric pressure. We found that p-d multiplets show considerable departures from LS coupling while lines in s-p multiplets adhere quite well to this coupling scheme. For N II, intersystem lines are relatively strong because of an accidental near-coincidence of triplet and singlet levels of the 3p configuration. All measured data have been incorporated into these new tables.

POSTER SESSION IA: PLASMA-SURFACE INTERACTIONS

Wednesday afternoon, 11 October 1995

Berkeley Marina Marriott

Belevedere/Angel Rooms, 16:15–18:00

IA 1 Simulations of Ions Impacting Si Surfaces: Effect of Incident Angle and Surface Coverage on Sputtering Yields, B.A. HELMER, D.B. GRAVES, and M.E. BARONE, University of California, Berkeley, CA — A very important parameter in plasma etching of submicron features for microelectronics applications is the ion impact angle dependence of etch yield. It is well known that physical sputtering yields show a maximum at impact angles of about 60° from the surface normal. However, there is experimental evidence that this angular dependence is reduced when reactive gases are present during sputtering.¹ We have examined this issue using classical molecular dynamics simulations of Ar^+ and Si^+ impacts onto silicon surfaces with varying amounts of fluorine on the surface and in the near-surface region. We varied ion impact energies from 1 to 50 eV and incident angles from 0° to 75° from the surface normal. For example, we observed the expected maximum sputtering yield near 60° for 50 eV Si^+ impacts onto an amorphous Si surface. For a Si surface with roughly 2 monolayers of F present, however, the impact angle has little effect on the Si sputtering yield. Implications for ion-assisted etching are discussed.

¹ H.F. Winters, J.W. Coburn, and T.J. Chuang, J. Vac. Sci. Technol. B1 469 (1983).

IA 2 Determination of Surface Recombination Probabilities of Radicals by Time-resolved Mass Spectrometry in $\text{H}_2\text{-CH}_4\text{-SiH}_4$ RF Discharges, P. KAE-NUNE, J. PERRIN, O. LEROY and J. JOLLY, Laboratoire PRIAM, ONERA/CNRS, Fort de Palaiseau, 91120 PALAISEAU, FRANCE — Threshold ionization mass spectrometry has been used to detect radicals in $\text{H}_2/\text{CH}_4/\text{SiH}_4$ RF discharges.¹ In the present work, this technique is applied to time-resolved measurements of the density of radicals in the vicinity of a heated electrode of a PECVD reactor, which enables the determination of the surface loss coefficient β of different radicals on different materials (H atoms on stainless steel, a-Si:H and SiO_2 , SiH_3 on a-Si:H and CH_3 on a-C:H). Time-resolved measurements are performed by using a pulsed RF plasma. The decay rate of the radical is recorded with a multichannel scaler connected to the output of the mass spectrometer and triggered synchronously with the plasma. When the plasma is turned off the decay rate of the radical results from diffusion (including the surface loss coefficient β , according to the Chantry's theory²) and may involve the mutual recombination of the radical (with a kinetic reaction rate constant k), which plays an important role for radicals like CH_3 . A 1D-modeling has been developed, in which a fourth order Runge-Kutta method is used to describe the temporal evolution of the radical density. The model takes into account the diffusion and the mutual recombination of the radical in the bulk of the plasma, and the surface loss coefficient on the electrodes. The β and k values are then deduced by fitting the experimental results.

¹ P. Kae-Nune, J. Perrin, J. Guillon and J. Jolly, Plasma Sources Science & Technol. 4, 1 (1995)

² P. J. Chantry, J. Appl. Phys. 62, 1141 (1987)

IA 3 Plasma-Electrode Interaction in Noble Gas Atmosphere*, J. SCHEIN, M. SCHUMANN, J. MENDEL, Ruhr-Universität Bochum, AEEO, Germany — For the investigation of arc spot ignition an arc is produced in a vacuum chamber filled with noble gas of high purity at atmospheric pressure. Perpendicular to the arc axis an electrode is positioned switched cathodically. The arc spot ignition on this cold cathodes is investigated by electrical and optical methods. Combining these methods it could be proved that there are different forms of arc spot ignition on cold cathodes: on the one hand an ignition initiated by a small precurrent and on the other hand a kind of breakdown without measurable indications before. These two kinds of

WEDNESDAY AFTERNOON

ignition can be associated to characteristic high-speed photographs. The first kind of ignition is always accompanied by the formation of a luminous layer on the cathode surface in combination with a channel connecting the bulk plasma and the electrode whereas in the second case only a plasma ball in front of the electrode surface can be seen. Preparing the electrode surface by mechanical polishing the first kind of ignition is dominant whereas when preparing by arcing the breakdown is observed. Thereby the high influence of the surface structure becomes obvious. Results of the electrical measurements for different materials will be presented supplemented by emission spectroscopy, high-speed photography and pictures of the surface structures.

* Work supported by DFG-SFB 191/A3.

POSTER SESSION IB: INDUCTIVELY COUPLED PLASMAS

Wednesday afternoon, 11 October 1995

Berkeley Marina Marriott

Belvedere/Angel Rooms, 16:15-18:00

IB 1 A Transformer Model of Electronegative Planar Inductive Discharges, J. T. GUDMUNDSSON, Department of Nuclear Engineering, and M. A. LIEBERMAN, Department of Electrical Engineering and Computer Sciences, University of California, Berkeley.

A planar inductive radio frequency discharge is driven by an r.f. supply through a lumped element matching network. The discharge is modeled as a non-ideal transformer where the inductive coil is taken as the primary circuit, the plasma is taken as the secondary circuit, and a capacitive coupling exists between the primary and secondary circuits. The mutual inductance between the primary and secondary circuits, the geometric self inductance of the secondary circuit, the resistance and inductance of the plasma, and the capacitive coupling are related to the plasma parameters. The model is solved along with the particle and energy balance relations in an electronegative plasma to determine the equilibrium and time-varying behavior of the discharge. The impedance seen in the primary coil due to plasma loading is related to the plasma parameters. The model is compared to measured (electropositive) Ar plasma properties and to measured electronegative plasmas such as O_2 , SF_6 , and SF_6/Ar .

Work supported by LLNL/PPRI Grant CP94-06/B283626, Lam Research Corporation, NSF Grant ECS-9217500, and DOE Grant DE-FG03-87ER13727.

IB 2 On the radial variation of sheath potentials and charged particle currents in planar inductively coupled plasmas, U. KORTSHAGEN, University of Wisconsin-Madison, G. MÜMKEN, Ruhr-Universität Bochum, Germany — In planar inductively coupled plasmas interesting behaviors of the sheath potentials and charged particle current densities have to be expected due to the fact that diffusion in more than one spatial dimension is not necessarily ambipolar but rather determined by the nature of the boundaries. At conducting walls only the total electron and ion currents have to be equal and not the local current densities. At dielectric, non-conducting walls the current densities have to be balanced locally; this fact may give rise to spatial profiles of surface charges.

These aspects have been examined experimentally as well as theoretically. Measurements of particle currents and potentials have been performed using probe arrays which were mounted in the bottom electrode of a planar ICP. The experimental results are compared to the predictions of a two-dimensional kinetic discharge model.

IB 3 Modelling, Project and Numerical Simulation of an Inductively Coupled Plasma Torch for the Deposition of High-Purity SiO_2 .¹ G. COCITO, L. COGNOLATO, C. PANCIATICHI, CSELT - Italy, G. DELLAPIANA, Politecnico di Torino - Italy, V. COLOMBO, Università di Bologna - Italy — An inductively coupled plasma torch has been realized to induce high T chemical reactions of O_2 and $SiCl_4$ to produce high purity, low OH , fused SiO_2 for fiber optic technology. The torch is attached to a 13.56 MHz, 5 kW RF generator and works at atm pressure; system geometry, inlet gas velocities, heat exchange and electrical coil configuration have been selected in accord with the physical modelling and numerical simulation results. Temperature, velocity and electromagnetic fields have been computed by using a time-dependent, 2D fluid code assuming LTE for the plasma,

laminar flow for inlet gases and 1D description of the electromagnetic field. Torch working conditions for various gas flows and powers for test Ar discharges are presented and compared with simulation. Conclusions are drawn concerning the possibilities of operating the system also with Ar - O_2 mixtures and finally with the desired reactive mixture of O_2 - $SiCl_4$.

¹Partially supported by ASP Scientific Association.

IB 4 Complex Impedance and Radical Measurements in Inductively Coupled Plasmas, D. M. SHAW, M. SUMIYA, D. VONA, C. CLARK, and G. J. COLLINS, Colorado State University - A commercially available plasma impedance probe is used to measure the complex impedance of a 20 cm diameter, 13.56 MHz inductively coupled plasma (ICP) reactor using several plasma gases at plasma powers and gas pressures varying from 2 - 50 mTorr and 50 - 1000 W respectively. Typical measured chamber impedance (Z) for 20 mTorr H_2 , He, O_2 and SF_6 plasmas at 475 W plasma power is $Z = 50 + j450 \Omega$ ($\pm 20\%$), while an Ar plasma at the same conditions has a much higher impedance of $Z = 420 + j690 \Omega$.

We employ a modified quartz crystal thin film growth rate monitor to measure the total radical flux versus radial position in both H_2 as well as O_2 ICP's. This method has a large (10^4) dynamic range and a spatial resolution of several mm. It has the disadvantages of not separating out the individual radical species, of not providing an absolute calibration of the radical flux (species per cm^2), and of saturating over total time of exposure. Nevertheless, its utility in providing rapid characterization of wide area total radical fluxes from 10^{14} to 10^{18} radicals $cm^{-2} sec^{-1}$ is demonstrated.

IB 5 Simulations of Profile Effects for Large Area ICP Sources,* P. VITELLO, R. BERGER, G. DIPESO, G.J. PARKER, and N. TISHCHENKO, LLNL - Recent developments in the application of high density plasmas to ultra large scale integrated circuit manufacturing has lead to a need to develop time-dependent multi-dimensional plasma simulation models. We present results here of a comparison between computer modeling and experimental results from the LLNL Large Area ICP Source. The Large Area Source is 30" diameter and is designed to study 400 mm processing. Computer simulations using the 2-D fluid code, INDUCT95, are used to explain variations in the plasma density profile measurements as a function of inductive power, pressure, coil design, and gas. Both Argon and N_2 discharges are considered. We show that there is excellent agreement between simulation and experimental data. Simulations show that high uniformity can be maintained when varying pressure if the chamber aspect ratio is also varied.

*This work was performed under the auspices of the U.S. Department of Energy by the Lawrence Livermore National Laboratory under contract W-7405-ENG-48.

IB 6 Modeling Large Area ICP Sources with Chlorine Chemistry,* R. BERGER, G. DIPESO, G.J. PARKER, N. TISHCHENKO, and P. VITELLO, LLNL - Chlorine discharges in high density, low pressure inductively coupled plasma (ICP) reactors present a variety of issues including multiple ion species (both positive and negative) and dissociation of molecular Cl_2 . We present results here of computer modeling of the LLNL Large Area ICP Source. The Large Area Source is 30" diameter and is designed to study 400 mm processing. Computer simulations using the 2-D fluid code, INDUCT95, are used to study variations in the plasma density profile as a function of inductive power, pressure, coil design, chamber aspect ratio, and surface recombination coefficient for the conversion of Cl to Cl_2 . A high degree of electro-negativity is predicted for low power operation ($\approx 100W$). For high powers ($\approx 1000W$), Cl_2 is found to be largely dissociated to Cl. Modeling results show that a high degree of uniformity is

possible over a 400 mm diameter area.

*This work was performed under the auspices of the U.S. Department of Energy by the Lawrence Livermore National Laboratory under contract W-7405-ENG-48.

IB 7

Theoretical and Experimental Studies of the Bell Jar Top Inductively Coupled Plasma, HAN-MING WU, MING LI, YUN YANG, JIA-PING YAN, DING-PU YUAN, Institute of Mechanics, Chinese Academy of Sciences, Beijing China— In the present paper, argon plasmas in a bell jar inductively coupled plasma (ICP) source are systematically studied over the range of pressure 5-20 mTorr and power input 0.2-0.5 kW. The research work consists of both theoretical calculation and experimental measurements. In the theoretical aspect: as far as the global balance is considered, the models can give reasonable results of the parameters, such as global electron temperature and plasma density. Then we develop a 2-D fluid model simulation with a self-consistent power deposition to obtain the spatial distributions of the plasma parameters. In the experimental aspect: using a tuned Langmuir double-probe technique, we reduce the rf interference and get the probe I-V characteristics. Time averaged electron temperature and plasma density are measured for some combination of pressure and applied rf power. The measurements agree well with the theoretical results qualitatively. It is found that the electron temperature distribution T_e are quite flat in the chamber. There is only 0.1 eV difference between the maximum and the minimum T_e . It is also seen that electron temperature depends primarily on pressure but is almost independent of the power input, except in very low pressure case. The plasma density goes up almost linearly with the power input. The diagnostic data of electron density uniformity seems not as good as the simulation predicts. Due to the inherent limitations of the double probe, the measured T_e should be lower than the true value.

POSTER SESSION IC: GEC REFERENCE CELL

Wednesday afternoon, 11 October 1995

Berkeley Marina Marriott

Belvedere/Angel Rooms, 16:15-18:00

IC 1 Modifications of the GEC Cell for Control During the Etching of Silicon, * A. Ricci, S. Shannon, C. Garvin, M. Weinstein, J. Grizzle, and M. Brake, U of Michigan - Modification to the GEC RF Reference Cell were made in order to conduct semiconductor dry etching research. Vacuum capability was enhanced resulting in lower base pressures of $\sim 10^{-8}$ torr and shorter pump down times with a turbo pump alone whereas previously we also needed a cryopump to achieve these pressures. Real time control of system parameters was implemented in order to perform basic system response tests, and the electrode cooling system was enhanced to allow for higher plasma power. The modified configuration is used to compare methods of measuring plasma absorbed power and correlation of absorbed power to etch rate and uniformity.

*Work supported in part by SRC 94-YC-085

IC 2 Time Resolved 2D Optical Imaging of Hydrogen and Argon Plasmas in the UK GEC Reference Reactor* C.M.O. MAHONY, W.G. GRAHAM, The Queen's University of Belfast, Northern Ireland. R.C. CHESHIRE and R. AL WAZZAN Oriel Instruments, Belfast, Northern Ireland. - Time resolved images of atomic argon (750.4 nm) and hydrogen (656.3 nm) emission have been recorded using a fast gated (5 ns) intensified charge coupled device (Oriel Instrum ICCD). We have obtained a complete map of the horizontal and vertical variation of these emissions and thus optical excitation over a range of plasma parameters. For argon the emission changes from relatively uniform across the plasma to being distinctly peaked at the sheath edge as the plasma becomes more collisional. In both argon and hydrogen the emission intensity is clearly seen to vary over the rf cycle. Different spatial behaviour is seen for hydrogen and argon. With hydrogen the bright emission region at the sheath edge is seen to move over the rf cycle whereas for argon it is always static. Unlike argon ions the lighter hydrogen ions can respond to the applied field and we propose that this is the cause of the observed difference.

*Work supported by the Engineering and Physical Science Research Council for Great Britain and Northern Ireland.

IC 3 Comparison of the Time Variation of Optical and Electrical Parameters in the UK GEC Reference Reactor*

C.M.O MAHONY, W.G. GRAHAM, The Queen's University of Belfast, Northern Ireland. - Simultaneous measurements have been made of time resolved plasma currents and electrode voltages along with time and spatially resolved optical emission spectroscopy in the UK GEC reference reactor. The measurements were taken over a range of pressures and radio frequency voltages while the reactor was operated in the asymmetrically driven mode using argon as the working gas. Plasma currents and electrode voltages were determined using a derivative I-V probe and optical emission spectroscopy for the 750.4 atomic argon line was carried out using single photon counting techniques. The time variation of the optical excitation at different vertical positions within the plasma was found by deconvolution of the optical emission signal $I(t)$. The optical excitation $E(t)$ is a function of $I(t)$, $dI(t)/dt$ and the relaxation time τ . The peak in optical excitation coincides with the peak in plasma current.

*Work supported by the Engineering and Physical Science Research Council for Great Britain and Northern Ireland.

IC 4 Modeling of GEC Reference Cell, M. MEYYAPPAN and T.R. GOVINDAN, Scientific Research Associates, Glastonbury, CT

- The GEC reference cell has been serving as the experimental platform to understand discharge mechanisms through systematic studies and experiments/model comparison. Careful electrical, optical and chemical measurements made in the Cell have been forthcoming¹. We have undertaken a modeling study of the Cell with an emphasis on comparison against these measurements. Both 1-d and 2-d models of the Cell are considered. The model equations consist of the three moments of the Boltzmann equation without the drift-diffusion approximation for momentum in order to extend the analysis to low pressures. Rate constants for inelastic collisions were generated from a 0-d Boltzmann solver. The asymmetry of the Cell warrants 2-d simulations. However, 2-d analysis in reactive systems is computationally intensive. We have developed a procedure to incorporate the asymmetry effects with the 1-d analysis, which captures many of the effects seen in cell measurements. Results are presented for argon and chlorine discharges and compared against data.

1. Special issue of the Journal of Research of the NIST, July 1995

IC 5 NF₃ Plasma Electrical Characterization in the GEC RF

Reference Cell, J.G. LANGAN and B.S. FELKER, Air Products and Chemicals, Inc. Allentown, PA 18195. NF₃ is used as a PECVD *in-situ* chamber cleaning gas to remove spurious deposition material from the process chamber walls. The speed of this process is extremely important when considering wafer throughput and cost. Since etch rates are controlled by a complex variable set, it is useful to specifically define and understand these variables for reactive plasma gases. For this reason, plasma impedance and power dissipated in Ar and NF₃ based plasmas are measured in a GEC RF Reference Cell under a variety of operating conditions. Values for the power dissipated in the plasma, impedance magnitude, and phase angle can be calculated using the de-embedding method¹. Both current and voltage waveforms are measured at the powered electrode, Fourier analyzed to remove the contributions of the higher harmonics, and analyzed for amplitude and phase angle. These values are corrected using the de-embedding method to remove the contributions of stray impedances to yield the "actual" discharge current and voltage allowing the impedance of the plasma and power dissipated to be calculated. The results for Ar are compared to those obtained by Sobolewski² under similar conditions.

WEDNESDAY AFTERNOON

1. R.F. Bauer and P. Penfield, IEEE Trans, MTT-22, 282 (1974).
2. M.A. Sobolewski, J.Vac. Sci. Tech. A 10, 3550 (1992).

POSTER SESSION ID: GLOW MODELING

Wednesday afternoon, 11 October 1995

Berkeley Marina Marriott

Belvedere/Angel Rooms, 16:15-18:00

ID 1 Plasma Computer Experiments Teaching Laboratory* C.K. BIRDSALL, V.P. GOPINATH, J. VERBONCOEUR, Univ. of Calif. Berkeley CA 94720 - A plasma simulation laboratory employing 1d3v PIC-MCC codes has been used to enhance a plasma lecture course, both of which emphasize the plasma physics of discharges and materials processing.

Simulations inserted into lecture courses on an occasional basis have long proven to be valuable teaching tools. The present weekly laboratory draws on 20 computer experiments from a workbook, companion to the lecture text.¹ The homework projects range from diffusion to DC and RF discharges in argon, with many questions asked, tracking the lectures.

The codes used are XES1, XPDP1 and XPDC1 (WWW <http://ptsg.eecs.berkeley.edu>) with numerous input files. The course does not require a background in numerical analysis, or recompilation of the software. All projects are performed by modifying standard sets of (laboratory) parameters, such as lengths, voltages, frequencies, and gas pressure. A computer demonstration will be available, as well as the workbook and examples of student homework. *Work supported in part by ONR Contract FD-N00014-90-J-1198 1. "Principles of Plasma Discharges and Materials Processing", M. A. Lieberman and A. J. Lichtenberg, Wiley, 1994.

ID 2 Implicit Simulation of Low Pressure rf Discharges,

M. M. TURNER, Dublin City University, Ireland - Particle simulation is a powerful but expensive technique for simulating low-pressure plasmas where kinetic effects should not be neglected. In high-density sources in particular, the stability and accuracy conditions that explicit particle simulations must satisfy become a prohibitive burden. Implicit algorithms remove these limitations, at some significant cost in algorithmic complexity. In this paper we discuss the implementation and performance of a highly modular implicit particle code, written in the C++ language and using many of its advanced features. The performance of this code is very close to a similar FORTRAN implementation.

ID 3 Modelling Of Cathode Sheath In Magnetron Discharges*, GRAEME LISTER, CRL, Hayes, UK**

Results of theoretical and numerical models of electron confinement in the cathode region of magnetron plasmas are presented. Experimental measurements¹ have shown that electron diffusion across the magnetic field lines parallel to the target corresponds to $2 < \omega_{ce} / \nu_e < 9$ here ω_{ce} is the electron cyclotron frequency and ν_e is the electron-atom elastic collision frequency ($\omega_{ce} / \nu_e = 16$ corresponds to Bohm diffusion). For low pressures, the Langmuir-Childs description of the sheath is adequate. However, at higher pressures, the ion mobility scales as $(E/N)^{1/2}$, and a collisional model of the sheath is appropriate. For many applications of magnetron discharges, the sheath is found to be sufficiently thin for electrons to enter the negative glow before losing energy through atomic excitation and ionisation. However, for high magnetic fields, electrons may be confined to the sheath region for sufficient time have appreciable inelastic collisions with the background gas.

¹Rosnagel S M and Kaufman H R 1987 *J. Vac. Sci. Technol.* A 8 30

* This work has been funded by British Nuclear Fuels plc

** Present address OSRAM SYLVANIA, Danvers, MA 01923

ID 4 Modeling of a Low-Current Glow Discharge with Transverse Magnetic Field, L. PEKKER, A. ERSHOV, Photran Corp., Lakeville, Minnesota - The low-current glow discharge with strong transverse magnetic field is investigated analytically and by Monte Carlo simulations. In the analytical model we assume that electron gyro radius is much smaller than the distance between the anode and the cathode so that the diffusion of electrons to the anode can be described in terms of a transverse mobility. The ion mean free path and ion gyro radius are assumed to be much greater than the cathode-anode gap, thus the influence of the magnetic field and collisions on movement of ions can be neglected. Based on this assumptions the longitudinal distributions of electrons and ions are obtained when the distortion of electrical field is small. It is shown that when magnetic field is strong enough the discharge is negatively charged. With an increase of current this leads¹ to a negative space charge dominated mode of glow discharge without cathode fall at all. Comparison with the Monte Carlo simulations has been done.

¹ L. Pekker, *Plasma Sources Sci. Technol.*, 4, 31, 1995.

ID 5 Rarefied Gas Flow Analysis in Plasma Etching Apparatus Using the Direct Simulation Monte Carlo Method,

M. IKEGAWA, Y. OGAWA, T. USUI, and J. TANAKA, Mechanical Engineering Research Laboratory, Hitachi Ltd. - The gas flow in low-pressure etching apparatus such as the magneto-microwave plasma reactor¹ is characterized as rarefied gas flow. The rarefied gas flow in etching plasma reactors was calculated with a direct simulation Monte Carlo program². The flow pattern in the plasma reactor was found to strongly depend on the Knudsen number and the gas supply structure. Also the ventilation of the etching reaction product in the plasma reactor was found to be improved at higher Knudsen numbers and have the best performance in the impact-flow type among the various gas supply structures.

1 M. Ikegawa, et al., *Jpn. J. Appl. Phys.* 31(1992)p2030.

2 M. Ikegawa, & J. Kobayashi, *JSME International Journal Series II*, 33, No.3 (1990)p463.

ID 6 A Numerical Study of the Expansion of a Plasma into a

Plasma, E. BESUELLE and F. DONEDDU, CEA, CE-Saclay, DCC/DPE, France - We investigate the non steady and non linear dynamics of the coupling of two cold plasmas, one created by Laser expanding into the other. Our numerical tools are a 1D Particle-In-Cell (PIC) code and two kinds of cylindrical fluids models: the first one considers two ionic populations with electrons in isothermal equilibrium; the second one is a four fluids model (two ionic fluids and two electronic ones), coupling the different populations by the Poisson equation and taking into account energy conservation equation for each fluid. The PIC code and the two fluids model exhibit that ions of both plasmas are accelerated, as globally described in [1]. Furthermore, the PIC code and the four fluids model show that, *in the beginning of the coupling, a singular motion of the electrons takes place. Those belonging to the expanding plasma move away, so that a deficit of electrons is created. The respect of quasineutrality imposes their replacement by electrons of the other plasma, whose electronic temperature locally increases for an adiabatical evolution.*

[1] Non-linear Dynamics and Acceleration of Ions when a Plasma Expands into a Plasma. A.V. GUREVITCH, R.Z. SAGDEEV, S.I. ANISIMOV, Y.V. MEDVEDEV. *Sov. Sci. Rev. A Phys., Soviet JETP*, 13, 1989, pp. 1-65.

ID 7 Voltage-current characteristics in low pressure, hollow cathode discharges. A. Fiala, L.C. Pitchford and J.P. Boeuf, CPAT, Université Paul Sabatier, Toulouse, France, P. Choi, LPML, Ecole Polytechnique, Paris, France and M. Nelson, Imperial College, London, United Kingdom - The measured and calculated voltage-current characteristic in a hollow cathode argon discharge at 1 torr will be presented. The calculations were performed using the 2-D hybrid fluid-Monte Carlo model presented previously¹, and this model gives a realistic description of the ionization source term in the highly nonuniform electric field as well as of the electrons oscillating between the sheaths inside the hollow cathode (pendulum electrons). The calculated v-i characteristic, determined by varying a series resistor, consists of distinct low current and high current parts, each with a positive slope, and separated by a considerable drop of the discharge maintenance potential corresponding to the penetration of the plasma into the cathode cavity and the onset of the HC effect. The same structure in the v-i characteristic is observed experimentally, and emission measurements confirm the mode prediction that the drop in the potential corresponds to an increasing volume of plasma in the hollow cathode cavity and hence increasingly efficient ionization due to the pendulum electrons.

1. A. Fiala, L.C. Pitchford and J.P. Boeuf, Phys. Rev. E, 49 5607 (1994).

ID 8 Plasma Chemistry of Low Pressure Processing Discharges, W.L. MORGAN, Kinema Research & Software†, Monument, CO 80132 - Using a 0-dimensional time-dependent plasma chemistry code, a 3-dimensional electron Monte Carlo code, and long mean free path models, I have investigated some of the important aspects of the plasma chemistry of a low pressure inductively coupled discharge in chlorine. The key gas phase processes in a pure Cl₂ discharge are dissociation, dissociative attachment, and ionization. The relative densities of electrons, Cl, Cl₂⁺, and Cl⁺ are strong functions of the degree of dissociation of the molecular chlorine. This, in turn, is strongly dependent upon the probability of reassociation of atomic Cl into Cl₂ on the chamber walls within the residence time of the gas in the processing chamber. Parametric studies of these dependencies will be presented. In addition, similar work on a more complex system, HBr/Cl₂/O₂, is currently underway.

Work partially supported by the Lawrence Livermore National Laboratory.

† See "http://www.kinema.com/kinema" on the World Wide Web.

ID 9 Modeling Electronegative Discharges at Low Pressure, I.G. KOUZNETSOV, A.J. LICHTENBERG and M.A. LIEBERMAN, University of California, Berkeley - The low pressure solution of an electropositive plasma¹ is generalized to include a finite particle flow at the interface with an electronegative plasma. We use this solution to extend a previous study,² which employed a macroscopic analytic model for a plasma discharge with a three component (electronegative) core and an electropositive edge region. In that study, both regions were treated in the high pressure approximation of constant mobility for the positive ions. The extension to low pressures uses a variable mobility model with constant mean free path for the positive ions within the electropositive region. A possibility of having an additional transition region is studied, in which case the flow at the edge of the electronegative region is sonic. The resulting algebraic equations are solved numerically over all parameter ranges and compared to simpler analytical approximations, for an oxygen discharge. This formalism is extended to two positive ion species (four plasma components).

¹V.A. Godyak and V.N. Maximov, Vestn. Moskovskogo Universiteta, Ser. *Physica i Astronomica* 6, 51 (1977); see also V.A. Godyak, *Soviet Radio Frequency Discharge Research*, Delphic Associates, Falls Church, VA (1986).

²A.J. Lichtenberg, V. Vahedi, M.A. Lieberman, and T. Rognlien, *J. Appl. Phys.* 75, 2339 (1994).

Work supported by NSF Grant ECS-9217500, DOE Grant DE-FG03-878R 13727, LLNL/PPRI Grant CP 94-06/B283626, and Lam Research Corporation.

ID 10 Electronegative Discharge Equilibria at Large Electronegativity,* Y.T. LEE**, A.J. LICHTENBERG and M.A. LIEBERMAN, University of California, Berkeley - In a previous study¹, a macroscopic analytic model was developed for a plasma discharge with a three-component (electronegative) core and an electropositive edge region. At high electronegativity the internal positive-negative ion recombination may dominate the positive ion diffusive loss from the core. In this situation the negative ion profile can differ significantly from the parabolic profile assumed in previous work¹, which is a good approximation at more modest electronegativities. Assuming Boltzmann equilibrium for the negative ions, we solve

the nonlinear ion diffusion equation to obtain the profiles and the fluxes. For a parallel plane chlorine plasma with $\alpha_0 = 50$ (α_0 is the ratio of the central Cl⁻ density to the nearly constant electron density, $\alpha_0 = n_0/n_{e0}$) we find a negative ion profile that is considerably flattened from that of a parabolic profile. We examine the assumption that the negative ions are in Boltzmann equilibrium, by solving the coupled equations in the absence of this assumption, but in the limit of large α_0 , finding quite similar profiles. The possible effect of an ion sound velocity limitation on the positive ion diffusive flux will also be discussed.

* Work supported by DOE Grant DE-FG03-87ER13727, NSF Grant ECS-9217500 LLNL/PPRI Grant CP94-06/B283626, and Lam Research Corporation

**Permanent address Lawrence Livermore National Laboratory

¹ A.J. Lichtenberg, V. Vahedi, M.A. Lieberman, and T. Rognlien, *J. Appl. Phys.* 75, 2339 (1994)

ID 11 Particle Simulation of Electronegative rf Discharges, D. A. W. HUTCHINSON and M. M. TURNER, Dublin City University, Ireland - The standard particle in cell with Monte Carlo collisions simulation method (PIC-MCC) is unsuited to situations where the densities of interesting plasma species are very divergent, as happens in electronegative discharges when the electron density is much less than the positive and negative ion densities, for example. In these circumstances it is difficult both to make proper and economical use of computer particles, and to arrange for the conservation laws to be enforced in collisions. In this paper we will describe an extension of the PIC-MCC scheme that meets these difficulties by allowing variable weights. We will discuss what we believe to be the advantages of this scheme over previous proposals¹, and we will present examples of applications.

[1] D. J. Cooperberg, V. Vahedi and C. K. Birdsall, paper 3B21, 15th International Conference on the Numerical Simulation of Plasmas, Valley Forge, 7-9 September 1995.

ID 12 PIC-MCC with variable particle weights. D. J. COOPERBERG, V. VAHEDI, AND C. K. BIRDSALL, *University of California at Berkeley**—In order to use particle-in-cell (PIC) simulation codes for modeling collisional plasmas such as self-sustained discharges, it is necessary to add interactions between charged and neutral particles. A Monte-Carlo collision (MCC) package for particles of various weights has been developed and is being tested. This scheme can in general reduce the number of computer particles needed to represent selected species which allows for a significant reduction in simulation size at runtime as in the case of highly electronegative discharges where the ion densities may be far greater than the electron density. Also, by choosing a constant number of computer particles to be used through the duration of the run, a consistent level of numerical fluctuation may be maintained. We have tested this scheme to simulate O₂ discharges at low powers and high pressures.

*This work supported by Office of Naval Research contract N00014-90-J-1198.

POSTER SESSION IE: FUNDAMENTAL PROCESSES IN DISCHARGES

Wednesday afternoon, 11 October 1995

Berkeley Marina Marriott

Belvedere/Angel Rooms, 16:15-18:00

IE 1 Penning Ionization of Cesium by Photoexcited Mercury as a Volumetric Source of High Density Plasma,* K. R. STALDER and R. J. VIDMAR, SRI International—We are studying efficient ways to develop high density plasmas and have identified Penning ionization as a potentially useful mechanism. In particular, the Penning ionization of cesium by metastable mercury appears to be particularly promising because of the favorable energetics of producing metastable mercury atoms that have electronic energies lying above the ionization potential of cesium. We are modeling the kinetics of the system, including the effects of buffer gases and molecular quenching gases. Excitation is produced by resonant photoexcitation of the Hg

3P_1 state followed by quenching with nitrogen to the 3P_0 state. Electron-ion recombination processes considered so far include three-body recombination. The electrons are heated by collisions with vibrationally excited nitrogen. The results indicate that cesium can be nearly 100% ionized to densities in excess of 10^{12} cm^{-3} .

* Work supported by AFOSR under Contract F49620-95-C-0009

IE 2 A Rare Gas - Rare Gas Metastable Model Potential, D. F. Hudson, NSWCDD/White Oak - A model potential has been created for the interactions between He metastables. There is at most, one free parameter which it may be possible to eliminate. The damping function is a variation of one used by Tang and Toennes [1] For He, the agreement with theory is within about 5% for the range 2 - 14 a_0 . The model will be described in detail along with applications to other rare gas systems.

1 Tang, K. T. and Toennies, J. P. J. Chem. Phys. **80**, 3726 (1984)

IE 3 Kinetics of Cs Formation from CsCl in the Positive Column of the Hydrogen Pulsed Discharge. JACEK BORYSOW, EDWARD AUGUSTYNIAK and ALEXANDER ERSHOV, Physics Department, Michigan Tech. University.

Time transients of the number densities of Cs in the ground electronic state were measured in a positive column of moderate-current hydrogen pulsed discharge. Metallic cesium was formed from cesium chloride. The population was computed from integrated high resolution laser absorption profiles of D2 line at 852 nm. Experiments were done at hydrogen number densities from $1.6 \times 10^{16} \text{ cm}^{-3}$ to $9.6 \times 10^{16} \text{ cm}^{-3}$ and current densities ranging from 0.3 to 1 A/cm². Number densities of CsCl varied from $5 \times 10^7 \text{ cm}^{-3}$ to $3 \times 10^8 \text{ cm}^{-3}$. The proposed kinetic model in a form of the rate equations reproduces accurately measured time transients of Cs population.

* Supported by ARPA contract # DAA07-94-C-R098.

IE 4 The Effect of Xenon on a Negative Hydrogen Ion Source,* P.G. STEEN and W.G. GRAHAM, The Queen's University of Belfast, Northern Ireland - The presence of caesium in hydrogen discharges is known to increase the negative hydrogen ion density by up to sixteen fold. The mechanism for this phenomenon is not understood. One of several theories suggests that caesium, as a heavy element, has a collisional cooling effect on the plasma. Before introducing caesium (and the problems with memory effects that it causes) the effect of addition of xenon, also a heavy element but unreactive, has been studied. Langmuir probe and photodetachment techniques have been used to measure the plasma parameters, including the negative ion density in a multicusp source running with hydrogen gas and small percentages of xenon gas. At total constant gas pressure the electron density doubles as the Xe concentration is increased to 20%. The electron temperature and plasma potential increase slightly. In all cases the most significant changes occur within the first 5% of added Xe. No significant change in the negative ion density was observed when Xenon was introduced.

* Work supported by the E.C. Human Capital and Mobility Programme.

IE 5 Radiative lifetime of the O(5S_2) metastable state and collisional coupling between the O($^5P_{1,2,3}$) fine structure sub-levels, I. PAK and N. SADEGHI, Labo. de Spectrométrie Physique, Université J. Fourier Grenoble I, FRANCE-

-A high density pulsed oxygen plasma ($p \sim 0.5$ to $10 \mu\text{bar}$; $n_e \sim$ a few 10^{11} cm^{-3}) produces metastable atoms O(5S_2) inside a Helicon reactor. From the pressure dependence of the decay time of their density in the afterglow, observed through the optical absorption on 777.42 nm ($^5P_2 \leftarrow ^5S_2$) transition, we deduce the radiative lifetime $\tau_0 = 91 \pm 5 \mu\text{s}$ and the rate coefficient for quenching by O₂ molecules $k = 1.7 \pm 0.5 \cdot 10^{-10} \text{ cm}^3 \text{ s}^{-1}$. In another set of experiments, O(5S_2) atoms, produced in rare gas glow discharge containing a trace of oxygen ($\phi_{\text{tube}} = 1 \text{ cm}$; $p \sim 0.2$ to 15 mbar ; $i_{\text{discharge}} \sim 1 \text{ mA}$), have been excited to one of the fine structure O(5P_2 or 5P_1) states by using a single mode diode laser tuned on 777 nm ($^5P_{J=1 \text{ or } 2} \leftarrow ^5S_2$) transitions. Rate coefficients for population transfers between the three fine structure sub-levels, induced by collision with He, Ne, Ar and Kr, as well as the quenching rate coefficients have been measured. In the case of krypton, we observe a large rate coefficient for the energy transfer from O(5P_J) to Kr atoms, populating probably the Kr($4p^55s$) states.

IE 6 Ion-ion Plasma Formation with Electrons Escaping in Electronegative Gases Pulse Discharges*

N.A.KHROMOV, S.N.LAZARYUK, V.A.ROMANENKO, A.A.KUDRYAVTSEV -For electronegative gas plasma decay can occur a transfer from electron-ion to ion-ion plasmas [1]. We have experimentally investigated sudden electron escaping for the time less than the free diffusion time of ions t_d in glass tube in oxygen and air at pressure 0.03...0.3 Torr during 0.5...2.0 ms pause between the pulse (10...50 μs) discharges and 0.01...1 A amplitude. The Langmuir's probe measurements were performed for various afterglow times. It is established that in the air in time $t_0 \sim 200 - 600 \mu\text{s} < t_d$ plasma sudden ($< 50 \mu\text{s}$) becomes almost electron free; a farther plasma decay is controlled by ion diffusion. Increasing of oxygen content in the air leads to substantial t_0 decrease. Obtained experimental data have a good agreement with our plasma decay model.

*Work supported by INTAS (project N 740) and RFFI (projects 1 94-02-03969 and 1 95-02-05064).

¹D.Smith et al. J.Phys D: Appl. Phys. **7**, 1944 (1974)

IE 7 Fluorescence of rare gas exciplexe excited by dielectric controlled discharges. C. CACHONCINLLE, E. ROBERT, A. KHACEF, and J.M. POUVESLE, Gremi/University of Orléans, France.

-High pressure (1-5 bars) rare gases (Rg: Ne, Ar, Kr and Xe) and mixture of Rg with Oxygen (O) have been excited using a Dielectric Controlled Discharge technics. Such media are well-known to produce useful fluorescence in the short wavelength spectral domain. Visible, UV and VUV time resolved spectroscopy have been performed on these plasmas in the nanosecond range time scale. Beside the VUV emission of the first and second continua of the rare gases, strong fluorescence have been recorded at higher wavelength and attributed to the so-called "third continua of rare gases" and the Rg-O exciplexe. Despite many experiments to better understand the molecular states that could be involved in the formation of the third continua (pure rare gas ionic excimer, singly or doubly ionised, neutral exciplexe of rare gas and impurities,...), their origin is still discussed in the literature. The new results presented in this work show that, on the contrary to what have been suggested in the past, no confusion can be made between third continua and the fluorescence related to Rg-O exciplexe.

IE 8 Model of VUV Photon-Induced Electron Emission in Low-Pressure Hydrogen Discharges.* A. V. PHELPS, JILA, U. of Colorado and NIST. - H_2 vuv photon-production¹, photoelectron emission², self-absorption^{1,3}, and quenching⁴ measurements are used to test models of the role of vuv photons in electrical breakdown and in steady-state, cathode-dominated discharges. For cathodes with a high electron yield² only for wavelengths λ below 100 nm, the Werner bands of H_2 are dominant. Lines ending on $v = 0$ are highly absorbed for a pd of 1 Torr-cm and those reradiated at $\lambda > 120$ nm are effectively lost. For a cathodes with a high yield for $\lambda \leq 130$ nm the Lyman band contributes and vibrationally excited H_2 appears to be required to obtain a significant reduction in electron yield. A vibrational excitation model is presented for the cathode fall region.

¹ J.M. Agello *et al.* Phys. Rev. A **29**, 636 (1984).

² G.L. Weissler, Handb. Phys. **21**, 304 (1956).

³ R. Geballe, Phys. Rev. **66**, 316 (1944); M.S. Bhalla, J.D. Craggs, and J.M. Meek, Proc. 5th Int'l. Conf. on Ionization Processes in Gases, (North-Holland, 1962, Amsterdam), Vol. 1, p. 315; R.B. Cairns and J.A.R. Samson, Proc. Phys Soc. **90**, 879 (1967).

⁴ W. Legler, Z. Phys. **173**, 169 (1963).

IE 9 Experimental studies and MCS on the Convex Profile of Luminous Layers. T. FUKUYAMA, H. ITOH and N. IKUTA, Chiba Inst. Tech., Japan. --- It is well known that luminous layers are observed in the Townsend discharge in rare gases¹. We observed the luminous layers in Ne using a uniform field diode with filament behind a mesh at the center of the cathode². The current is less than $1 \mu A$. The profile of luminous layers commonly show convex forms toward the cathode. A precise MCS is applied to make clear this phenomena not only Ne but also Ar and Xe. For this purpose, the cylindrical discharge space is divided to small segment in radial and axial directions. The quantities concerning with the electron swarm are sampled in these segment. Electrons are released from the centre of the cathode with zero energy. Axial distributions of mean energy, drift velocity and each excitation numbers are in good agreement with the observed results. The mean energy distribution of the axial direction at the center axis is larger than the outers. Electrons lose energy in mostly elastic collisions till reaching on the outskirts of the cylindrical discharge space. This tendency is more evident in Ar and Xe than in Ne due to higher elastic cross sections. This fact suggests that the convex profile of luminous layers are explained without considering the space charge with the tube and on the wall.

¹G. Holst and E. Oosterhuis: Phil. Mag., **46**, 1117, 1923.

²T. Fukuyama, H. Itoh et al: ESCAMP1994, 230 and 232, 1994.

THURSDAY MORNING

SESSION KA: GEC REFERENCE CELL

Thursday morning, 12 October 1995

Berkeley Marian Marriott

Yerba Buena/Treasure Rooms, 8:00-10:00

Bill Graham, presiding

Invited Papers

8:00

KA 1 Electron density measurements in the GEC reactor.* L.

J. OVERZET, University of Texas at Dallas, Richardson, TX 75083.

— I have compiled some of the electron density measurements taken in GEC reactors and compared the results. The electron densities have been measured by microwave interferometry at 8.6, 35 and 80 GHz, by Langmuir probes and by laser induced fluorescence. The agreement between the techniques is close especially when one considers the differences between the cells and the techniques that have been used. For example, the close agreement spans symmetrically and asymmetrically driven cells with both aluminum and steel electrodes. The data have also brought attention to several features of the measurement techniques. For example, the microwave interferometry results at low pressures exhibit closer agreement when plotted as a function of the discharge voltage than they do when plotted as a function of the discharge current. This appears to indicate either that measurements of the discharge current continue to be more difficult, or that the voltage plays a more significant role in determining the density.

* Work supported in part by the National Science Foundation and The State of Texas Advanced Research Program.

8:30

KA 2 Electrical Characterization of Radio-Frequency

Glow Discharges, M. A. SOBOLEWSKI, National Institute of Standards and Technology.

The reproducibility of low temperature glow discharges is an important concern, both in plasma processing applications and in fundamental research. These discharges can be sensitive to a variety of experimental factors that often are poorly controlled, resulting in changes in a single discharge cell over time or differences between ostensibly identical cells. This talk will describe experimental efforts to identify and understand the sources of this irreproducibility, concentrating on studies of discharges in argon, in the GEC RF Reference Cell, operated at 13.56 MHz. For these discharges, the effects of gas phase impurities, the condition of the electrode surfaces, and variations in the electrical circuitry that powers the cell have been systematically characterized in controlled experiments, using current and voltage waveform measurements. After reviewing these studies, more recent work will be presented showing how the changes in the current and voltage characteristics can be interpreted and the origin of the changes elucidated, using simultaneous floating potential measurements, measurements of electron density by Langmuir probes and microwave interferometry, and modeling work. The implications of these results on standard cell efforts, reactor design, and plasma process control will also be discussed.

Contributed Papers

9:00

KA 3 Mass Spectrometric Investigation of Positive Ions and

Neutrals in SF₆ RF Discharges in the GEC Reference Cell,R. FOEST, INP Greifswald, Germany, J.K. OLTHOFF and R.J. VAN

BRUNT, NIST — SF₆ is widely used as an etching gas in the plasma processing of semiconductor materials. We report experimental results obtained in a GEC Reference cell for pure SF₆ at pressures from 4 to 33 Pa and applied rf voltages from 100 to 300 V. Ions and neutrals are extracted from the plasma through a 0.1 mm diameter orifice in the

grounded electrode and analyzed by mass and energy filters. Relative intensities of neutral species are presented along with the degree of dissociation of SF₆, which is about 0.25 at low power and increases to 0.65 at higher powers. Kinetic energy distributions of ions produced in the plasma are measured at the grounded electrode. Relative ion intensities are obtained by integration of the kinetic energy distribution functions over the energy range. The most abundant positive ions are SF₃⁺ and SF₅⁺ comprising nearly 90% of the ion flux, followed by other SF_x⁺ ions (x = 0, 1, 2, 4), F⁺, SOF₃⁺, and HF⁺. Moreover we also detect S₂F₇⁺, S₂F₆⁺ and S₂OF₅⁺. The shapes of the kinetic energy distributions are discussed and related to the sheath properties and measured electrical waveforms, as a function of pressure and applied voltage.

9:15

KA 4 Two dimensional excited state distributions in inductively

coupled argon discharges, * G. A. HEBNER, Sandia NationalLaboratories, Albuquerque NM - The spatially dependent excited

state density in inductively coupled argon discharges has been determined using absorption spectroscopy. Absorption measurements were performed by collimating the output from a single mode Ti:Sapphire laser using a six inch diameter beam expander, passing the beam through the discharge region and imaging the transmitted beam onto a CCD camera. The line integrated density of the 1s₃, 1s₄, 1s₃ and 1s₂ levels and the Doppler width was then determined by fitting the absorption lineshape. For an argon pressure of 10 mTorr and rf plasma power of 160 W, the line integrated density varied between 2 × 10¹⁶ m⁻² for the 1s₃ state to 2 × 10¹⁵ m⁻² for the 1s₂ state. Line integrated density and Doppler width as a function of rf power (50 to 300 W), pressure (4 to 50 mTorr) and lower electrode bias will be presented.

* This work was supported by the United States Department of Energy and SEMATECH.

9:30

KA 5 2-D Fluid Model of the GEC Reference Cell with

Inductively Coupled Power, J. D. BUKOWSKI, P. VITELLO†,

and D. B. GRAVES, U.C. Berkeley and †LLNL - We have modeled

the GEC Reference Cell with inductively coupled rf power and compared the predictions to the experimental measurements of Miller, et al [1]. Measurements include spatially resolved electric probe profiles of electron density, electron temperature and plasma potential as a function of applied power. In addition, line averaged electron density measurements were made with microwave interferometry. The model-experiment comparison was done for both Ar and Cl₂ discharges, using published or widely available data for rate and transport coefficients. Comparisons of spatial profiles of electron density, plasma potential and electron temperature were in good quantitative to semi-quantitative agreement for Ar discharges. In the case of Cl₂, electron temperature and plasma potential were reasonably well predicted by the model, but the absolute value of the predicted plasma density was about a factor of 2 too high, as compared to the measurements. Chlorine discharge model predictions of the spatial profiles of the neutral composition (Cl, Cl₂) and temperature and the negative ion profiles will also be presented.

[1] P.A. Miller, G.A. Hebner, K.E. Greenberg, P.D. Pochan, and B.P. Aragon, *J. Res. Natl. Inst. Stand. Technol.*, submitted 1994

9:45

KA 6 Chemically Reacting 3-D Flow in the GEC Ref-

erence Cell, D. C. WADSWORTH, Hughes STX and Phillips

Laboratory (Propulsion Directorate) - High-temperature, multi-

species neutral reacting flow through the GEC RF cell has been

modeled for a range of low pressure operating conditions using

the Direct Simulation Monte Carlo technique. The technique

allows accurate simulation of a variety of transport phenomena in the low pressure or rarefied gas dynamic regime, including species separation effects and the development of Knudsen or slip layers near surfaces such as the substrate. Of additional interest is the resolution of non-uniform flow near the substrate due to the three-dimensional nature of the cell. Visualization of results provides insight into the complex flow expected in the general 3-d plasma reactor. Parametric calculations of this type are expected to assist in ongoing experimental diagnostics of cell performance and facilitate optimization of cell geometries and operating conditions.

SESSION KB: ELECTRON COLLISIONS

Thursday morning, 12 October 1995

Berkeley Marina Marriott

Belvedere Room, 8:00-10:00

Ilya Fabrikant, presiding

8:00

KB 1 Electron-Impact Excitation of Xenon, M.A.KHAKOO#, S.TRAJMAR+, S.WANG+, I.KANIK+, L.R.LECLAIR+, C.FONTES*, R.E.H.CLARK*, J.ABDALLAH, Jr* and G.CSANAK*, #Cal.St. U. Fullerton, *Jet Propulsion Laboratory and *Los Alamos National Laboratory. Experimental and theoretical differential cross sections (DCS) for the 20 lowest electronic states of Xenon in the 10 to 80eV range will be reported. The relative (with respect to elastic scattering) inelastic scattering intensities were normalized by utilizing the known elastic DCS's¹ and calibrating the instrument response on the basis of time-of-flight measurements. The calculations are based on the unitarized distorted wave approximation and first-order many-body theory and used the Los Alamos National Laboratory codes². Extensive comparisons between experimental and calculated results will be presented.

Supported by *NASA, *DOE, #NSF-RUI and #DOE-AWUI.

1. D.F.Register et al. *J.Phys.B.* **12**, 1685 (1986).
2. R.E.H.Clark et al. *Phys.Rev.* **A40**, 2935 (1994).

8:15

KB 2 Application of Magneto-Optical Atom Traps for Measuring Electron-Atom Ionization and Total Scattered Cross Sections.* R. SCOTT SCHAPE, PAUL FENG, THAD G. WALKER, L.W. ANDERSON AND CHUN C. LIN, Univ of Wisconsin-Madison. An electron beam is passed through laser-cooled Rb atoms held in a magneto-optical trap. The recoil velocity imparted to the scattered Rb atoms allows them to escape the trap so that the fractional loss rate of the trapped atoms due to electron-atom collisions can be used to determine the electron scattering cross section. In one set of experiments the trap was turned off during the electron beam pulse and remained off for up to 18ms after the electron-beam pulse to allow even the slowest recoiled Rb atoms to escape the trap. The total scattering cross sections determined in this way are in good agreement with previous measurements by atomic beam recoil experiments and beam transmission techniques. For measurement of ionization cross sections, the trap is turned on immediately after the electron beam pulse so that the scattered Rb atoms do not escape the trap. The Rb ions produced by electron-impact ionization are not resonant to the trapping lasers so that the measured loss rate gives the ionization cross section. *Supported by Air Force Office of Scientific Research, the National Science Foundation and the Packard Foundation.

1. R.S. Schappe et al., *Europhysics Letters* **29**, 439(1995).
2. P. J. Visconti et al, *Phys Rev. A* **3**, 1310(1971).
3. S.P. Parikh et al., *Phys. Rev. A* **47**, 1535(1993).

8:30

KB 3 Use of Improved Electron-Helium Differential Ionization Cross Sections in Monte Carlo Simulations, J. E. LAWLER¹, V. KRATSOV², and D. H. MADISON² ¹Univ. of Wisconsin-Madison ²Univ. of Missouri-Rolla --Monte Carlo simulations of electron avalanches in the cathode region of a glow discharge in helium are performed using improved theoretical differential ionization cross sections for helium calculated using the first order distorted wave Born approximation. In the cross section

calculation, final state correlations between the two continuum electrons, which are known to be important, are taken into account using effective charges. This approach has been shown to give good agreement with experimental cross section measurements [1] (differential and integrated). The simulations using more accurate cross sections are compared with earlier simulations[2]. The ionization per electron as a function of position in the cathode fall and negative glow is similar to the earlier simulations, but the new simulations have a more realistic treatment of energy dependent momentum transfer during ionizing and other inelastic collisions.

1. S. Jones, D.H. Madison and M.K. Srivastava, *J. Phys. B* **25**, 1899 (1992).
2. E. A. Den Hartog et al., *Phys. Rev.* **A38**, 2471 (1988).

8:45

KB 4 Dissociative Excitation of Molecular Ions - * A. E. OREL, UC Davis and T. N. RESCIGNO Lawrence Livermore National Laboratory - A knowledge of basic dissociative collision process involving low-energy electrons and molecules plays a crucial role in the understanding and modelling of low-temperature processing plasmas. In contrast to the situation with respect to neutral target gases, there is almost no data, either experimental or theoretical, on the cross sections for dissociative excitation of molecular ions. We have undertaken a theoretical study of this process using the complex Kohn variational method, modified to account for Coulomb boundary conditions. For several target ions, we have undertaken large-scale multistate close-coupling calculations using elaborate trial wave functions. We will illustrate the method with results on the dissociative excitation of CH⁺ and OH⁺.

*This work was performed under the auspices of the U.S. Department of Energy by LLNL under contract W-7405-ENG-48.

9:00

KB 5 Experimental Electron Impact Cross Section and Linear Polarization for the Nitrogen $C^3\Pi_u, v=0 \rightarrow B^3\Pi_g, v'=0$ Transition* CONNOR FLYNN AND BERNHARD STUMPF, Dept. of Physics, University of Idaho. -- We have measured the linear polarization and the apparent excitation function of the nitrogen $C^3\Pi_u, v=0 \rightarrow B^3\Pi_g, v'$ transition (337.13 nm) from threshold (11.03 eV) to 500 eV. The electron beam is produced by a multi-stage electron gun [1] and has a thermal energy spread of about 0.25 eV. The experiment is carried out in the static target mode with a nitrogen pressure of about 10^{-5} Torr. The 337.13 nm transition is selected with an interference filter or with a monochromator. Our measured cross section agrees best with data by Finn, Aarts, and Doering [2] and is in overall good agreement with data by Imami and Borst [3]. As expected for a molecular vibrational transition with unresolved rotational structure, the measured linear polarization is rather small, a few percent at low energies and practically zero at high energies.

*Supported in part by NSF/Idaho-EPCoR under grant OSR-9350539 and by a grant from the State Board of Education of the State of Idaho.

- [1] Z. Wei, C. Flynn, A. Redd, and B. Stumpf, *Phys. Rev. A* **47**, 1918 (1993)
- [2] T. G. Finn, J. F. Aarts, and J. P. Doering, *J. Chem. Phys.* **56**, 5632 (1972)
- [3] M. Imami and W. L. Borst, *J. Chem. Phys.* **61**, 1115 (1974)

9:15

KB 6 Cross Sections for Electron Collisions with H₂O,* S. K. SRIVASTAVA and SHUANGHAI ZHENG#, JET PROPULSION LABORATORY, California Institute of Technology - Electron collision cross sections for water are important for modelling various planetary and electrical discharge plasmas and energy degradation calculations. The cross sections of interest are ; 1) Elastic scattering, 2) Momentum transfer, 3) Inelastic scattering, 4) Ionization, and 5) Attachment. We have recently completed a survey on these cross sections and have critically evaluated their accuracies. We have also measured ionization and dissociative ionization cross sections near the threshold region and find large differences with the previously published data.

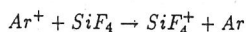
THURSDAY MORNING

Our recently measured cross sections and the survey will be presented at the conference.

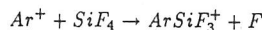
* Work supported in part by the Planetary Atmospheres Program of NASA and in Part by AFOSR.
NRC-NASA Resident Research Associate

9:30

KB 7 Dissociative Ionization and Charge Transfer in SiF_4 ,* R. NAGPAL, P. HAALAND, and A. GARSCADDEN, WL/POOC-3, Wright-Patterson AFB, OH 45433- Dissociative ionization cross sections of SiF_4 have been examined by Fourier Transform Mass Spectrometry (FTMS) from threshold to 50 eV. At low gas pressures, formation of SiF_3^+ is observed as the dominant ionization channel. In the electron energy range between 20-50 eV, the cross sections for the formation of SiF_3^+ are greater than those for Ar^+ by ≈ 10 -25%. When combined with published values for inelastic scattering of electrons by SiF_4 , the computed Townsend ionization coefficients are substantially larger than the experimental values. Adjustments of low-energy cross-sections (vibrations and dissociation) are used to reconcile the FTMS data with the swarm analyses. Although the yield of SiF_4^+ by electron impact is very low, we find rapid charge transfer from ground state argon ions to SiF_4 :



At higher gas pressures, a cluster ion is also observed which we ascribe to the reaction:



*Work Supported by Air Force Office of Scientific Research.

9:45

KB 8 Electron Attachment to S_2OF_{10} ,* P.G. Datskos, I. Sauer, J. Hoy, L. A. Pinnaduwege, Oak Ridge National Laboratory and The University of Tennessee - The disulfur compound bis (pentafluorosulfur)oxide (S_2OF_{10}) is a byproduct of spark induced breakdown of sulfur hexafluoride (SF_6) when either O_2 or H_2O is present,¹ and, in the case of oxygen, is formed at the expense of the highly toxic byproduct S_2F_{10} . Both S_2OF_{10} and S_2F_{10} are detected with high sensitivity by electron capture detection, providing impetus for determining the rate constants for electron capture, particularly at low electron energies. The total electron attachment rate constant $k_a(\langle \epsilon \rangle)$ for S_2OF_{10} has been measured, in a buffer gas of N_2 , as a function of the mean electron energy $\langle \epsilon \rangle$ (0.046 - 0.911 eV) using an electron swarm technique. The electron attachment rate constant $k_a(\langle \epsilon \rangle)$ increases monotonically with decreasing $\langle \epsilon \rangle$ below 0.911 eV and its magnitude is larger than that of SF_6 . From the measured $k_a(\langle \epsilon \rangle)$ the total electron attachment cross section $\sigma_a(\epsilon)$, determined using an unfolding technique, is larger than the maximum s-wave capture limit $\pi\lambda^2$ and is consistent with previous measurements from low pressure beam experiments.²

* Work supported in part by the Office of Energy Management, DOE, under contract DE-AC05-84OR21400 with Lockheed Martin Energy Systems, Inc., and the University of Tennessee Science Alliance Program.

¹ I. Sauer, S. M. Mahajan, and R. A. Cacheiro, *Gaseous Dielectrics VII* (L. G. Christophorou and D. R. James, eds.), Plenum, 1994, p. 423.

² J. K. Olthoff, K. L. Stricklett, R. J. Van Brunt, J. H. Moore, J. A. Tossell, and I. Sauer, *J. Chem. Phys.* 98(12), 9466 (1993).

SESSION LA: DUSTY PLASMAS

Thursday morning, 12 October 1995

Berkeley Marina Marriott

Yerba Buena/Treasure Rooms, 10:15-11:45

C. Cui, presiding

10:15

LA 1 Ordered structures in a strongly-coupled dusty plasma using a GEC Reference Cell

J. Goree and R.A. Quinn, U. Iowa, Iowa City, IA, and C. Cui, Applied Materials, Santa Clara, CA

Experiments with the newly discovered Coulomb lattice structures, termed "plasma crystals" are described. These stable structures are

formed by charged microspheres levitated above the lower electrode of rf discharges. We used a GEC Reference Cell, operated using krypton at ≤ 1 Watt 13.56 MHz with the upper electrode replaced with a window. Coordinates of particles are determined from digitized video images of a laser-illuminated slice of the particle cloud. From these, pair and bond-orientational correlation functions are analyzed, yielding a quantitative description of the phase of the plasma crystal structures. For the data of Cui, Goree and Quinn, the scale lengths are on the order of 4 and 50 inter-particle spacings respectively, indicating a hexatic phase, which is a state theoretically predicted to be part of a gradual melting transition in 2-D systems. Defect maps are also consistent with this determination of phase.

10:30

LA 2 Homogeneous Aggregation of Dust Particles in Plasmas, P. Haaland, A. Garscadden, B. Ganguly, and J. Williams, WL/POOC3, Wright-Patterson AFB, OH 45433. Fine particles with diameters in the μm range can be grown by accretion of positive ions in laboratory plasmas. Although they are roughly spherical, these dust particles have remarkable, cauliflower-like morphology when viewed by low-voltage scanning electron microscopy. Negative charge on spherical particles can be computed from probe-theory and leads to floating potentials of a few volts. The coulomb repulsion between grains is far greater than their thermal kinetic energy, consistent with homogeneous growth into the observed spherical particles. However, the coulomb repulsion would seem to preclude a structural motif of connected beads that is also observed *ex situ*. The cauliflower morphology, which can have domains of high curvature, permits field emission of electrons and thereby alters the floating potential of some grains enough to collapse the inter-grain repulsion and permit condensation into connected dust dimers and beads.

10:45

LA 3 Comparison of calculated and measured location of potential traps for dust particles in rf discharges, A. MERAD, J.P. BOEUF, and L.C. PITCHFORD, CPAT, CNRS Toulouse, France and J.-L. DORIER and Ch. HOLLENSTEIN, CRPP-EPF Lausanne, Switzerland - Systematic comparisons between 2-D calculations¹ of the location of potential traps for dust particles and measurements² of the dust particle scattering intensity profiles as well as comparisons between the measured emission profiles and the calculated ionization rate have been made voltage at 0.2 mbar for different conditions of geometry and rf voltage. A small concentration of amorphous silicon dust particles was trapped in argon discharges at low power so that the dominant force acting on the dust particles is the electrostatic force. The scattering intensity profile gives a mapping of the dust particle location and the emission intensity can be qualitatively compared to the calculated ionization rate. Good agreement is found in all cases, and, in particular, the calculations and the experiments both show that the relative locations of the potential and ionization rate maxima are highly dependent on the chamber geometry.

1. J.P. Boeuf and L.C. Pitchford, *Phys. Rev.E* 51, 1376 (1995).

2. J.-L. Dorier, Ch. Hollenstein and A.A. Howling, *J. Vac. Sci. Technol.* A13, 918 (1995).

11:00

LA 4 Particle Nucleation, Growth and Transport in Plasma Processing Reactors* HELEN H. HWANG, FRED Y. HUANG and MARK J. KUSHNER Univ. of Illinois, Dept. of Elect. and Comp. Engr., Urbana, IL 61801 USA - Particle contamination of wafers in plasma processing reactors is a continuing concern. The transport of particles is dominated by electrostatic, ion-drag, thermophoretic and fluid-drag forces, all of which have different dependencies on particle size. Therefore rates of nucleation and growth of particles are important to both production of particles and their transport. We have developed a 2-d simulation of the nucleation, growth and transport of particles in plasma processing reactors. The model tracks the growth and trajectories of individual particles while considering collisions resulting in accretion, charging, neutralization, Brownian

motion, and self diffusion in addition to the previously mentioned forces. We will discuss results for particle growth in Ar/SiH₄. The trajectories of accreting particles are first towards the center of the reactor and then towards the sheath edges. The details of the trajectories depend on power deposition and gas flow since these parameters determine the rate of growth and residence time.

*Work supported by SRC, Sandia National Lab/Sematech, NSF and the Univ. of Wisconsin ERC for Plasma Aided Manufacturing.

11:15

LA 5 In Situ Diagnostics of the Temporal Evolution of Plasma Generated Particle Distributions by Laser Light Scattering; URSULA I. SCHMIDT and DAVID B. GRAVES; University of California at Berkeley, Dept. of Chemical Engineering

Contamination due to plasma-generated particulates is one of the major issues affecting the yield loss in microelectronics fabrication. In addition to particle measurements in the downstream gas flow or on the wafer surface after the plasma process, laser light scattering performed in situ during the process provides further information about particulates. Particulate sizes and number densities can be derived both spatially resolved and as a function of time. The laser light scattering system we will describe allows the quantitative determination of particulate size and number density in an rf discharge by detecting the scattering intensity at two separate angles (angular dissymmetry) or at two different orientations of the polarization plane (polarization dissymmetry), respectively. We will discuss the calibration procedure required in order to obtain quantitative results for particulate size and number density. Based on this data analysis, we will report on the temporal evolution of the spatial distribution of aluminum particles in an Ar discharge. For example, the scattering pattern can change from a continuous cloud of particles filling the entire inter-electrode gap to a narrow band of intense scattering near the grounded electrode. Other changes of light scattering patterns with time have been observed under different conditions. The implications of these observations in terms of particle generation and evolution in plasmas are discussed.

11:30

LA 6 Simulation of the Behavior of Dust Contaminants in Plasma Processing Devices

Giovanni Lapenta and J.U. Brackbill
lapenta@ulisse.lanl.gov
Los Alamos National Laboratory

Abstract

Dust contaminants reduce severely the yield of the plasma processing stages of semiconductor manufacturing by falling on semiconductor wafers and damaging irreversibly the chips being produced. Recent studies¹ have shown that dust contaminants are trapped in specific regions at the sheath edge over and around the wafer. Careful design of the processing device and particularly of the substrate holder can potentially reduce the dust contamination and increase the yield. In the present work, we present a complete self consistent simulation package² to study the behavior of dust contaminants. The method is based on a fluid simulation of the glow discharge coupled with a description of the dust motion. The method can be used to predict the trapping of dust in specific regions and can guide the development of new design configurations that increase the yield.

SESSION LB: FLAT PANEL DISPLAYS

Thursday morning, 12 October 1995

Berkeley Marina Marriott
Belvedere Room, 10:15-12:00
Bob McGrath, presiding

10:15

LB 1 Backscattering of Secondary Electrons in an AC Plasma Display Cell. J. P. VERBONCOEUR, *Lawrence Livermore National Laboratory*—In the characterization of ac plasma panels, the secondary emission model plays a crucial role in the evolution of the discharge. Ions created by electron-neutral ionization are accelerated through the cathode fall, generating secondary electrons upon impact with the cathode. The secondary electrons obtain sufficient energy

through the cathode fall to generate one or more ionization events, sustaining the discharge. A small change in the secondary electron flux can result in dramatic changes in the evolution of the discharge.¹

In this study, the secondary electron emission current is examined in neon-xenon mixtures for pressures and fields typical of ac plasma panels. Typical fluid models are unable to model the full kinetics of the secondaries in the cathode fall, particularly backscattering. A PIC-MCC code is employed to determine the backscattered current, and provide a modified secondary emission coefficient for use in fluid models.

This work performed at Lawrence Livermore National Laboratory under the auspices of the U.S. Department of Energy under Contract Number W-7405-ENG-48.

¹O. Sahni and C. Lanza, "Influence of the secondary electron emission coefficient of argon on Paschen breakdown curves in ac plasma panels for neon+0.1% argon mixture", *J. Appl. Phys.* 47, 5107 (1976).

10:30

LB 2 1-D Multi-Species (He/Xe) Fluid Model of a Color AC Plasma Display Panel*. RAMANA VEERASINGAM**, R. B. CAMPBELL and R. T. McGRATH, *Sandia National Laboratories, New Mexico* - The color ac plasma display panel (AC-PDP) is an especially viable technology for large screen area video display monitors. We have developed a 1-D fluid model to simulate the plasma dynamics in a color AC-PDP with a goal to understand the operation of a panel including: bi-stable voltage margins, power dissipation, UV emission and light output. The model follows several excited states of helium and xenon and includes photon emission from xenon dimers and Holstein corrected emission from decaying excited states of atomic xenon. The model includes Poisson's equation, a surface charge buildup equation, and a circuit equation. Ionization and excitation rates are determined from O-D Boltzmann calculations and are parametrized as a function of E/N. Two methods of determining the bistable margin including: (i) multi-pulse simulations and (ii) from the voltage transfer characteristic are performed. The model has been benchmarked to experiments and is presently used as a tool to investigate the various operating ranges in parameter space through simulations to guide in the design of AC-PDP panels. We will present results from our simulations benchmarked with experiments.

* Work supported by US DOE. ** The Pennsylvania State University

10:45

LB 3 Assessment of Computational Methods for Simulating AC Plasma Display Panels, G.J.Parker, J.P. Verboncoeur, B.M. Penetrante, P.A. Vitello, and J. Shon", *Lawrence Livermore National Laboratory, Sandia-Livermore National Laboratory*— This paper compares fluid and particle simulations for configurations typical of double-substrate AC plasma display panels. The purpose is to test the validity of various approximations used in the simulations. Various concentrations of neon/xenon gas mixtures are simulated and the results compared to experimental observations. One fluid model consists of the usual "local field" approximation where the electron transport and rate coefficients depend on the local and instantaneous value of the electric field. Another fluid model solves the electron temperature equation instead. Particle-in-cell/Monte-Carlo-collision simulations are also shown. Results are compared to experimental observations for different Ne/Xe concentrations. A fast zero dimensional model has been developed to give quick voltage transfer curves and electron energy loss channels of reasonable accuracy.

This Work performed at Lawrence Livermore National Laboratory under the auspices of the U.S. Dept. of Energy under contract number W-7405-ENG-48.

11:00

LB 4 Using GEC cell equipment for ac-PDP research*, P.J. DRALLOS, V.P. NAGORNY, and W. WILLIAMSON, JR., *Dept. of Physics and Astronomy, Univ. of Toledo, Toledo, OH 43606* - A single ac-PDP picture element occupies a volume of approximately 10⁻⁶ cm³. This small physical size contributes to the difficulties of performing experimental measurements and diagnostics of the ac-PDP discharges. It happens that, by scaling the discharge length, L, inversely with the pres-

THURSDAY AFTERNOON

sure, p , the scaled geometry can be comfortably accommodated with standard GEC reference cell equipment. Our analytic theory predicts that some of the plasma diagnostics will remain constant, while others will scale proportionally to L or L^2 . Computer simulations which support these predictions will be shown, with some examples explaining how the GEC cell representation can be related to actual PDP dynamics. We will also describe and show simulations of a proposed GEC cell experiment, designed to measure the effective secondary electron emission coefficient from MgO surfaces by impact of thermal, xenon ions.

* This work supported by the USDOE under contract No. DE-AC04-76P007898.

11:15

LB 5 Interpreting ac-PDP modeling and experimental results*, V.P. NAGORNY, P.J. DRALLOS, and W. WILLIAMSON, JR., Dept. of Physics and Astronomy, Univ. of Toledo, Toledo, OH 43606 - Computer models, being approximations of the real world, may vary from one researcher to another. Consequently, direct comparisons between different models or experiments are not always straightforward. Occasionally, both experiment and theory may each be correct, yet may still appear to disagree with one another¹. Comparisons among different ac-PDP models and experiments, of inappropriate parameters and diagnostics, have led to a considerable amount of confusion. Our research has identified some previously unpublished parameters which can be used to enable more meaningful comparisons to be made among other models and experiments. We will present a brief outline of our theory, and show some illustrative examples of our analysis procedures. Common mistakes and misinterpretations will also be discussed.

1. Amikam Aharoni, Physics Today 43#6, p. 33 (1995).

* This work supported by the USDOE under contract No. DE-AC04-76P007898.

11:30

LB 6 Trapping of Radiation in Plasma Flat Panel Displays* M.E. RILEY and W. J. ALFORD, Sandia National Labs. - We analyze the mechanisms that are relevant for radiation trapping in a near-atmospheric-pressure mixture of Xe and He typical of plasma flat panel displays. The trapping of the Xe 147 nm emission is reasonably described by the Holstein formula¹ with the Huennekens-Colbert² procedure for combining Doppler and pressure broadening. In addition to the trapping analysis, we present a space-dependent approximation for the trapped decay rate that can be useful in simulations of the discharge kinetics. The decay operator is local in space and should be easily included in implicit plasma codes.

*Work performed at Sandia National Labs and supported by US DoE under contract DE-AC04-94AL85000.

¹T. Holstein, Phys. Rev. 72, 1212 (1947) and Phys. Rev. 83, 1159 (1951).

²J. Huennekens and T. Colbert, J. Quant. Spectros. Radiat. Transfer, 41, 439 (1988).

11:45

LB 7 2-D Model of Plasma Panel Display Cells in "Barrier-Rib" Geometries, J.P. BOEUF and L.C. PITCHFORD, CPAT, CNRS, Toulouse, France - We have developed a 2-D fluid model of AC plasma display panels which is suitable for arbitrary Cartesian geometries. AC plasma display cells are dielectric barrier discharges, where the electrodes consist of a series of parallel metallic strips covered with a dielectric layer. In the simplest configuration, the dielectric faces, separated by about 100 μm , are oriented so that their electrode arrays are orthogonal. A transient discharge can form at the intersection of a line and a column electrode. We present here results in Ne-Xe (90-10) at 500 Torr and for a "barrier rib" geometry in which the adjacent cells (spaced every 200 μm) are separated by rectangular dielectric ribs attached to one of the dielectric faces. We

will show results of the characteristics of the plasma display cells for different conditions and the spreading of the plasma along the dielectric face as surface charges accumulate. Under these conditions, the current pulse duration is on the order of 10-20 ns. Results will also be presented for coplanar electrodes where the model predicts longer pulse durations.

SESSION MA: MATERIALS PROCESSING: DEPOSITION

Thursday afternoon, 12 October 1995

Berkeley Marina Marriott

Yerba Buena/Treasure Rooms, 13:30-15:00

Ken Stalder, presiding

13:30

MA 1 Bias-Enhanced Nucleation of Diamond by Microwave Plasma CVD: Surface Effects, SATHEESH K. AMBADI, P. R. EMMERT, and A. GARSCADDEN, Wright Laboratory, WPAFB - Applying a negative bias to substrates for short periods of time prior to growth has proved to be advantageous in achieving high nucleation densities ($\sim 10^9$ - 10^{12} cm^{-2}) during diamond film deposition. Biasing does not cause surface damage as opposed to other surface pretreatment methods. The understanding of the growth of the intermediate layer of carbon deposited during biasing and achieving control of the nucleation mechanism are essential for epitaxial growth of diamond films. Experiments carried out using a microwave plasma with negatively biased substrates show that the nucleation density of diamond increases with bias time up to about 30 minutes and then decreases with longer biasing times. This behavior is found to correlate strongly with discharge current measurements during biasing, and the surface topography of the intermediate layer deposited during biasing. Calculations have been carried out linking the electron emission processes (secondary and field emission) and the sheath thickness variations with time to the measured time-dependent bias current and coverage. The role of the intermediate carbon layer deposited during biasing in promoting enhanced nucleation will also be discussed.

13:45

MA 2 Ultra-Sensitive Optical Absorption Spectroscopy of a Microwave Plasma Assisted Diamond Growth Facility* W.B. JAMESON, C.J. ERICKSON, K.L. MENNINGEN, M.A. CHILDS, L.W. ANDERSON, J.E. LAWLER, U. of Wisconsin, Madison - Ultra-sensitive multi-element absorption spectroscopy was performed on a Microwave Plasma Assisted Chemical Vapor Deposition (MPACVD) diamond growth facility. A MPACVD facility was designed and constructed, in which diamond films were grown. The absolute methyl radical column density [CH_3], and the line average of the gas temperature were measured as functions of position in the discharge for input methane concentration from 0 to 1%. The average absolute methyl radical density by volume [CH_3] was obtained using a path length of 6 cm and varied from 1 to 6×10^{13} cm^{-3} . The gas temperature was measured using H_2 emission spectrum and was found to be 1200 ± 100 K throughout the discharge. An upper bound of 10^{10} cm^{-3} was placed on the CH density, and from this an upper bound of 0.008 was placed on the hydrogen dissociation fraction [$\text{H}/[\text{H}_2]$] from the reactions linking CH and CH_3 in local thermodynamic equilibrium.

*Supported by the Army Research Office

14:00

MA 3 Surface Topography of Intermediate Films Deposited during Substrate Biasing and Enhanced Nucleation of Diamond by Microwave Plasma-Assisted Deposition, P. R. EMMERT, and SATHEESH K. AMBADI, Wright Laboratory, WPAFB - Experiments have been carried using a microwave plasma (H_2/CH_4) to achieve high nucleation densities of diamond and to understand the processes responsible for the nucleation enhancement obtained by negatively biasing the substrates (4" polished silicon wafers). The bias times were varied from 5 to 50 minutes. Intermediate films with significant diamond content were observed on all substrates except for the lowest biasing times (5 minutes); however, the

intermediate film quality deteriorated rapidly for biasing times in excess of 30 minutes. Scanning Electron Microscopy and Atomic Force Microscopy were used to obtain the surface topography of the films and the film thickness was measured using surface profilometry. Subsequent deposition (for 60 minutes) on these films without biasing and reduced CH₄ resulted in diamond nucleation densities (~10⁹ - 10¹⁰ cm⁻²) that correlated well with the tip size distribution obtained after biasing alone. Experimental results for the tip-size distribution and the nucleation density variation with biasing time will be presented. The effects of changing the ion flux and ion kinetic energy on the deposited intermediate layer during biasing and on diamond nucleation will also be discussed.

14:15

MA 4

Ion Chemistry and Deposition from ((C₂H₅)₂N)₄Ti, PETER HAALAND, WL/POOC3, Wright Patterson AFB, OH 45433, Dissociative ionization of the title compound, which is a precursor for plasma-enhanced chemical vapor deposition of Ti_xN_y passivation layers, has been examined by Fourier Transform Ion Cyclotron Resonance Mass Spectrometry. Of the 6970 positive ions which might be formed fewer than twenty are observed, and of these none contain titanium atoms. *Ab initio* electronic structure calculations show oxidation out of the t₂ highest occupied molecular orbital causes substantial Jahn-Teller distortion of the parent ((C₂H₅)₂N)₄Ti⁺ ion and leaves positive character on the amine nitrogens rather than the titanium atom. These results imply that plasma-enhanced CVD of titanium nitride films occurs by neutral, rather than charged, radical precursors.

14:30

Reaction Mechanisms in the PECVD of a-C:H:O:N Films, S.F. DURRANT, E.C. RANGEL and M.A. BICA DE MORAES IFGW, UNICAMP, Campinas, SP, Brazil - Plasma/polymer surface reactions in the PECVD of propanol/nitrogen mixtures in a glow discharge were investigated. Initially, a film from such a mixture was deposited. Then, temporal trends in plasma concentrations of the species H, CO, CN, CH and OH following cutting of either of the principal gas flows were determined by a dynamic form^{1,2} of actinometric optical emission spectrometry. In plasmas of propanol alone the species H, CO, CH and OH were detected, indicating the role of gas-phase reactions in their production. However, in plasmas of nitrogen alone, these species, along with CN, were also detected. Thus plasma nitrogen plays a role in the production of these species via surface reactions.

[1] S.F. Durrant, E.C. Rangel and M.A. Bica de Moraes, *J. Vac. Sci. Technol. A*, in press (1995).

[2] S.F. Durrant and M.A. Bica de Moraes, *J. Vac. Sci. Technol. A*, in press (1995).

14:45

Diagnostic Measurements of Gas Species, Temperatures and Plasma Properties of Subsonic and Supersonic Arcjet Plasmas Used to Deposit Diamond Thin Films, J. B. JEFFRIES and K. R. STALDER, SRI International—We have developed and applied a number of diagnostic probes of the gas phase processes that occur in arcjet plasmas which are used to deposit diamond thin films. Laser-induced fluorescence (LIF) methods can measure the spatial distribution of various molecular and atomic species throughout the arcjet region. LIF can also measure the temperatures of various species. Optical emission is used to observe species that are not accessible with LIF. Spatially-resolved mass spectroscopic sampling of the boundary layer yields information on the two-dimensional distribution of important growth species and their temperatures near the deposition substrate. Finally, plasma probing using Langmuir probe techniques yields information on the temperature and density of charged species in the plasma jet. All of these diagnostics taken together enable us to quantify and model the diamond growth environment. We will briefly discuss these techniques and

results.

* Work supported by ARPA via the Naval Research Laboratory, and ARO under Contract DAAH04-93-K-0001

SESSION MB: DIAGNOSTICS: ELECTRICAL METHODS

Thursday afternoon, 12 October 1995

Berkeley Marina Marriott

Belvedere Room, 13:30-15:00

Bert Ellingboe, presiding

Invited Paper

13:30

MB 1 Ion Current Based Probe Diagnostics (a critical review), V.A. GODYAK, OSRAM SYLVANIA INC., 71 Cherry Hill Dr. Beverly, MA 01915 - This presentation reviews the practical aspects of probe diagnostics based on the ion part of the Langmuir probe characteristics (single, double and triple probe techniques). It has been known for a long time (Langmuir was the first to have noticed this) that the plasma parameters obtained using the ion part of the probe characteristic may differ considerably from that found using the electron part of the probe characteristic. From a detailed discussion of numerous assumptions on which different ion current theories are based, it is shown that in the majority of plasma experiments these assumptions are not valid. As a result, incorrect values of the ion density, electron temperature and plasma potential are frequently obtained. On the basis of numerous studies carried out over the last 30 years, it is shown that orbital motion theory for ion collection to the probe, which has become so popular in recent years, is a most unreliable one for inferring plasma parameters. On the other hand, a few cases are specified where the ion part of the probe characteristics could give correct information.

Contributed Papers

14:00

MB 2 Ion Dynamics in Pulsed & Sinusoidally Driven Electrostatic Probes N. ST.J. BRAITHWAITE* AND M. A. LIEBERMAN ECS Department, UC Berkeley, CA 94720 - Experiments and particle simulations have been performed in planar geometry in which a probe is excited by a sinusoidal source or a rectangular voltage pulse. The total current includes displacement and conduction components; the former are associated with electron dynamics and the modulation of space charge in the sheath while the latter concerns the charge collected by the probe. With sinusoidal excitation it is found that the phase of the net current measured in the external circuit changes markedly at frequencies comparable with the ion plasma frequency. At both higher and lower frequencies the probe current is in quadrature with the probe potential, whereas near ω_{pi} there is an in-phase component which almost halves the phase difference. The effect is seen in experiments performed in an argon ICP and in scaled simulations. With rectangular pulses, a related effect is seen in the charge collected by an electrostatically screened particle detector. In all experiments, stray displacement currents are minimized through the use of triaxial cable with an actively driven screen. It is concluded that these observations can be attributed to ion inertia and are accordingly sensitive to the mass of ions involved.

*The Open University, UK.

14:15

MB 3 Probe Detection of Phased EEDFs in RF Discharges*, F.F. CHEN and D.D. BLACKWELL, UCLA--Landau damping can cause fast electron tails ("beams") to be created during the accelerating phase of the RF electric field. To measure electron energy distribution functions (EEDFs) in an RF plasma requires careful compensation for RF potential fluctuations. Normally, the probe tip or energy analyzer collector is driven to follow the floating potential (V_f) of an electrode close to the collector. This

THURSDAY AFTERNOON

method works for a steady-state beam; but if the beam is pulsed, V_f swings negative just when the fast electrons are present. The time-averaged probe characteristic then does not "see" the beam at all. Ironically, if the beam is well separated from the bulk distribution, it can be detected by a poorly RF compensated probe, though the Maxwellian part will be completely distorted. We have checked our computations experimentally with an electron gun which adds a fast electron component to a helicon plasma. The assertions made above have been borne out. We also describe attempts to design a probe that is compensated with the space potential, rather than the floating potential.

*Supported by SRC, Wisconsin ERC, and LLNL-PPRI.

14:30

MB 4 Accuracy of Electric Probes in Low Frequency RF Plasmas,* M. TUSZEWSKI and J.A. TOBIN, Los Alamos National Laboratory - The densities of 0.46 MHz rf inductively coupled plasmas are estimated by combining 35 GHz microwave interferometer, cylindrical probe, and mass spectrometer data. Measurements are made inside a 0.4-m-diameter cylindrical vacuum vessel, 0.2-m downstream from the source. The peak densities n_e and n_i are inferred in the range 10^9 - 10^{11} cm⁻³ for rf powers of 200-500 W and argon and nitrogen gas fills of 1-10 mTorr. The n_e values are obtained from interferometry data and from probe radial profiles. The n_i values are obtained from ion saturation currents using probe orbital theory. Three probes are tested: a single probe, a single rf-compensated probe, and a symmetrical double probe. The main results are: (1) ratios $n_i/n_e = 1 \pm 0.2$ are obtained for all argon data, (2) ratios n_i/n_e up to 5 are obtained with nitrogen at low rf powers and high gas fills, (3) large n_i/n_e values correlate well with large probe rf voltages, and (4) significant improvements are obtained with rf compensation and with a well-shielded double probe.

* Work supported by the US Department of Energy.

14:45

MB 5 The Effect of Metastable-Metastable Collisional Ionization on the Electron Energy Distribution Function of pulsed discharges.* L. J. OVERZET, M. B. HOPKINS[†], and CHRIS BOWLES University of Texas at Dallas, Richardson, TX 75083.

— A time resolved Langmuir probe technique has been used to obtain evidence of metastable-metastable ionization processes in the afterglow of pulsed discharges in helium and argon. While these processes have been postulated and are understood,¹ proof of their importance in the electron energy distribution function (EEDF) during the afterglow period had not yet been found. We have found significant peaks in the EEDF corresponding to the helium and argon metastable-metastable ionization processes near 15 eV and 8 eV respectively. We have seen increasing electron densities in both helium and argon afterglows caused by this ionization process as well.

* Work supported in part by the National Science Foundation and The State of Texas Advanced Research Program.

¹ See for example: K. E. Greenberg and G. A. Hebner J. Appl. Phys. 73, 8126 (1993).

[†] Dublin City University, Dublin, Ireland

POSTER SESSION NA: DEPOSITION

Thursday afternoon, 12 October 1995

Berkeley Marina Marriott

Belvedere/Angel Rooms, 15:45-17:30

NA 1 Actinometric Optical Emission Spectroscopic Study of Fluorinated Film-depositing Plasmas, S.F. DURRANT, N.C. DA CRUZ and M.A. BICA DE MORAES,

IFGW, UNICAMP, Campinas, SP, Brazil - Discharges were produced in tetramethylsilane/sulfur hexafluoride/helium mixtures in a deposition system fed with radiofrequency power (40 Mhz, 100 W max. power)¹. Conventional actinometric optical emission spectrometry¹ was used to determine trends in the concentrations of plasma species such as Si, F, CF₂, H, and CH as a function of the proportion of SF₆ in the feed. In addition, a dynamic form of actinometry² was employed in which the SF₆ flow was cut following the deposition of a fluorinated film. The measured temporal trends in the plasma concentrations give clues as to the importance of plasma/polymer-surface reactions, which, for example, are partly responsible for the production of plasma F and CF₂. The dynamic method is simple to implement and widely applicable.

[1] S.F. Durrant, N. Marçal, S.G. Castro, R.C.G. Vinhas, M.A. Bica de Moraes & J.H. Nicola, Thin Solid Films, 259, 139 (1995).

[2] S.F. Durrant, E.C. Rangel & M.A. Bica de Moraes, J. Vac. Sci. Technol. A, in press (1995).

NA 2 Production of MOCVD plasma for Cu thin film deposition*, M. SHIRATANI, K. WATANABE, H. J. JIN, H. KAWASAKI, T. FUKUZAWA, T. KINOSHITA and Y. WATANABE. Department of Electrical Engineering, Kyushu University - We have developed a new plasma CVD reactor for thin film deposition with a material supply system which offers accurate and reproducible feed of metal organic material to the reactor.¹ Using the reactor, Cu films of high purity and low resistivity have been successfully produced. Compositions and deposition rates of the films depend appreciably on material of a substrate such as Si, SiO₂ and Al, indicating that surface reactions play an important role in the deposition processes. Furthermore, radicals produced due to decomposition of Cu(hfa)₂ and/or H₂ by electron impact have been found to be necessary for the deposition processes. Density of Cu atoms measured by a light absorption method was 10^8 - 10^9 cm⁻³, which was not enough to obtain the observed deposition rates.

*Work supported by a Grant-in-Aid for Scientific Research by the Ministry of Education, Science and Culture of Japan.

¹M. Shiratani, K. Shibata, H. Kawasaki, T. Fukuzawa, T. Kinoshita and Y. Watanabe, Proc. 12th Symp. Plasma Processing (edited by T. Makabe, Sendai, Japan) 71 (1995).

NA 3 Measurements of Electron Densities and Temperatures in Supersonic Arcjet Plasmas Operating Under Diamond Growth Conditions,* K. R. STALDER, E. A. BRINKMAN, and J. B. JEFFRIES, SRI International—We have measured the spatial variation of plasma parameters in a supersonic DC arcjet plasma used in the deposition of diamond thin films. A Langmuir probe was inserted into the plasma jet from the side. The plasma density was approximately 10^{11} cm⁻³ 25-mm downstream from the arcjet exit orifice. The electron temperature was 8.7 eV, or 100,000 K, which is approximately twenty to thirty times hotter than the gas temperature. Since the arcjet gas pressure ranged from 23 to 32 torr, the corresponding electron-neutral collision frequency was approximately 10^{10} - 10^{11} s⁻¹. The electron thermal equilibration time under these conditions is about 1 to 10 μ s which is just slightly shorter than the gas transit time to the probe. The non-equilibrium nature of the electrons in this situation is thus explained by the time scales for electron thermalization compared to the gas transit time. We will present data for the spatial variation of these plasma parameters and interpret them in light of the gas species determined from laser-induced fluorescence measurements.

* Work supported by ARO under Contract DAAH04-93-K-0001

NA 4 Effects of Carbon Source Gases on Diamond Thin Film Formation using RF Plasma CVD Assisted by Microwave Plasma, K. YAMADA, E. MIZUNO, S. KATO, M. HIRAMATSU, M. NAWATA, M. IKEDA*, M. HORI* and T. GOTO*, Meijo Univ. and *Nagoya Univ. Japan - For the formation of diamond thin films,

CH₃ and H radicals have been regarded as important reactive species. In this work, we investigated the effects of CH₃ radical density on diamond film formation using a parallel plate RF (13.56 MHz) plasma CVD reactor, which mainly produced CH₃ radical, equipped with H radical source by remote microwave (2.45 GHz) plasma. Diamond film was deposited by changing the mixture ratio of CH₃OH and CH₄ at the total pressure of 1.33 Pa, H₂ / H₂O pressure of 5.34 / 6.67 Pa, RF power of 100 W, microwave power of 100 W and substrate temperature of 600 °C. CH₃ radical density in CH₄ plasma are found to be higher by one order of magnitude than that in CH₃OH plasma using infrared diode laser absorption spectroscopy. However, deposition rate of diamond film was almost constant with the variation of the mixture ratio of CH₃OH and CH₄. Diamond formation in this condition was considered to be affected by the amount of H radicals. The effects of fluorocarbon gas on diamond formation have been also investigated.

NA 5 Gas Phase Composition During Thermal Plasma Assisted CVD of Diamond Films. D.W. ERNIE, P.G. GREUEL, and J.T. ROBERTS, U. of Minnesota - Mass spectrometric studies of the growth precursor and other gaseous species present near a molybdenum substrate surface during diamond film deposition from a 15 kW, 3.3 MHz inductively coupled torch operating between 50 to 400 torr in CH₄/H₂/Ar and C₂H₂/H₂/Ar mixtures have continued.¹ Quantitative measurements of the stable species CH₄, C₂H₂, C₂H₄, and C₂H₆, and of the CH_x (x≤3) unstable radical species, will be presented as a function of discharge parameters. It has been found that the most abundant C₂ species is C₂H₂, followed by C₂H₄, with little detectable C₂H₆. The stable species composition varies only slightly when the feedstock is changed from CH₄ to C₂H₂. Calibration of the threshold ionization technique used for detection of the CH_x radicals has yielded absolute concentrations of CH₃ and CH₂ radicals consistent with computer simulations. These results will be compared with previous theoretical and experimental studies and implications for diamond growth mechanisms will be discussed.

*Work supported by NSF Grant No. ECD-8721545, Engineering Research Center for Plasma-Aided Manufacturing.

¹ H.J. Yoon *et al.*, 47th GEC, Gaithersburg, Paper MA-5 (1994).

NA 6 Particle Formation and Optical Emission in RF Discharge of SiH₄. B. JELENKOVIC, A. LARACUENTE and A. GALLAGHER, JILA, U. of Colorado and NIST - The SiH₄ rf discharge was investigated for particle formation and their effect on optical emission intensities in the range of pressure 0.15-0.5 Torr, flow 5-10 sccm and silicon deposition rates 0.5-2 Å/s. The discharge was operated between 90x52 mm electrodes, with a 17 mm gap. The Mie scattering and optical emission was measured along the longer dimension, i.e., direction of gas flow. The optical emission data show a maximum around the down stream edge of the electrodes (gas exit) at the lower pressures (< 0.25 Torr). When low pressure is combined with low flow, we see pressure dependent position of a maxima of Mie scattering near the gas exit. SiH₄* emission increases at the position of increased Mie scattering. At other pressures and flows an increase of Mie scattering can be seen well beyond the gas exit (> 3 cm), where very little discharge emission is detected. The discharge resistivity continuously increases with pressure, i.e. voltage current phase shift changes from 75 to 60°. At these higher pressures we do not see significant particle formation. This might be due to the smaller sizes of particles and/or the absence of trapping electric fields near the gas exit.

NA 7 Electron Density and Temperature in Low-Pressure RF SiH₄ Plasmas Diluted with H₂, He, Ar and Xe. H. NOMURA, A. KONO AND T. GOTO, Nagoya Univ., Japan - Effects of He, Ar, Xe and H₂ dilution on the electron density (N_e) and temperature (T_e) in a capacitively-coupled RF (13.56 MHz) SiH₄ plasma have been investigated in order to correlate the results with our recent SiH_x density measurements in the plasma.

The electron density and its loss rate (R_L) in the afterglow were measured using a microwave-cavity-resonance technique. The behavior of T_e was estimated from N_e and optical emission intensity measurements. SiH₄ addition to the dilution gases caused marked increase of R_L , indicating the generation of electron-attaching molecules (or particles) in the plasma. T_e increased with increasing dilution (up to dilution ratios of 95%) for all gas mixtures, but for Xe dilution it then decreased to approach a value in a pure Xe discharge. The results could be understood from simple particle-balance consideration. The behaviors of N_e and R_L upon dilution differ considerably for different dilution gases, suggesting a complicated mechanism of producing electron-attaching molecules.

NA 8 Production and Loss of SiH_x Radicals in a Low-Pressure RF SiH₄ Plasma,* H. NOMURA, K. AKIMOTO,

A. KONO AND T. GOTO, Nagoya Univ., Japan - The rate constants (k_r) for the reactions of SiH and SiH₂ with SiH₄ at low pressures (0.07-1 Torr) have been determined from laser-induced-fluorescence measurements of the decay rate of the radical densities in the afterglow of an RF SiH₄/Ar discharge. The k_r values of the two reactions were of similar magnitudes (e.g., $4-5 \times 10^{-11} \text{ cm}^3/\text{s}$ at 70 mTorr) and decreased with decreasing total pressure, indicating that the major reaction channels are three-body association reactions forming Si₂H₃ and Si₂H₆ even in the present low-pressure conditions. The results were used, with the aid of previous measurements of other rate constants and radical densities, to estimate the SiH_x (x=0-3) production frequencies in low-pressure SiH₄ plasmas. The results indicate that despite the low densities of SiH_x (x=0-2) in the plasma the sum of their production frequencies is comparable to, or considerably larger than (when the plasma is diluted with Ar), the SiH₃ production frequency.

*Work supported by the Ministry of Education, Science and Culture of Japan.

NA 9 Possible coagulation process of particulates in rf silane plasmas*, M. SHIRATANI, S. SANJAY, Y. UEDA, H. OHKURA, S. FUJIO, H. KAWASAKI, T. FUKUZAWA and Y. WATANABE, Department of Electrical Engineering, Kyushu University - We have shown that particulates grow through three phases of nucleation and subsequent initial growth, rapid growth and growth saturation. A particulate growth process in the rapid growth phase is studied using an amplitude modulated rf discharge.¹ Morphology of particulates shows that coagulation of particulates plays a crucial role in this phase; a coagulation rate of 400 s⁻¹ observed is extremely high compared to a thermal collision rate of 5 s⁻¹ between particulates; the coagulation rate increases considerably with an amplitude of rf discharge voltage and a self-bias voltage. Coagulation between oppositely charged particulates is proposed as a possible process to explain properly these experimental features.

*Work supported by a Grant-in-Aid for Scientific Research by the Ministry of Education, Science and Culture of Japan.

¹M. Shiratani, H. Kawasaki, T. Fukuzawa, and Y. Watanabe, Surface Rev. Lett. (in press).

NA 10 Numerical Modeling of the Physical Chemistry in SiH₄ RF Discharges and Comparison with Radical Density Measurements by Threshold Ionization Mass Spectrometry. O. LEROY, J. PERRIN, P. KAE-NUNE, J. JOLLY, and G. GOUSSET, Laboratoire PRIAM, ONERA/CNRS, Fort de Palaiseau, 91120 PALAISEAU, FRANCE -

Radical density measurements have been carried out in a GEC reference cell-like low pressure discharge in pure SiH₄ in the vicinity of a heated electrode. The threshold ionization technique was used to measure the density of SiH₃, SiH₂, SiH, and H. A 1D-modeling has been developed in order to understand the mechanisms responsible of the a-Si:H deposition. The model is not self-consistent, as some parameters measured or calculated externally are injected: the temperature profile between the electrodes (measured by CARS or calculated by a thermal model taking into account the temperature accommodation between the gas and the surfaces), the source functions for the radical creation by electronic

impact on neutral molecules (calculated from electrical models), the pressure (assumed constant), and the partial densities of neutral species (deduced from mass spectrometry measurements). The model solves the transport and continuity equation by treating the diffusion of the monomer SiH_n ($n=0-3$) and dimer Si_2H_n ($n=2,5$) radicals in the mixture of the four neutral gases (SiH_4 , Si_2H_6 , Si_2H_4 and H_2) in stationary conditions. The density of each radical is calculated between the electrodes and the deposition rate on the heated electrode is deduced. In the bulk of the plasma, kinetic reactions are expressed through reaction rate coefficients. On the electrodes, the destruction of each radical is expressed by the Milne's boundary condition taken into account a loss coefficient rate β . A comparison between the measured densities and the calculated ones is performed in typical conditions of a-Si:H deposition.

POSTER SESSION NB: MAGNETICALLY ENHANCED PLASMAS

Thursday afternoon, 12 October 1995
Berkeley Marina Marriott
Belvedere/Angel Rooms, 15:45-17:30

NB 1 Modeling of ECR Processes, M. MEYYAPPAN and T.R. GOVINDAN, Scientific Research Associates, Glastonbury, CT - High density plasmas such as ECR have been increasingly used in processing of semiconductor materials. Modeling of the plasma process can be valuable in equipment design, process optimization and control. We have recently developed a comprehensive model for ECR processing and applied to argon discharges¹. Comparison of the model results against diagnostics was very good. Encouraged by the success of the model, we have extended the analysis to reactive plasmas. The model couples discharge physics and chemistry with flow and heat transfer in the reactor. Governing species, flow, electron energy, ion energy, and gas energy equations are radially averaged to obtain 1-d model equations. Homogeneous and surface chemistry mechanisms have been included. Results are presented for a chlorine discharge in an etching environment and compared against measurements. We show from self-consistent simulations how the pressure and neutral density variations strongly affect the plasma dynamics.

1. M. Meyyappan and T.R. Govindan, 187th ECS Meeting, Reno, May 1995.

NB 2 Influence of Wall Surface on CF_x ($x=1-3$) Radicals and Film Deposition in CHF_3/H_2 ECR Etching Plasma, M.HORI, K.TAKAHASHI and T.GOTO, Nagoya Univ. - The variation of CF, CF_2 and CF_3 radical and F atom densities has been investigated with changing the composition (F/C) of film deposited on reactor wall surface in CHF_3/H_2 ECR plasma. CF, CF_2 and CF_3 radical densities in the plasma were measured using infrared diode laser absorption spectroscopy and F atom using actinometry technique. The composition (F/C) of the films deposited on the reactor wall was found to be successfully changed with varying H_2 partial pressures from 0.01 Pa to 1.33Pa at 300W using XPS and FT-IR analyses. The only CF radical density in CHF_3/H_2 plasma was greatly affected by composition (F/C) of the films deposited on the reactor walls. Thus, the loss probability of CF radical decreased as the F/C ratio of films deposited on the reactor wall decreased. Furthermore, it was found that the behavior of CF radical density in the plasma followed the deposition rate of film formed on the substrate. The mechanism of fluorocarbon film formation in CHF_3/H_2 ECR plasma is discussed by connecting the behavior of CF_x ($x=1-3$) radical and F atom densities in the plasma with the characteristics of wall surfaces.

NB 3 Measurement of Radical Densities Associated with C_4F_8 Plasma from a Large Area ECR Plasma Source, S. DEN^{1,2}, T. KUNO¹, K. TAKAHASHI¹, M. ITO¹, M. HORI¹, Y. HAYASHI², Y. SAKAMOTO³ and T. GOTO¹, Nagoya Univ.¹,

Irie Koken Co. Ltd.², and Nichimen Electronic Technology Corporation³ - C_4F_8 gas has been employed to get a high selective etching of SiO_2 over underlayer materials in high density plasma etching processes. Radical species from the C_4F_8 plasma are considered to play an important role in SiO_2 etching rate and selectivity. To clarify the surface reactions involved in these processes, we have undertaken to quantify the radical densities associated with C_4F_8 plasma. As a source, a large area (200mm) electron cyclotron resonance plasma source was used (Nichimen Electronic Technology Corp.: Pure Plasma 300D-ECR). Typical characteristics include electron densities $>10^{11}\text{cm}^{-3}$ and ioncurrent uniformities $<+/-5\%$. Radical densities were measured using infrared diode laser absorption spectroscopy and actinometric technique. Our results show that the F and CF radical densities increase linearly with input microwave power, while the CF_2 radical exhibits non-linear dependency. These results and their effects on Si surface reaction processes will be discussed.

NB 4 Plasma Production and Loss in a Helicon Plasma, J. GILLAND, R. BREUN, and N. HERSHKOWITZ, University of Wisconsin-Madison* - A steady state helicon plasma depends on the relative production rate from rf heated electron-neutral collisions and the losses due to axial and radial diffusion. Under suitable conditions, the ionization rate is high enough to induce the phenomenon of "neutral pumping", in which the neutral gas pressure outside of the plasma column decreases dramatically upon initiation of the helicon plasma. This phenomenon is examined for a range of plasma parameters and end conditions, including material limiters and uniform, cusped, and zero applied magnetic axial fields. Measurements of end loss current through limiters or endplates to ground, as well as axial variation of plasma density and temperature are being made. An argon plasma column of 2 cm radius, 1 m length has been produced with electron densities up to $3 \times 10^{13}\text{cm}^{-3}$ using helicon waves at 13.56 Mhz and rf power from 300 to 800 W. The neutral pressure in the chamber was observed to drop by a factor of 1/3 upon initiation of the helicon wave for some conditions.

*Funded by National Science Foundation Grant No. ECS-9120326

NB 5 Silicon Etching by SF_6 in a Pulsed Helicon Reactor, A.J. PERRY, A. HERRICK and R.W. BOSWELL, ANU, Australia - We present the results of a study of the etching of silicon in a pulsed SF_6 plasma at 1.5mTorr. The silicon etch rate was measured using infrared laser interferometry as a function of the pulse length (from 0.2 to 800 ms) for a fixed duty cycle of 33%. The fluorine concentration in the plasma was determined from time resolved actinometry. Using these data and results from continuous etching which show that the etch rate is proportional to the fluorine density, we determined that the decay time of the fluorine concentration after the plasma is extinguished is 10msec, much shorter than the residence time in the system. This implies that fluorine consumption by the silicon wafer dominates all other losses in the system.

NB 6 Experiment and theory of bucket-lift electron heating in a helicon source.* A.W. MOLVIK, R.H. COHEN, A.R. ELLINGBOE, E.B. HOOPER T.D. ROGNLIEN, and B.W. STALLARD, Lawrence Livermore National Laboratory - Helicon discharges efficiently produce 10^{12}cm^{-3} range densities. Experiments¹ have shown that argon emission intensity is modulated at the 13.56 MHz rf frequency, and that the peak emission propagated axially at a velocity corresponding to that of the helicon waves, consistent with a few tens of eV electrons trapped in the traveling wave, e.g. "Bucket lift" heating. An analytic model of the heating rate is presented which places quantitative restrictions on the trapping rate, the collisional loss rate, and bucket acceleration rates. Using a gridded energy analyzer, we have measured a 13.56 MHz modulation of electrons above 35 eV, consistent with particles trapped in waves. The LLNL Helicon Source consists of solenoidal magnets and a Nagoya Type III antenna

surrounding a 15 cm inner diameter Pyrex tube. At one end, the tube expands to a 30 cm diameter aluminum vessel surrounded by a picket fence array of permanent magnets. The antenna is driven by up to 3 kW at 13.56 MHz. This helicon source is being studied and optimized for application to a large area plasma source.²

* Performed by LLNL for DoE under contract W-7405-ENG-48.

1. A. R. Ellingboe, et al., Phys. of Plasmas, June, 1995.
2. R. D. Benjamin, P. O. Egan and R. W. Richardson, This meeting.

NB 7 Comparison of Experimental and Simulation Model Plasma Profiles for a Helicon Source * J.A. BYERS, R.H. COHEN, A.R. ELLINGBOE, A.W. MOLVIK, T.D. ROGNLIEN, B.W. STALLARD, AND P.A. VITELLO, *Lawrence Livermore National Laboratory*—Results of plasma parameters from a large-area helicon source are compared with a magnetized version of the 2-D INDUCT94 transport code. The discharge tube radius is 7.6 cm with a 10% uniform, axial B-field over a 20 cm length. The helicon wave is excited by a Nagoya Type III antenna using up to 3 kW from a 13.56 MHz source yielding electron densities $\sim 5 \times 10^{12} \text{ cm}^{-3}$. Measurements are obtained from Langmuir probes, a calorimeter, RF \vec{B} probes, and an electron energy analyzer. For the modeling, the wave fields are calculated using the ANTENA code and a comparable code developed at ORNL giving collisional and Landau electron heating rates. Bucket-lift heating due to wave-trapped electrons is described in an accompanying paper. We have developed fourth-order differencing algorithms in the code to minimize the numerical diffusion on the rectangular mesh for cases where the expanding magnetic field lines cross the mesh at a finite angle and will report on their effectiveness. Comparisons are made for the profiles of plasma density, calorimeter heat flux, and RF wave fields.

*Work performed under USDoE contract W-7405-ENG-48 at LLNL

NB 8 Quasineutral Particle Simulation Code for ECR Plasma Processing Devices, GLENN JOYCE, MARTIN LAMPE, W. M. MANHEIMER, STEVEN P. SLINKER, and RICHARD F. FERNSLER, NRL - We report on the continued development of a fast-running quasineutral 2-D (r-z) particle simulation code for low-pressure processing plasmas. The technique avoids fast time scales and short spatial scales by using a guiding center representation for the electrons, and by calculating the internal electric field from the requirement of quasineutrality, rather than from Poisson's equation. The sheath potentials are determined from a two-dimensional generalization of the "logical sheath" condition¹. We show that the sheath potentials are coupled to cross-field ion flow in a way which requires implicit solution of a 1-D nonlinear diffusion problem, embedded within the larger 2-D explicit simulation. We show that the model is sufficient to represent kinetic features such as Landau damping of low-frequency waves. Modeling and numerical techniques will be discussed in the present paper, and Ar transport calculations will be discussed in a companion paper.

- * Work supported by Office of Naval Research.
1. S.E. Parker, et al., J. Comp. Phys. 104, 41 (1993).

NB 9 Simulation Study of Plasma Transport in ECR Reactors* MARTIN LAMPE, GLENN JOYCE, W. M. MANHEIMER, STEVEN P. SLINKER, and RICHARD F. FERNSLER, NRL - We have used a recently-developed axisymmetric quasineutral particle simulation code¹ to study heating and transport of Ar plasma in a standard two-magnet ECR reactor configuration, in which the electrons are always strongly magnetized, but the degree of magnetization of the ions varies spatially and depends on plasma conditions. We show how cross-field plasma transport depends on whether field lines terminate on insulating or conducting surfaces. For each case, we compute the spatial extent and uniformity of the plasma temperatures, density, and distribution function, as functions of the strength and spatial variation of the heating source, the magnetic configuration, the various collisional processes, and the

longitudinal and cross-field transport processes. Results will be compared to experiment.

- *Work supported by Office of Naval Research
1. Code features discussed in the adjacent poster by Joyce, et al.

NB 10 A study about the Resonance Cone in a Cold Magnetized Plasma, E. BESUELLE, CEA, CE-Saclay, DCC/DPE, France - The phenomenon of resonance cone of a wave in a magnetized plasma has been already used to measure n_e , but without taking into account the collisions. The thermal effects leading to a fine structure around the principal resonance cone have been particularly studied in the last 20 years. We study here the case of a cold magnetized plasma, in which the collisions frequency ν of the electrons with other particles is of the order of ω_{ce} (if $B \approx 5 \text{ G}$, $T_e \approx 0.1 \text{ eV}$, $n_e \approx 10^{11} \text{ cm}^{-3}$, then $\nu \approx \omega_{ce}$ and $\omega_{pe} \approx 200\omega_{ce}$). The calculation of the potential ϕ emitted by the antenna, without neglecting any pole of the dispersion relation, gives then: $\phi \propto 1 / (z^2 + K_{//}/K_{\perp}\rho^2)^{1/2}$, where $K_{//}$ and K_{\perp} represent the diagonal terms of the tensor $\mathbf{K} = \epsilon/\epsilon_0$. It appears that the characteristics of the resonance cone (when it exists) are modified by the collisional effects, so that the classical formula used to determine ω_{pe} is no more valid. Furthermore, we show that the resonance cone exists only if $\text{Re}(K_{//}/K_{\perp}) < 0$, the upper hybrid branch vanishing for $\nu/\omega_{ce} \geq 0.22$ and the lower one for $\nu/\omega_{ce} \geq 0.40$. This phenomenon may lead to a new method of determining n_e and T_e : first, the detection of an existing resonance cone will give n_e ; then, a fitting of the resonance cone profile would lead to an estimation of T_e .

NB 11 Thomson Scattering Diagnostics of a Magnetic Neutral Loop Discharge Plasma, K. UCHINO, T. SAKODA, M. BOWDEN, K. MURAOKA, M. MAEDA, M. ITOH and T. UCHIDA, *Kyushu U. and ULVAC Japan, Ltd.* - A magnetic neutral loop discharge (NLD) has been proposed as a new plasma source for plasma processing.¹ Because the electron motions become nonlinear around the magnetic neutral loop, the plasma can be heated efficiently by applying an RF inductive field in the low pressure regime of around 1 mTorr. In order to characterize the production and the transport processes in the NLD plasma, laser Thomson scattering was applied to diagnose the plasma. Electron velocity distribution functions around the magnetic neutral loop were measured by this method, reliably and without disturbing the plasma.

- 1 T. Uchida, Jpn. J. Appl. Phys. 33, L43 (1994).

POSTER SESSION NC: ELECTRICAL METHODS
Thursday afternoon, 12 October 1995
Berkeley Marina Marriott
Belvedere/Angel Rooms, 15:45-17:30

NC 1 Investigation of the dependence of discharge parameters of a 13.56 MHz parallel plate discharge on plate spacing, C.M. Deegan and M.B. Hopkins, *Dublin City University, Ireland.* - Published probe measurements in rf plasmas have shown considerable discrepancies in measurements of certain plasma parameters, electron temperature in particular^{1, 2}. It is suggested that this may be due to the variations in chamber geometry and electrode spacing from system to system. A capacitively coupled system, used previously to characterise low-pressure rf discharges, has been modified to facilitate variation of the space between the parallel plates. This may vary from two to nine centimetres. A current-voltage probe as well as Langmuir probes are installed on the system to monitor plasma parameters and to investigate if these parameters are affected by the plate spacing.

¹ R.A. Doyle, M.M. Turner and M.B. Hopkins, *Appl. Phys. Letts.*, 69 (25) (1993)

² Goydak and Piejak, *Phys. Rev. Letts.*, 65, 8 (1990)

NC 2 Time Resolved Plasma Parameter Measurements in Pulsed Discharges.* L. J. OVERZET, CHRIS BOWLES, M. B. HOPKINS[†], and BRIAN SMITH University of Texas at Dallas, Richardson, TX 75083. — A Langmuir probe (LP), microwave interferometer (MWI), and RF current-voltage probes have been combined to measure the plasma parameters as a function of time. The LP and MWI measurements indicate nearly the same electron density in helium, nitrogen and argon while the RF excitation is on; but, the two techniques can indicate very different charge densities and time dependencies during the power off period. In one case the MWI indicated a density that was slightly rising when the LP indicated a quickly decreasing density! The electron temperature at discharge turn on for 500 mTorr argon and helium discharges was found to be initially very large and to decrease with time; but, the electron temperature of 100 mTorr argon discharges was found to be nearly constant during the discharge turn on. At discharge turn off, the electron temperature decreases to less than 0.5 eV.

* Work supported in part by the National Science Foundation and The State of Texas Advanced Research Program.

[†] Dublin City University, Dublin, Ireland

NC 3 Inductive Probe Characterization of a CF₄ Discharge in a Planar Radio-Frequency Inductively Coupled Plasma Source.*

R. A. Stewart, J. Griesbach, A. E. Wendt, and J. A. Meyer, U. of Wisconsin-Madison - Plasma characterization of many reactive gas discharges using Langmuir probes is difficult due to deposition of films on the probe collecting surface. Recently, the use of an inductive loop probe has been demonstrated for measuring electromagnetic fields in an argon discharge.¹ Using the measured rf field quantities \vec{B}_z and \vec{B}_r , the rf electric field (E_ϕ) and the local plasma permittivity (ϵ) can be calculated directly. Electron density (n_e) is then estimated using a local relation between ϵ and n_e . In this study we have demonstrated the use of inductive probes to measure the spatial distribution of electromagnetic fields in a CF₄ discharge generated in a planar radio-frequency (13.56 MHz) inductively coupled plasma (ICP) source. Both spatial profiles $n_e(r, z)$ and variations of n_e at discharge center with pressure and power have been obtained.

*Work supported by NSF Grant EEC-8721545.

¹J. A. Meyer and A. E. Wendt, to appear in *J. Appl. Phys.*, 78, July 1 (1995)

NC 4 Surface Temperature Measurements in Inductive Discharges in Xenon and in Argon. R. PIEJAK, V. GODYAK and B. ALEXANDROVICH, OSRAM SYLVANIA INC., 71 Cherry Hill Drive, Beverly 01915 - Temperature within an rf inductive discharge driven at 6.8 MHz have been measured by inserting into the discharge a miniature thermocouple surrounded by a thin glass capillary tube. The discharge vessel is cylindrical in shape: 4" long and 8" ID and is maintained by a pancake (flat) coil located at one end of the cylinder. Measurements were made in the mid plane of the vacuum vessel at the center and at a radius of 4 cm from the center over a range of gas pressure between 0.3 mTorr and 1 Torr in xenon. At 100W on the coil, the temperature in the center reached 200°C at 0.3 mTorr and 440°C at 1 Torr. Many of the same measurements were also made in argon for comparison. Measurements were made at a fixed powers (100W and 200W) applied to the coil. A complete radial temperature profile at 30 mTorr was also measured in both gases. The temperature data presented here is useful for at least two reasons: 1) this data is helpful in choosing appropriate probe materials to survive the temperature in the discharge and 2) this data allows one to determine the neutral gas density (an especially important parameter to modelers) from the (measured) gas pressure.

NC 5 P.C.-based Langmuir Probe Diagnostic. C.O'MORAIN, A. GRAYDON, Scientific Systems Ltd., Ireland, M.HOPKINS, A. HUGHES, Dublin City University, Ireland. - A P.C.-based Langmuir probe diagnostic has been designed based on the earlier work of Hopkins et al¹. The developed system allows spatial and temporal measurement of internal plasma parameters and of the electron energy distribution function (EEDF) in RF and DC discharges. In RF discharges the system employs a miniature probe (shaft diameter 6 mm) which includes a high frequency network to compensate for the presence of RF on the plasma potential. The system can incorporate a second auxiliary probe to track the floating potential compensating for low frequency noise and plasma potential shifts caused by finite sheath resistance. The system can also operate in box car mode allowing time-resolved sampling (resolution 2 μ sec) of plasma parameters and EEDFs. Details of the probe acquisition electronics, software and miniature probe heads will be discussed. The software includes novel automatic data reduction algorithms and smart probe tip cleaning routines. Data obtained using this system from a range of plasma sources will be presented.

¹ M.B. Hopkins et al, *Rev. Sci. Instrum.* 57 (9), (1986).

NC 6

Electron Energy Distributions in the Bell Jar Top Inductively Coupled Plasma. HAN-MING WU, YUN YANG, DING-PU YUAN, JIA-PING YAN, MING LI, Institute of Mechanics, Chinese Academy of Sciences, Beijing China - The argon and SF₆ plasmas in a bell jar inductively coupled plasma (ICP) source are systematically studied by means of measurement with a tuned Langmuir probe. Using a tuned Langmuir double-probe technique, we reduce the rf interference and get the probe I-V characteristics and finally present the electron energy distribution functions (EEDF). Time averaged electron temperature and plasma density are measured for some combination of pressure and applied rf power. The Te measurements agree the theoretical results reasonable well. Whereas the diagnostic data of Te uniformity seems not as good as the local-approach simulation predictions. The EEDFs at variant spatial points are studied with different operation parameters.

POSTER SESSION ND: PLASMA DISPLAYS

Thursday afternoon, 12 October 1995

Berkeley Marina Marriott

Belvedere/Angel Rooms, 15:45-17:30

ND 1

On the Dynamics of the Gas Discharge in an ac pdp Cell.* V.P. NAGORNY, P.J. DRALLOS AND W. WILLIAMSON, JR., Dept. of Phys. and Astronomy, The U. of Toledo, Toledo, OH 43606 - The dynamics of a gas discharge between electrodes covered with an insulator is described. One can meet such a situation in a plasma display panel. We investigate a regime of the discharge when the voltage applied to a gap is initially significantly higher than the breakdown voltage, such that $U_{gap} - U_{br} \sim U_{br}$. We find the characteristic time scale of the development of the discharge and the maximum value of the current density as a function of parameters of the cell and initial parameters of the discharge. The regime under investigation is of special interest because, as was previously shown [1], the opposite regime, $U_{gap} - U_{br} \ll U_{br}$, is unstable during periodic operation of the cell.

*Work supported by the US DOE under the contract No. DE-AC04-76P00789.

¹V.P. Nagorny, P.J. Drallos and W. Williamson, Jr., *J. Appl. Phys.* 77, p.3645 (1995).

ND 2 Hybrid Model of Plasma Panel Display Cell in a Planar Geometry. A. HIRECH, J. MEUNIER, Ph. BELENGUER, J.P. BOEUF, and L.C. PITCHFORD, CPAT, CNRS, Toulouse, France - We recently presented¹ model calculations of the characteristics of a AC plasma display panel cell in mixtures of neon (90%) and xenon (10%) at pressures on the order of 500 torr and for a gap spacing of 100 μm . We supposed in these calculations that the electron excitation and rate coefficients depend on the local value of E/n . Because the electric field is rapidly varying in space (compared to the mean free path for energy loss collisions), the assumption of local equilibrium is questionable. In this communication, we present calculations, for the same conditions as were reported previously, using a hybrid fluid-particle model to identify the effects of non-local electron excitation and ionization on the predicted characteristics of a plasma display panel cell. Results from the hybrid model are in good agreement with our previous results for the Ne-Xe (90-10) mixture previously reported. These and other results for higher concentrations of xenon will be presented and the range of conditions for which the local field approximation is valid will be discussed.

1. J. Meunier, Ph. Belenguer and J.P. Boeuf, to appear in J. Appl. Phys, 15 July 1995.

ND 3 Multidimensional Fluid Simulations of an AC Plasma Display Panel (AC-PDP)*. ROBERT B. CAMPBELL, RAMANA VEERASINGAM**, ROBERT T. McGRATH - The design of AC PDPs is facilitated by the insight gained by a multidimensional computational tool under development. The model consists of reaction-diffusion-convection equations for ions, electrons, neutral metastables, dimers, and excited species, solved simultaneously with Poisson's equation using fully-implicit numerical methods. The 2-D version of the code routinely operates in the high intensity glow discharge regime where space charge effects are very significant. The rate coefficients for electron driven processes are evaluated with a 0-D Boltzmann solver, and parametrized as a function of E/n , and corrected for non-LFA effects. The transport of excited species due to radiation trapping is explicitly included, as is the calculation of photon fluxes on material surfaces. The code treats mixtures, with the He-Xe Penning mixture receiving the most attention to date. We have found that our best understanding of the discharge dynamics is achieved by viewing computer-generated videos of the plasma evolution. A variety of these video simulations will be the centerpiece of our presentation at the meeting, where we shall vary electrode and barrier geometries, applied voltage, and secondary emission characteristics of the surfaces.

* Work supported by US DOE. ** The Pennsylvania State University

ND 4 The effect of mixture ratio in He/Xe ac-PDPs*, P.J. DRALLOS, V.P. NAGORNY, and W. WILLIAMSON, JR., Dept. of Physics and Astronomy, Univ. of Toledo, Toledo, OH 43606 - The operational dynamics of an ac-PDP cell are investigated with regard to the source gas mixture via computer simulation. Single pulse and steady state multiple firing simulations are performed, from which several important design parameters can be characterized. The characterizations include important design parameters such as voltage margin, voltage transfer, and light efficiency. The results presented are for two-component, helium-xenon mixtures of various relative proportions. The simulations were performed with a hybrid, kinetic-fluid computational model. Electron-driven rates are derived from electron Boltzmann kinetic calculations and incorporated into self-consistent, fluid-Poisson simulations.

* This work supported by the USDOE under contract No. DE-AC04-76P007898.

ND 5 Ionization and excitation rates for a multi-species He/Xe gas mixture determined from Boltzmann calculations*. RAMANA VEERASINGAM**, R. B. CAMPBELL, R. T. McGRATH, M. E. RILEY, W. J. ALFORD, J. W. SHON, J. ABDALLAH***, R. CLARK***, and C. FONTES***, Sandia National Laboratories, New Mexico - In support of multi dimensional fluid models developed for the ac plasma display panel (AC-PDP), it is necessary to obtain cross-sections for the various electron driven excitation and ionization processes and to compute reaction rates parametrized on local field strength. We calculate reaction rates using a 0-D Boltzmann kinetic code with cross-sections determined from ab-initio calculations of xenon for a 7 level reduced xenon model. The 7 level model captures the essential spectral emission one would expect from xenon in a plasma display panel. We will present the xenon model and the reaction rates for varying concentrations of xenon in helium parametrized as functions of E/n . These rates are used in our 1-d and 2-d fluid simulations of the AC-PDP.

* Work supported by US DOE.

** The Pennsylvania State University, *** Los Alamos National Laboratories

FRIDAY MORNING

SESSION PA: MAGNETICALLY ENHANCED PLASMAS

Friday morning, 13 October 1995

Berkeley Marina Marriott

Yerba Buena/Treasure Rooms, 8:00-9:45

Martin Lampe, presiding

8:00

PA 1 Antenna Design for Helicon Sources*, D. ARNUSH and F.F. CHEN, UCLA--We describe a simple method for designing antennas to couple efficiently to helicon modes in a low-pressure, magnetized discharge. The k -spectrum of antennas composed of straight, circular, and helical segments can be expressed analytically and plotted for each azimuthal mode number m . Reflections from end boundaries are neglected. The resonant k -numbers for helicon modes can also be calculated from the dispersion relation for given tube radius, density, magnetic field, and m -number, taking into account the radial density profile. Those modes with k 's near the peak of the antenna's spectrum will have good coupling. Conversely, for a given helicon mode, the geometry of the antenna can be varied until its spectrum peaks at the right value of k . To obtain the magnitude of the coupling, we have simplified the ANTENA code by taking the limit of small electron mass. The roles of the plasma dielectric, the boundaries, and the spurious high- k root are then made clear. We can take arbitrary density profiles into account by simply substituting the dispersion characteristics computed for a nonuniform plasma for the well-known ones for a uniform plasma, thus greatly simplifying the code.

*Supported by NSF, SRC, Wisconsin ERC, and LLNL-PPRI.

8:15

PA 2 Capacitive, Inductive and Wave Coupling in a Helicon Plasma A.R. ELLINGBOE*, R.W. BOSWELL, A. DEGELING AND CHAN OUK JUNG**, ANU, Australia, **Samsung Korea. Three distinct modes of rf coupling have been measured in the large WOMBAT plasma system excited by a double half turn antenna. In capacitive mode, the density is low and quite uniform with a high plasma potential and high directly coupled rf fields. The inductive mode occurs at higher rf powers and is characterized by significantly higher densities, a lower plasma potential and a radial density distribution with a minimum in the centre. Axial measurements of the wave fields suggest a wavelength significantly longer than the source. The transition between these modes occurs at densities of around 10^{10} cm^{-3} and radial measurements of the axial magnetic wave-fields suggest this is related to the skin depth. At still higher rf powers, the jump to Helicon mode can be quite dramatic with a further increase in the central density, decrease in the plasma potential and a radial density distribution tending to gaussian. The jump depends on the ratio of the steady axial magnetic field to the density and wave field measurements confirm the existence of $m=1$ helicon waves with wavelengths shorter than the source.

*Present address: University of California, Lawrence Livermore National Laboratory, P.O. Box 808, Livermore, CA 94551

8:30

PA 3 Cross Field Diffusion in a Helicon Plasma. A.J. PERRY, R.W. BOSWELL AND H.M. PERSING, ANU, Australia. - As the input power to a Helicon plasma is increased there is a discontinuous increase in the density which is identified with the change from capacitive to inductive/wave coupling to the plasma. Below this transition the radial profile of the plasma potential V_p is centrally peaked ($V_p(\text{max}) \sim 50\text{V}$), producing an electric field that drives ions out of the plasma radially. Measurements with an emissive probe show that V_p is also strongly modulated ($\Delta V - V_p$) at the rf drive frequency suggesting the presence of large rf fields in the source. In the high density mode V_p is low (15-20V), independent of power and the modulation has dropped to $\sim kT_e/2e$. The radial profile of V_p is flat. These data suggest that in the low mode there is

an anomalously high cross-field diffusion of electrons which establishes the radial fields accelerating ions to the walls. This diffusion may be driven by the large rf fields present in the plasma. As the density increases, the fields are screened out, the radial electron loss diminishes and the radial V_p is flat. The reduced radial diffusion of both charged species produces a still higher density as the major loss surface is reduced to axial losses.

8:45

PA 4 An Experimental Study of Breakdown in a Pulsed Helicon Plasma. R. W. BOSWELL and D. VENDER, ANU, Australia. - Fast time resolved measurements of ion and electron energy distributions in the first 200 μsec of a discharge in a 20 cm diameter glass Helicon source show that 10 μsec after the rf is turned on, an intense burst of electrons is produced with average energy of 200 eV and lasting about 1 μsec . This initial pulse of high energy electrons can be explained by resonant secondary electron multiplication (the multipactor effect) of electrons which are accelerated in the rf fields produced by the Helicon antenna. These electrons ionize the background gas very rapidly and a plasma with high electron temperature and hence high plasma potential can be created in about 1 μsec . Subsequently, further ionization occurs and after 20 μsec , the plasma potential has fallen to about 200 V and the electron temperature to about 20 eV. The electron temperature continues falling and reaches a steady state value of 8 eV in about 30 μsec . The density and plasma potential reach steady state after about 70 μsec .

9:00

PA 5 Very low B field Helicon-ECR ICP Source. N. HERSHKOWITZ, T. LHO, J. MILLER and J. AMONDSO, University of Wisconsin-Madison-- Cylindrical argon plasmas are produced in a uniform magnetic field oriented parallel to the cylinder axis, by a spiral inductively coupled source (ICP) at the end of a plasma column. RF is applied at 13.56 MHz. The magnetic field is varied from 0 to 120 gauss. "Resonances" in plasma density are observed when the B field satisfies $B = nB_r$, for low values of the integer $n > 0$, where B_r is the B field which corresponds to an electron cyclotron resonance frequency equal to the rf frequency. Three different operating regimes are identified. These are a low density mode with $B = 0$, a mode with higher density with B non-zero (and propagating waves) and a higher density inductive mode when B is returned to 0. The three modes exhibit different axial and radial density and potential profiles. When B is present, the source can operate with either helicon or electron cyclotron waves.

9:15

PA 6 Measurement of CH₃ Radical Density in ECR and Parallel-Plate RF Plasmas.* M.IKEDA, K.AISO, M.HORI, and T.GOTO, Nagoya Univ. - In order to elucidate the mechanism of diamond film formation, the behaviors of CH₃ radical in ECR downstream and parallel-plate RF (13.56 MHz) plasmas were investigated using infrared diode laser absorption spectroscopy. In the case of ECR plasma, microwave power was modulated with on-period of 50 ms and off-period of 110 ms. In the case of RF plasma, RF power was modulated with on period of 20 ms and off-period of 38 ms. CH₃ radical densities were estimated to be of the order of 10^{11} cm^{-3} in the ECR CH₃OH plasma and less than 10^{10} cm^{-3} in the ECR CH₄ plasma at pressure of 1.3 Pa, flow rate of 30 sccm

and microwave power of 300 W. On the other hand, CH₃ radical densities in RF CH₃OH and CH₄ plasmas were estimated to be of the order of 10¹¹ and 10¹² cm⁻³, respectively, at pressure of 7 Pa, flow rate of 8 sccm and power density of 0.8 Wcm⁻². The comparison of CH₃ radical density in RF CH₃OH plasma with that in CH₄ plasma are discussed from the viewpoint of the diamond film formation.

*Work supported by a Grant-in-Aid for Scientific Research of Japan.

9:30

PA 7 VUV and Mass Spectroscopic Characterization of Cl₂/Ar and CH₄/H₂/Ar ECR Plasmas, C.R. EDDY, JR., B. THOMS, S. DOUGLASS*, S. MCELVANEY, G. MEHLMAN and J.E. BUTLER, *Naval Research Laboratory and SFA, Inc.* - VUV emission from Cl₂/Ar and CH₄/H₂/Ar ECR microwave plasmas has been recorded over the wavelength range from 1100 to 2500 Å. In addition to identifying the dominant dissociation processes in these discharges, neutral temperatures have been measured in the range from 0.1 to 0.3 eV. The effects of changes in discharge parameters (i.e., pressure, power, etc.) and the location and bias of the substrate platen on plasma radiation, in terms of plasma parameters, are also presented. Further, a high resolution, wide range mass spectrometer has been used to characterize the plasma flux incident on the substrate platen in both of these plasma chemistries which are commonly used to etch semiconductor materials. Neutrals, positive ions, and negative ions are sampled through a 0.625" dia. aperture in the substrate platen in the absence of the substrate. The change in the ratio of these different types of species is evaluated as a function of process pressure, microwave power, input gas composition and the location of the resonance condition.

*National Research Council Associate

SESSION PB: KINETIC EFFECTS AND RF GLOWS

Friday morning, 13 October 1995

Berkeley Marina Marriott

Belvedere Room, 8:00-9:45

M. Surendra, presiding

8:00

PB 1 On the validity of various approximations for determining a spatially dependent EEDF, U. KORTSHAGEN, University of Wisconsin-Madison — Much effort has been devoted to developing efficient models for spatially dependent electron kinetics in weakly ionized plasmas. While low pressure discharges can be modeled in the "nonlocal approximation", the "local approximation" seems to be suited for high pressures. The intermediate pressure range, however, requires more general techniques (numerical solution of kinetic equations, Monte Carlo or convective scheme approaches).

The possibility of extending the applicable range of the "nonlocal approach" by accounting for a first order correction is discussed. The validity of all three approaches (nonlocal, corrected nonlocal, local) is studied on the basis of the numerical solution of the complete, space-dependent Boltzmann equation for rare gases as well as molecular gases.

8:15

PB 2 Fast Electron Distribution in a Cylindrical Hollow Cathode *, V.I.KOLOBOV G.J.PARKER and W.N.G.HITCHON, Plasma ERC, U. of Wisconsin-Madison and LLNL - We have studied the fast electron kinetics in a cylindrical hollow cathode discharge using two approaches. One is based on the "Convected Scheme" (CS)¹. The other assumes small energy and momentum change of fast electrons in collisions with neutrals. By employing a spatial averaging of the Boltzmann equation, it allows a simple solution for the electron distribution function (EDF) in a regime with significant "pendulum effect"². The principal features of the nonlocal electron kinetics in the cavity incorporated in both models include: electron confinement by

the radial electric field, generation of progeny electrons in the cathode sheath, and electron momentum and energy change in collisions. The influence of the EDF anisotropy on calculated radial profiles of the light emission of different lines will be discussed and compared to experimental data.

* Work supported in part by NSF Grant ECD-8721545

¹ G.J.Parker, W.N.G.Hitchon and J.E.Lawler, Phys. Rev. E **50**, 3210 (1994)

² V.I.Kolobov and L.D.Tsendin, submitted to PSST (1995)

8:30

PB 3 Plasma-Sheath Transition and Bohm Criterion for Multicomponent Systems, K.-U. RIEMANN, Inst. f. Theor. Phys., Ruhr-Univ. Bochum, D-44780 Bochum, Germany. — In the asymptotic limit $\lambda_D \rightarrow 0$ of a small Debye length the problem of the plasma boundary layer is split up into the separate problems of a quasineutral presheath and of a plane collision-free sheath. The formation of a stationary sheath requires that the ions entering the sheath region fulfill a sheath condition (the "Bohm criterion"). In the case of one ion component, the Bohm criterion yields unique sheath edge boundary conditions for the sheath — as well as for the presheath analysis. If more than one ion species are present, the situation is essentially complicated. We investigate the conditions for the plasma sheath transition in a multicomponent system both in the frames of hydrodynamic and of kinetic theory and discuss the appropriate generalisations of the Bohm criterion accounting for various positive and negative ion components. As in the case of only one ion component, the generalized Bohm criterion is usually fulfilled in the equality form. It is demonstrated, how this *one* condition may be used to find boundary conditions for *all* ion components.

8:45

PB 4

Immersed Boundary Method for Plasma Simulation in Complex Geometries

J.U. Brackbill and Giovanni Lapenta
Los Alamos National Laboratory

Abstract

A reliable simulation package for industrial devices must handle complex geometries. In many industrial applications of plasma physics, it is crucial to include small features or curved surfaces. Standard simulation methods are formulated on rectangular meshes and must be rewritten to extend them to more general meshes. In the present work, we apply the immersed boundary method³ to extend particle simulation methods to 2D and 3D complex geometries. This method uses object particles with specified material properties to represent geometric features of arbitrary size and shape. Complicated plasma/material interactions are included⁴, and adaptive grids and particle rezoning techniques⁵ are used to focus the computational effort in the regions of interest.

Applications to fluid PIC simulation of plasma processing devices and to kinetic simulation of dust contaminants are presented.

9:00

PB 5 Electron Sheath Heating in capacitively coupled RF Discharges,* U. BUDDEMEIER, Ruhr-Universität Bochum, Germany, and U. KORTSHAGEN, University of Wisconsin-Madison — The efficiency of the electron sheath heating in capacitively RF discharges in the weakly collisional regime is studied. This heating process can be described as diffusion in energy space, allowing it to be included as an additional energy diffusion term in the Boltzmann equation. In order to obtain the energy diffusion coefficient, the electron-sheath interaction is analyzed numerically, the temporal sequence of interactions is studied by means of a particle simulation.

FRIDAY MORNING

The sheath heating efficiency turns out to be strongly dependent on the RF sheath voltage. EDFs measured in a symmetrically driven RF discharge are compared to a parametric, 1D kinetic model based on the "nonlocal approximation".¹ Reasonable agreement is obtained using a simplified expression of the diffusion coefficient from the numerical calculations. Furthermore, a heating mode transition is observed, which is possibly connected to the RF voltage dependence of the heating efficiency.

* supported by the Deutsche Forschungs Gemeinschaft (SFB 191)
¹ U. Buddemeier, U. Kortshagen, and I. Pukropski, Appl. Phys. Lett. in press (July 1995).

9:15

PB 6

Wellknown two mechanisms in the maintenance of the rf glow discharge are the ionization multiplication by electrons in the sheath-plasma boundary. One is realized by reflected electrons in electropositive gases, and the other by migrating electrons into the double layer in strong electronegative gases. The third mechanism of the maintenance is realized in the bulk plasma region in the rf discharge in O₂. Oxygen belongs to a weakly electronegative gas. Except for lower pressure, electron attachment rate prevails against the ionization in the boundary region between the ion sheath and the plasma. Atomic oxygens O⁻ produced by dissociative attachment are confined in the bulk plasma by positive ion sheaths. Also a large amount of atomic oxygen is produced by way of a dissociative electronic excitation by electrons. The decay of atomic oxygen is controlled by a surface recombination on the electrode. Therefore both of O⁻ and O distribute with a peak at plasma center. Then, the electron detachment reaction between O⁻ and O occurs at high efficiency in the bulk plasma, and ejected electrons contributes to the rf maintenance.

*Work supported by a Grant-in-Aid for Scientific Research on "Free Radical Science". Toshiaki Makabe

3-14-1 Hiyoshi, Yokohama 223 Japan
045-563-1141(ex.3358)
makabe@mkbe.elec.keio.ac.jp

9:30

PB 7

Electron Beam Sustained Reactive Ion Etching rf Discharges* MARK J. KUSHNER and DAVID N. RUZIC, Univ. of Illinois, Dept. of Elect. and Comp. Engr., Urbana, IL 61801 USA - The trend in plasma etching is towards reactors in which the ion flux and ion energy to the wafer can be separately controlled. This is accomplished by ionization being provided dominantly by a source other than the applied rf bias on the substrate. ICP and ECR reactors, which use this principle, optimally operate at low gas pressures (< 10s mTorr). To address higher pressures, a hybrid electron beam/RIE discharge system (EB-RIE) has been developed. In the EB-RIE system, a planar electron beam (1-3 kV) is injected into the plasma chamber above and parallel to the wafer. An rf bias is separately applied to the substrate. A 2-d model of the EB-RIE reactor has been developed to investigate scaling of this device. The model is a hybrid simulation which combines an electron Monte Carlo module with a fluid simulation. Results will be discussed for Ar and Ar/Cl₂ gas mixtures in which the beam energy, gas pressure and positioning of the beam are varied. The effects of these parameters on plasma density, dc bias, and uniformity of the reactive fluxes to the substrate will be presented.

* Work supported by NSF, SRC, Sandia National Lab/Sematech, and the U. of Wisconsin ERC for Plasma Aided Manufacturing.

SESSION QA: PLASMA IMMERSION IMPLANTATION

Friday morning, 13 October 1995

Berkeley Marina Marriott

Yerba Buena/Treasure Rooms, 10:00-12:00

M. Lieberman, presiding

Invited Paper

10:00

QA 1 Applications of Plasma Immersion Ion Implantation for Semiconductor Processing, * NATHAN W. CHEUNG, Department of Electrical Engineering and Computer Sciences University of California, Berkeley, California, 94720 - The *Plasma Immersion Ion Implantation (PIII)* technique shows great promise for large-area and high dose-rate processing of electronic materials. This paper will review the current understanding of plasma-surface interactions. Examples such as plasma doping for ultra-shallow junctions and high aspect-ratio Si trenches, selective plating of metals, damage induced impurities gettering, and subsurface material synthesis of silicon-on-insulator will be used to illustrate the unique applications of PIII for electronic materials modification. We will also discuss the processing requirements and limitations of PIII: concomitant implantation and sputtering, oxide charging, and substrate heating.

* Work supported by NSF, JSEP, and SEMATECH

Contributed Papers

10:30

QA 2 Plasma Source Ion Implantation Process for Surface Modification of Aluminum Alloys* L. ZHANG, K. MENTE, J.H. BOOSKE†, J.L. SHOHET, C. BAUM, R. MAU, E. BARRIOS, J.R. JACOBS, P. SANDSTROM, Plasma ERC, U. of Wisconsin, and A.J. BERNARDINI, Litton Industries -- In this paper we will describe the results of a comprehensive study of nitrogen plasma source ion implantation (N-PSII) for corrosion protection of aluminum alloys. Microstructural analyses of PSII treated 6061 Al established that the N-PSII had produced a layered surface structure, consisting of an Al oxide layer, a mixed layer of Al oxide and an Al nitride (AlN), a pure AlN layer and a band of Al matrix with dense AlN precipitates. By correlating the analytical results with the corrosion test results, it has been verified that the improved corrosion resistance in PSII-treated coupons is due to the formation of a continuous AlN layer. It was also found that the formation of a continuous AlN layer is mainly determined by the implant energy and the total integrated implantation dose, and relatively insensitive to factors such as the plasma source, pulse length, or frequency. More detailed results of the comprehensive study will be presented, including such factors and effects as implant energy and dose, alloy type, and tribological and electrical properties of the treated surfaces.

* Supported by the NSF under grant ECD-8721545.

† Supported in part by NSF PYI grant ECS-9057675

10:45

QA 3 Theory of the collisional presheath in a strong magnetic field, K.-U. RIEMANN, T. DAUBE, and H. SCHMITZ (Ruhr-Univ. Bochum, D-44780 Bochum, Germany) — The formation of a stationary space charge region (sheath) in front of an absorbing wall requires that the ions are pre-accelerated to ion sound speed (Bohm criterion) in a quasineutral presheath. Usually the presheath mechanism depends decisively on collisional friction of the ions, on ionization or on geometric ion current concentration. The possibility of a 'magnetic presheath' where the ion dynamics is dominated by a magnetic field (nearly) parallel to the wall, was discussed controversially. Recent hydrodynamic analyses [1,2] were able to resolve previous contradictions and to clarify the mechanism of the magnetic presheath. Simultaneously, however,

it became evident that the fluid theory is not suitable to give a reliable description of the plasma sheath transition. Therefore we have investigated the special case of a wall parallel magnetic field kinetically. Comparison with PIC-MC simulations show that the stationary solution of the problem is unstable.

- [1] K.-U. Riemann. *Phys. Plasmas* 1, 552 (1994)
 [2] P.C. Stangeby. *Phys. Plasmas* 2, 702 (1995)

Invited Paper

11:00

QA 4 Industrial Development of Plasma-Based Ion Implantation from an Industrial Perspective, JESSE N. MATOSSIAN, Hughes Research Laboratories, Malibu, CA. Plasma-based ion implantation, for tribological improvements of materials, combines plasma-source technology with high-voltage, high-power-switching technology, and materials science. Since 1988, the technology has been the focus of research and development for industrial usage. Sizeable research activities have been under way at universities, national laboratories, and industrial companies. Hughes Research Laboratories (HRL) has been one of these industrial companies. Major technology achievements at HRL include the first demonstration of high-voltage (100-200 kV), high-power (100-kW) implantation of gaseous ions in a large-scale (4-ft-diameter x 8-ft-long) implantation facility, the first demonstration of a large-scale (3000-lb object) implant, and the development of a technique for x-ray reduction. This talk reviews HRL's experience, perspective, and lessons-learned to industrialize plasma-based ion implantation technology for internal, as well as commercial use. Included in this review is an update of several activities ongoing in the US and abroad, that represent major steps toward industrial acceptance and industrial usage of the technology for tribological applications.

Contributed Papers

11:30

QA 5 Unified Model of the rf Plasma Sheath* M.E. RILEY, Sandia National Labs. - By developing an approximation to the first integral of the Poisson equation, one can obtain solutions for the current-voltage characteristics of an rf plasma sheath that are valid over the whole range of inertial response of the ions to an imposed rf voltage or current. The theory adequately reproduces the time-dependent current-voltage characteristics of the two extreme cases corresponding to the high frequency, current-controlled Lieberman rf sheath theory¹ and the low frequency, adiabatic Metzger-Ernie-Oskam theory.² Implementation of the model in a plasma simulation requires incorporation of one additional ordinary differential equation in time which contains the ion fall time through the sheath as a damping parameter.

*Work performed at Sandia National Labs and supported by US DoE under contract DE-AC04-94AL85000.

- ¹M.A. Lieberman, *IEEE Trans. Plasma Sci.* 16, 638 (1988).
²A. Metzger, D.W. Ernie, and H.J. Oskam, *J. Appl. Phys.*, 60, 3081 (1986).

11:45

QA 6 Surface Modification of Polymers for Improved Adhesion of Vapor Deposited Metallic Films*, B.A. RATCHEV, R. SPETH, G.S. WAS[†], R. MAU, J.H. BOOSKE^{**}, J. JACOBS, R. BRUEN, J.L. SHOHET, AND G. FERNANDEZ[#], Engineering Research Center for Plasma-Aided Manufacturing, Univ. of Wisconsin-Madison. Results are presented of a study of ion beam and RF-plasma-physical-sputter pretreatments of Lexan Polycarbonate (PC) and ABS polymers for the purpose of improved

adhesion of vapor deposited aluminum films. The effects on the adhesion characteristics, the type of ions (or plasma) used, and the type of surface bombardment (presputter or simultaneous with deposition) will be discussed. Both methods indicated dramatic improvement in adhesion with "clean" polymer surfaces. XPS studies suggest that the Al is bonded in identical ways at the treated and untreated (control) surfaces. The conclusion is that improved adhesion is due to surface sputter cleaning.

* supported by NSF grant ECD-8721545

[†] Depts. of Nucl. Engr. and Mat. Sci. & Engr., Univ. of Michigan

[#] Vacuum Technologies, Inc., Reedsburg, WI

^{**} Supported in part by NSF PYI grant ECS-9057675

SESSION QB: ENVIRONMENTAL APPLICATIONS

Friday morning, 13 October 1995

Berkeley Marina Marriott

Belvedere Room, 10:00-12:00

Ann Gentile, presiding

Invited Paper

10:00

QB1 Destruction of Chlorinated Hydrocarbons Using a Packed Bed Corona Reactor, T. ORLANDO, R. TONKYN, and S. BARLOW, Environmental Molecular Sciences Center, Pacific Northwest Laboratory*, Richland, WA 99352--We report on the effects of gas composition, relative humidity, and packing material on the ability of a small packed bed corona reactor to destroy low concentrations (<1200 ppm) of CCl₄ and C₂HCl₃. Measurements of the contaminant removal and by-product appearance in the effluent gas as a function of energy dissipated in the reactor have been made at atmospheric pressure. We have compared the energy consumption in dry and moist air, as well as dry and moist nitrogen. At low concentrations, TCE destruction was considerably more efficient in dry N₂ than in dry air, although CCl₄ destruction efficiency was unchanged. A simple kinetic model has been developed that is consistent with the data. Several packing materials have been tried in order to determine whether changing the physical or chemical properties of the packing can alter the efficiency of the overall process.

* PNL is a multiprogram national laboratory operated for the U.S. Department of Energy by Battelle Memorial Institute under contract DE-AC06-76RLO 1830.

Contributed Papers

10:30

QB 2 Streamer Dynamics in Dielectric Barrier Discharges for Plasma Remediation of SO_x/N_xO_y: Single and Multiple Streamers¹ ANN C. GENTILE,² JEFF YANG and MARK J. KUSHNER, Univ. of Illinois, Dept. of Elect. and Comp. Engr., Urbana, IL 61801 USA - Dielectric Barrier Discharges (DBDs) are being investigated for remediation of SO_x and N_xO_y from atmospheric gas streams produced by combustion of fossil fuels. Plasmas in DBDs consist of microstreamers (10s-100s μm diameter, 10s - 100s ns long). Locally high gas temperatures can initiate advection and produce rarefied channels. We have developed a plasma chemistry model including Navier-Stokes equations to investigate DBD remediation of SO_x/N_xO_y. Results will be discussed for single (1-d) and multiple streamers (2-d). Electron impact generated N atoms produced in the streamer remediate NO (N + NO → N₂ + O) while high gas temperatures regenerate NO (N + O₂ → NO + O). Transport improves efficiency by diffusing NO into and convecting N out of the streamer region thereby channeling N into reduction rather than reassociation. Closely spaced streamers are less efficient because they mutually interfere with these transport processes.

¹ Work supported by NSF and Office of Naval Research.

² Present Address: Sandia National Lab., Livermore, CA 94551

FRIDAY MORNING

10:45

QB 3 Laser Induced Breakdown Spectroscopy for Detection of Lead and Cadmium in Concrete. ANDREW V. PAKHOMOV, WILLIAM NICHOLS and JACEK BORYSOW, Physics Department, Michigan Tech. University - Time resolved laser induced breakdown spectroscopy was applied for measurement of lead and cadmium content in concrete at levels down to 1 ppm. The breakdown was formed at the sample surface by Q-switched Nd:YAG laser operating at 1.06 μm and repetition rate of 10 Hz.

The heavy metal contamination can be determined on absolute scale down to 100 ppm while detection limits are in the order of 10 ppm. Contamination levels are inferred from the ratio of integrated emission lines by heavy metals to known reference lines of the matrix. Results appear to be independent of the incident laser energy which was varied from 250 to 400 mJ/pulse. Optimum sampling times were determined from analysis of plasma temporal evolution between 0.1 to 10 μs .

* Supported by ARPA grant # DAAE07-94-C-R098.

11:00

QB 4 Plasma-Assisted Decomposition of Hydrocarbons Using Electron Beam and Pulsed Corona Processing, B.M. PENETRANTE, M.C. HSIAO, J.N. BARDSLEY, B.T. MERRITT, G.E. VOGTLIN, P.H. WALLMAN, Lawrence Livermore National Laboratory, A. KUTHI, C.P. BURKHART, J.R. BAYLESS, First Point Scientific, Inc. -- The objective of this study is to assess the applicability of non-thermal plasma systems for hydrocarbon emission control. Such a system could potentially be used, for example, to control hydrocarbon emissions during cold start in gasoline engines. The two critical issues are electrical energy consumption and byproduct identification. Our investigation used a compact electron beam reactor and a pulsed corona reactor to study the effects of reactor type and electron energy distribution on the decomposition chemistry and electrical energy efficiency. Our electron beam reactor used a novel design to deliver a cylindrically symmetric electron beam that is projected radially inward to the flow duct. Our pulsed corona reactor used a wire-cylinder configuration with a magnetic pulse compression power supply. We characterized the energy consumption of the plasma process for the decomposition of a variety of hydrocarbons, including propene, ethylene, methane, benzene, acetone and methanol.

*Work performed in part at Lawrence Livermore National Laboratory under the auspices of the U.S. Department of Energy under Contract Number W-7405-ENG-48, with support from the Advanced Energy Projects Division of the Office of Energy Research and a Cooperative Research and Development Agreement with Cummins Engine Company. The electron beam processing equipment was developed under a National Science Foundation grant, Contract Number III-9122767.

11:15

QB 5 Absorption and Emission Spectroscopy of Barrier Discharges in N_2+NO and O_2+NO Mixtures, I.P. VINOGRADOV and K. WIESEMANN, Ruhr-Universität, Bochum, Germany.

An experiment for studying NO and NO₂ chemistry in barrier discharges was built up and first data in N_2+NO and O_2+NO mixtures were obtained by applying absorption and fluorescence spectroscopy. The NO reduction

efficiency in the discharge depends on the operating frequency and the distance between dielectric and electrode, i.e. on power absorption of the discharge. From relative band and line intensities of NO, N₂, N₂⁺ and N it can be deduced that the electron energy distribution function changes when changing the frequency of the applied voltage. In O₂+NO discharges a N₂(C-B) fluorescence system is observed indicating dissociation of NO to occur. A possible mechanism is discussed.

11:30

QB 6 Temperatures and Electron Densities in Laser-Induced Breakdown. SERIFE YALÇIN, * DAVID R. CROSLLEY, GREGORY P. SMITH, and GREGORY W. FARIS, Molecular Physics Laboratory, SRI International, Menlo Park, CA 94025. Laser-induced breakdown of air and other gases with metal-containing aerosols has been investigated for application to in situ detection of toxic metals. Atomic ion and emission lines from metals, oxygen, and nitrogen were used to measure temporally and spatially resolved temperatures, while the breadths of lines from hydrogen atoms (produced via H₂O in the flow) and nitrogen atoms were used to determine electron densities. A typical spark cools from ~20000K to 14000K between 0.3 and 1.7 μs following the breakdown pulse, during which time the electron density decreases from $2 \times 10^{18}/\text{cm}^3$ to $2 \times 10^{17}/\text{cm}^3$. The spark temperature does not vary with laser pulse energy or the nature of the carrier gas, a result quite encouraging for application to metal detection.

Supported by the Environmental Protection Agency.

*Visiting student; permanent address: Middle East Technical University, Ankara, Turkey

11:45

QB 7 Coupling between electrical-particle-gas dynamics and chemical kinetics model for NO reduction from flue gases excited by pulsed corona discharge, M. YOUSFI, O. EICHWALD, A. HAMANI, A.HENNAD, M.D. BENABDESSADOK, M. OULD MAHMOUD, Univ. Paul Sabatier, URA du CNRS n° 277, CPAT118, Route de Narbonne, 31 062 Toulouse Cédex, FRANCE- Flue gases (including N₂, O₂, H₂O, CO₂ and a few ppm of oxides as NO_x or SO₂) can be excited by pulsed corona discharges which produce energetic electrons in ionized channels left behind the successive streamers. These free electrons are able to dissociate, ionize and excite molecules of flue gases thus producing primary (O, OH) and secondary (HO₂, O₃) radicals. This leads, following complex interactions, to the transformation of polluting agents in acids and then into salts when NH₃ is added in flue gas in a stoichiometric ratio. In this paper, we are interested by the evolution of the different chemical species (electrons, ions, excited species, radicals, oxides, neutrals, ...) involved in the transformation of polluting agents. So, we have developed a chemical kinetics model for NO reduction from typical flue gases including a few ppm of NO_x. It is coupled to a multi-dimensional electrical fluid model giving the dynamics of charged particles and more particularly the initial conditions needed for the chemical kinetics model. It is also coupled to a particle model for charged particles determining the electron and ion transport coefficients needed for electrical model and electron-molecule reaction coefficients needed for chemical kinetics model; the specific profiles of charged particles due to non-thermal and non-equilibrium effects in gas are also given by the particle model. It is finally coupled to a gas dynamics model giving the temperature profile of neutral gas needed for chemical kinetics model. So the results obtained from such a hybrid model are analyzed as a function of discharge parameters and the main reaction channels involved in NO removal are emphasized.

AUTHOR INDEX

- Abdallah, J. — ND5
 Abdallah, J., Jr. — BB2, KB1
 Abraham, I.C. — BA3
 Abraham-Shrauner, B. — DC2
 Abramzon, N. — DB7
 Aiso, K. — PA6
 Akimoto, K. — NA8
 Alexandrovich, B. — NC4
 Alford, W.J. — LB6, ND5
 Algatti, M.A. — EA12
 Allen, T.M. — EA13
 Alvarez, I. — EB6
 Ambadi, Sathesh K. — MA1, MA3
 Amondson, J. — PA5
 Amorim, J. — EA7
 Anderson, H.M. — AA2, BA1, DB3, EA8
 Anderson, L.W. — BB3, KB2, MA2
 Aoki, N. — EA2
 Arnush, D. — PA1
 Athavale, Satish — HA6
 Augustyniak, Edward — E1 3
- Balooch, M. — HA3
 Baravian, G. — EA7
 Bardsley, J.N. — QB4
 Barlow, S. — QB1
 Barnes, Michael — AA3
 Barone, M.E. — A1 1, HA4
 Barrios, E. — QA2
 Bartel, T. — FA1
 Bartelega, J.M. — EA12
 Baum, C. — QA2
 Bayless, J.R. — QB4
 Beale, Dan — EB8
 Becker, K. — DB7, HB5
 Belenguer, Ph. — ND2
 Bell, F.H. — BA2, BA6
 Benabdessadok, M.D. — QB7
 Benck, E. — EA6
 Benjamin, N.M. — AA2
 Benjamin, R.D. — AA1
 Berger, R. — B1 5, B1 6
 Bergeson, S.D. — EA14
 Bernardini, A.J. — QA2
 Bessis, D. — DB2
 Besuelle, E. — D1 6, NB10
 Bica de Moraes, M.A. — MA5, NA1
 Birdsall, C.K. — D1 1, D1 12, DD1, EB4
 Blackwell, D.D. — MB3
 Blanks, K.A. — DB7
 Bletzinger, P. — DD2, EA10
 Boesten, L. — DB9, GB1
 Boeuf, J.P. — D1 7, LA3, LB7, ND2
 Boffard, John B. — BB3
 Bonham, R.A. — DB11
 Booske, J.H. — QA2, QA6
 Booth, J.P. — EA5, EB9
 Borthwick, I.S. — CA6
 Borysow, Jacek — E1 3, EA4, QB3
 Boswell, R.W. — AA2, NB5, PA2, PA3, PA4
 Bowden, M. — NB11
 Bowden, M.D. — EA1, EA2, FA8
 Bowles, Chris — MB5, NC2
 Božin, J. — CB1
 Brackbill, J.U. — LA6, PB4
 Braithwaite, N.St.J. — EB9
 Brake, M. — C1 1
 Bretagne, J. — CB8, EB3
 Breun, R. — NB4
 Breun, R.A. — BA3
 Brinkman, E.A. — NA3
 Brinkman, Elizabeth A. — EA9
- Brown, S.R. — CA7
 Bruen, R. — QA6
 Buchenauer, D. — BA4
 Buddemeier, U. — PB5
 Buenker, R.J. — FB5
 Buie, M.J. — CA4
 Bukowski, J.D. — DC4, KA5
 Burgers, M. — CB2
 Burkhart, C.P. — QB4
 Burrow, P.D. — GB2
 Butler, J.E. — PA7
 Bwoden, M.D. — EA3
 Byers, J.A. — NB7
- Cachoncinlle, C. — E1 7
 Cammack, David A. — AB4
 Campbell, R.B. — LB2, ND5
 Campbell, Robert B. — ND3
 Cartwright, D.C. — BB2
 Champion, R.L. — EB2, FB4, HA2
 Chan, V.K. — GB2
 Charrada, K. — DA5
 Chatain, F. — HB3
 Chen, F.F. — MB3, PA1
 Chen, L. — DC3
 Cheshire, R.C. — C1 2
 Cheung, Nathan W. — QA1
 Childs, M.A. — MA2
 Choi, P. — D1 7
 Cisneros, C. — EB6
 Clark, C. — B1 4
 Clark, R. — ND5
 Clark, R.E.H. — BB2, KB1
 Coburn, J.W. — DC3
 Cocito, G. — B1 3
 Cognolato, L. — B1 3
 Cohen, R.H. — FA2, NB6, NB7
 Collins, G.J. — B1 4
 Collision, Wenli Z. — AA5
 Collison, Wenli Z. — AA7
 Colombo, V. — B1 3
 Coonan, B.A. — FA3
 Cooper, R. — CB2
 Cooperberg, D.J. — D1 12, DD1
 Cronrath, W. — EA3
 Crosley, David R. — QB6
 Csanak, G. — BB2, KB1
 Cui, C. — LA1
 Cunge, G. — EB9
 Czuprynski, P. — BA8
- Da Cruz, N.C. — NA1
 Dahiya, R.P. — DC7
 Dalvie, M. — AA4, BA7
 Date, H. — CB5, DC1
 Datskos, P.G. — KB8
 Daube, T. — QA3
 Deegan, C.M. — NC1
 Degeling, A. — PA2
 de Hoog, F.J. — CA8
 Dellapiana, G. — B1 3
 Den, S. — NB3
 Den Hartog, E.A. — DB3
 Derouard, J. — EA5, HB3
 Deters, T.M. — HB6
 De Urquijo, J. — EB6
 Deutsch, H. — HB5
 Dillon, M.A. — CB2, DB9, GB1
 Dipeso, G. — B1 5, B1 6
 Disch, S.B. — BA3
 Doneddu, F. — D1 6
 Dorier, J.-L. — LA3
 Douglass, S. — PA7
 Drallos, P.J. — LB4, LB5, ND1, ND4
- Duckworth, R.C. — CA7
 Durrant, S.F. — MA5, NA1
- Economou, D. — FA1
 Economou, Demetre — HA6
 Eddy, C.R., Jr. — PA7
 Egan, P.O. — AA1
 Eichwald, O. — QB7
 Ellingboe, A.R. — NB6, NB7, PA2
 Emmert, P.R. — MA1, MA3
 Erickson, C.J. — MA2
 Ernie, D.W. — NA5
 Ershov, A. — D1 4
 Ershov, Alexander — E1 3, EA4
- Fabrikant, I.I. — BB5
 Falconer, I.S. — DD3
 Faris, Gregory W. — QB6
 Felfli, Z. — DB1, DB2
 Felker, B.S. — C1 5
 Feng, Paul — KB2
 Fernandez, G. — QA6
 Fernsler, Richard F. — NB8, NB9
 Fiala, A. — D1 7
 Flamm, Daniel L. — AA8
 Flynn, Connor — KB5
 Foest, R. — EB1, KA3
 Fontes, C. — KB1, ND5
 Forrister, R.M. — EA8, EB10
 Fox, C.A. — BA4, BA5
 Fuhr, J.R. — HB6
 Fujii, K. — BB1
 Fujio, S. — NA9
 Fukuyama, T. — E1 9
 Fukuzawa, T. — NA2, NA9
- Gallagher, A. — NA6
 Gallagher, Jean W. — HB1
 Gallup, G.A. — GB2
 Ganguly, B. — LA2
 Ganguly, B.N. — DD2, EA10
 Gao, D.W. — EA1
 Garcia, G.A. — DB5
 Garrett, A.W. — EA13
 Garscadden, A. — EA10, EA11, KB7, LA2, MA1
 Garvin, C. — C1 1
 Gentile, Ann C. — QB2
 Giapis, K.P. — HA5
 Gibson, N.D. — DA1, FA4
 Gill, C.G. — EA13
 Gilland, J. — NB4
 Glasson, T. — EA5
 Godyak, V. — NC4
 Godyak, V.A. — MB1
 Golde, M.F. — DB4, FB3
 Gomide, J.V.B. — DB5
 Gopinath, V.P. — D1 1
 Gordon, M.H. — CA3
 Goree, J. — LA1
 Goto, T. — DC5, NA4, NA7, NA8, NB2, NB3, PA6
 Gougousi, T. — DB4, FB3
 Gousset, G. — CB8, EB3, NA10
 Govindan, T.R. — C1 4, NB1
 Graham, W.G. — C1 2, C1 3, E1 4, HA1
 Grapperhaus, Michael J. — AA5, AA7
 Graves, David B. — LA5
 Graves, D.B. — A1 1, CB5, DC3, DC4, HA4, KA5
 Graydon, A. — NC5
 Green, David S. — HB4
 Greuel, P.G. — NA5
- Griesbach, J. — NC3
 Grizzle, J. — C1 1
 Gussman, M.W. — DA2
 Gu, J.P. — FB5
 Guarnieri, C.R. — AA4
 Gudmundsson, J.T. — B1 1
- Haaland, P. — KB7, LA2
 Haaland, Peter — MA4
 Haas, F.A. — FA7
 Haffad, A. — DB2
 Hamaguchi, S. — BA7
 Hamani, A. — QB7
 Hamza, A.V. — HA3
 Han, X.L. — CA7
 Hardy, K. — FB6
 Haverlag, M. — CA8
 Hayashi, T. — EB12
 Hayashi, Y. — DC6, NB3
 Hebner, G.A. — EB5, KA4
 Helm, H. — DB6
 Helmer, B.A. — A1 1
 Hemberger, P.H. — EA13
 Hennad, A. — QB7
 Herrick, A. — NB5
 Herron, John T. — HB4
 Hershkowitz, N. — NB4, PA5
 Hewett, D. — BA7
 Hiramatsu, M. — DC5, NA4
 Hirech, A. — ND2
 Hirsch, G. — FB5
 Hitchon, W.N.G. — EB8, FA6, PB2
 Hoekstra, Robert J. — AA5
 Holland, John — AA3
 Hollenstein, Ch. — LA3
 Honda, R.Y. — EA12
 Hooper, E.B. — NB6
 Hopkins, M. — NC5
 Hopkins, M.B. — FA3, MB5, NC1, NC2
 Hori, M. — DC5, NA4, NB2, NB3, PA6
 Hori, T. — EA3, FA8
 Hoy, J. — KB8
 Hsiao, M.C. — QB4
 Hsu, W.L. — BA4
 Huang, Fred Y. — LA4
 Hudgens, Jeffrey W. — HB4
 Hudson, D.F. — E1 2
 Huestis, D.L. — DB6
 Hughes, A. — NC5
 Huo, W.M. — GB3
 Hutchinson, D.A.W. — D1 11
 Hwang, G.S. — HA5
 Hwang, Helen H. — LA4
- Ikedo, M. — DC5, NA4, PA6
 Ikegawa, M. — D1 5
 Ikuta, N. — E1 9, EB11
 Ingold, J.H. — AB2
 Ito, M. — NB3
 Itoh, H. — E1 9, EB11, EB12
 Itoh, M. — NB11
 Izawa, M. — CA2
- Jacobs, J. — QA6
 Jacobs, J.R. — QA2
 James, B.W. — DD3
 Jameson, W.B. — MA2
 Jeffries, Jay B. — EA9
 Jeffries, J.B. — MA6, NA3
 Jelenkovic, B. — NA6
 Jelenković, B.M. — CB1
 Jewett, R.F. — AA2
 Jin, H.J. — NA2

- Johannes, J. — FA1
 Johnsen, R. — DB4, FB3
 Johnston, M. — BB1
 Jolly, J. — A1 2, NA10
 Joubert, O. — BA2, BA6
 Joyce, Glenn — NB8, NB9
 Jung, Chan Ouk — PA2
- Kae-Nune, P. — A1 2, NA10
 Kanik, I. — KB1
 Kato, M. — EA15
 Kato, S. — DC5, NA4
 Kawamura, E. — EB4
 Kawasaki, H. — NA2, NA9
 Kayama, M.E. — EA12
 Keiter, E.R. — EB8
 Kelkar, U.M. — CA3
 Kelly, P.B. — EA13
 Khacef, A. — E1 7
 Khachan, J. — DD3
 Khakoo, M.A. — KB1
 Khan, Babar A. — AB4
 Khromov, N.A. — E1 6
 Kimura, M. — CB2, CB3, FB5
 Kinoshita, T. — NA2
 Kirmse, K.H.R. — BA3
 Kitajima, T. — CA2
 Kitamori, K. — AA6, DC1
 Kolobov, V.I. — FA6, PB2
 Kolobov, V.L. — EB8
 Kono, A. — NA7, NA8
 Kortshagen, U. — B1 2, DA1, FA4, PB1, PB5
 Kota, G.P. — DC3
 Kouznetsov, I.G. — D1 9
 Kowari, K. — CB4
 Krajcar-Bronić, I. — CB3
 Kramer, K.M. — EB8
 Kratsov, V. — KB3
 Kroesen, G.M.W. — CA8
 Kudryavtsev, A.A. — E1 6
 Kuno, T. — NB3
 Kurunczi, P. — DB7
 Kushner, Mark J. — AA5, AA7, HB2, LA4, PB7, QB2
 Kuthi, A. — QB4
- Lagus, Mark E. — BB3
 Lampe, Martin — NB8, NB9
 Langan, J.G. — C1 5
 Lapatovich, W.P. — AB3
 Lapenta, Giovanni — LA6, PB4
 Laracuente, A. — NA6
 Larson, R.S. — BA5
 Lawler, J.E. — DA1, DB3, EA14, FA4, KB3, MA2
 Lazaryuk, S.N. — E1 6
 LeClair, L.R. — KB1
 Lee, Y.T. — D1 10
 Leroy, O. — A1 2, NA10
 Levin, A. — HB5
 Lewis, J. — CA4
 Lho, T. — PA5
 Li, Ming — B1 7, DC4, NC6
 Li, Y.M. — DA6
 Lichtenberg, A.J. — D1 9, D1 10
 Lieberman, M.A. — B1 1, D1 9, D1 10, EB4, MB2
 Lin, Chun C. — BB3, KB2
 Lin, Frank — AA3
 Lister, Graeme — D1 3
 Lymberopoulos, D. — FA1
- Madison, D.H. — KB3
 Maeda, K. — CB6
 Maeda, M. — EA1, EA2, EA3, EA15, FA8, NB11
 Mahmoud, M. Ould — QB7
- Mahony, C.M.O. — C1 2, C1 3
 Makabe, T. — CA2, CB6, PB6
 Malik, H.K. — DC7
 Mangano, S. — AA2
 Manheimer, W.M. — NB8, NB9
 Martinez, H. — EB6
 Masai, T. — DB9
 Matossian, Jesse N. — QA4
 Mau, R. — FA5, QA2, QA6
 McConkey, J.W. — DB8
 Mcelvaney, S. — PA7
 McGrath, Robert T. — ND3
 McGrath, R.T. — LB2, ND5
 McMillin, B.K. — CA1
 Mechlińska-Drewko, J. — DB10
 Meeks, E. — BA4, BA5
 Mehlman, G. — PA7
 Meister, D. — EB7
 Melden, G.J. — EB10
 Menningen, K.L. — MA2
 Mente, K. — QA2
 Mentel, J. — A1 3
 Merad, A. — LA3
 Merritt, B.T. — QB4
 Meunier, J. — ND2
 Meyer, J.A. — BA3, FA5, NC3
 Meyyappan, M. — C1 4, NB1
 Mi, L. — DB11
 Michel, J.P. — DB7
 Miller, J. — PA5
 Mizuno, E. — DC5, NA4
 Moalem, M. — HA3
 Molvik, A.W. — NB6, NB7
 Morgan, W.L. — D1 8
 Mota, R.P. — EA12
 Msezane, A.Z. — DB1, DB2
 Mullin, C.S. — AA1
 Mullman, K.L. — EA14
 Mümken, G. — B1 2
 Muraoka, K. — EA1, EA2, EA3, EA15, FA8, NB11
 Murnick, D.E. — DA4
 Musielok, J. — HB6
- Nagorny, V.P. — LB4, LB5, ND1, ND4
 Nagpal, R. — EA11, KB7
 Nakano, N. — PB6
 Nawata, M. — DC5, NA4
 Neiger, M. — DA3
 Nelson, M. — D1 7
 Niazi, K. — DD5
 Nichols, William — QB3
 Nickel, J. — BB1
 Nogar, N.S. — EA13
 Nomura, H. — NA7, NA8
 Norimoto, K. — EB12
- Ogawa, Y. — D1 5
 Ohkura, H. — NA9
 Okutsuno, H. — EB11
 Othoff, J.K. — CB7, EB1, EB2, FB2, KA3
 O'Morain, C. — NC5
 Orel, A.E. — KB4
 Orlando, T. — QB1
 Overzet, L. — DD4
 Overzet, L.J. — KA1, MB5, NC2
- Pak, I. — E1 5
 Pakhomov, Andrew V. — QB3
 Panciatici, C. — B1 3
 Parker, G.J. — B1 5, B1 6, FA6, LB3, PB2
 Pastorius, L.A. — DB8
 Paterson, A.M. — CA6
 Pekker, L. — D1 4
 Peko, B.L. — FB4
- Penetrante, B.M. — LB3, QB4
 Pereira, D. — DB5
 Perrin, J. — A1 2, NA10
 Perry, A.J. — AA2, NB5, PA3
 Perry, N.J. — CA7
 Persing, H.M. — PA3
 Peterson, J.R. — FB6
 Petrović, Z.Lj. — CB1
 Phelps, A.V. — E1 8
 Piech, Garrett A. — BB3
 Piejak, R. — NC4
 Pinker, Ronald D. — AB4
 Pinnaduwege, L.A. — KB8
 Pitchford, L.C. — D1 7, LA3, LB7, ND2
 Poslavsky, L. — CA4
 Pouvesle, J.M. — E1 7
- Quinn, R.A. — LA1
- Radovanov, S.B. — EB10
 Ramos, G.B. — FB6
 Rangel, E.C. — MA5
 Rao, M.V.V.S. — CB7, EB2
 Ratchev, B.A. — QA6
 Rescigno, T.N. — KB4
 Ricci, A. — C1 1
 Richardson, R.A. — AA1
 Riemann, K.-U. — PB3, QA3
 Riley, M.E. — LB6, ND5, QA5
 Robert, E. — E1 7
 Roberts, J. — EA6
 Roberts, J.T. — NA5
 Rognlien, T.D. — FA2, NB6, NB7
 Romanenko, V.A. — E1 6
 Rousseau, A. — EB3
 Rowe, B.R. — FB1
 Roznerski, W. — DB10
 Ruzic, David N. — PB7
- Sadeghi, N. — E1 5, EA5, HB3
 Sakai, Y. — AA6, CA5, DC1
 Sakamoto, Y. — NB3
 Sakoda, T. — NB11
 Sandstrom, P. — QA2
 Sanjay, S. — NA9
 Sauer, I. — KB8
 Scalabrin, A. — DB5
 Schappe, R. Scott — KB2
 Schein, J. — A1 3
 Schlammkowitz, M. — FB6
 Schmidt, Ursula I. — LA5
 Schmitz, H. — QA3
 Schumann, M. — A1 3
 Sekizawa, H. — EB11
 Shannon, S. — C1 1
 Shaw, D.M. — B1 4
 Sheldon, J. — FB6
 Shi, X. — GB2
 Shi, Z. — BB4
 Shibata, M. — PB6
 Shimozuma, M. — CB5
 Shiratani, M. — NA2, NA9
 Shizgal, B.D. — CB4
 Shoheit, J.L. — QA2, QA6
 Shon, J. — BA4, LB3
 Shon, J.W. — BA5, ND5
 Sieck, L. Wayne — HB4
- Šimko, T. — CB8
- Slinker, Steven P. — NB8, NB9
 Smith, B. — DD4
 Smith, Brian — NC2
 Smith, Gregory P. — QB6
 Sobolewski, M.A. — KA2
 Sommerer, Timothy J. — AB1
 Speth, R. — QA6
- Splichal, M.P. — BA1
 Sporleder, C.R. — DB11
 Srivastava, S.K. — KB6
 Stalder, K.R. — E1 1, MA6, NA3
 Stallard, B.W. — NB6, NB7
 Steen, P.G. — E1 4
 Stewart, R.A. — BA3, DC4, NC3
 Stewart, R.S. — CA6
 St. J. Braithwaite, N. — FA7, MB2
 Stoffels, E. — CA8
 Stoffels, W.W. — CA8
 Stratil, P. — EA7
 Stumpf, Bernhard — KB5
 Su, M.C. — CA7
 Sugawara, H. — CA5
 Sultan, G. — EA7
 Sumiya, M. — B1 4
 Surendra, M. — AA4
 Suzuki, M. — DC1
 Suzuki, S. — EB11
 Swansiger, B. — BA4
- Tachibana, K. — DC6
 Tagashira, H. — AA6, CA5, CB5, DC1
 Tagawa, H. — EA1
 Takahashi, A. — EA15
 Takahashi, K. — NB2, NB3
 Tanaka, H. — DB9, GB1
 Tanaka, J. — D1 5
 Tarnovsky, V. — HB5
 Teixeira, J.C. — EA12
 Thoms, B. — PA7
 Thrum, T. — DA3
 Tishchenko, N. — B1 5, B1 6
 Tobin, J. — MB4
 Tonkyn, R. — QB1
 Trajmar, S. — BB1, KB1
 Tserepi, A. — EA5
 Tucek, J.C. — HA2
 Turner, M.M. — D1 2, D1 11, FA3
 Tuszewski, M. — MB4
- Uchida, S. — CA5
 Uchida, T. — NB11
 Uchino, K. — EA1, EA2, EA3, EA15, FA8, NB11
 Ueda, Y. — NA9
 Ulrich, A. — DA4
 Usui, T. — D1 5
- Vahedi, V. — BA7, D1 12, EB4
 Vallier, L. — BA8
 Van Brunt, R.J. — CB7, EB1, EB2, KA3
 Veerasingam, Ramana — LB2, ND3, ND5
 Velikić, Z. — CB1
 Vender, D. — PA4
 Ventzek, P.L.G. — AA6, CA5, CB5, DC1
 Verboncoeur, J. — D1 1
 Verboncoeur, John — AA8
 Verboncoeur, J.P. — LB1, LB3
 Veres, G. — HB6
 Vidmar, R.J. — E1 1
 Vinogradov, I.P. — QB5
 Vitello, P. — B1 5, B1 6, KA5
 Vitello, P.A. — AA4, LB3, NB7
 Vogtlin, G.E. — QB4
 Vona, D. — B1 4
 Vosen, S.R. — BA5
 Vušković, L. — BB4
- Wadsworth, D.C. — KA6
 Walker, Thad G. — KB2
 Wallman, P.H. — QB4
 Walton, S.G. — HA2

Wang, S. — KB1
Wang, Wei-E. — HA3
Wang, Y. — EB2
Wang, Yicheng — FB4
Was, G.S. — QA6
Watanabe, K. — NA2
Watanabe, Y. — NA2, NA9
Wazzan, R. Al. — C1 2
Weber, T. — EA6
Wei, H. — BB4
Weinstein, M. — C1 1
Welch, M. — CA4

Wendt, A.E. — BA3, FA5, NC3
Wickliffe, M.E. — DB3
Wiese, W.L. — HB6
Wiesemann, K. — QB5
Wieser, J. — DA4
Williams, J. — LA2
Williamson, W., Jr. — LB4, LB5,
ND1, ND4
Wise, R. — FA1
Woods, R.C. — BA3
Woodworth, J.R. — EB7
Wouters, M.J. — DD3

Wu, Han-Ming — B1 7, NC6
Wu, J.Z. — BA3
Yalçin, Serife — QB6
Yamada, K. — DC5, NA4
Yamada, N. — AA6
Yamakoshi, H. — EA15
Yan, Jian-Ping — NC6
Yan, Jia-Ping — B1 7
Yang, Jeff — QB2
Yang, S. — FA7

Yang, Yun — B1 7, NC6
Ying, C.H. — BB4
Yoneyama, Shima — AA8
Yousfi, M. — QB7
Yuan, Ding-Pu — B1 7, NC6
Yuri, M. — DB9, GB1
Zachariah, M.R. — CA1
Zhang, L. — QA2
Zheng, Shuanghai — KB6
Zissis, G. — DA5

NOTES

NOTES

BULLETIN

OF THE AMERICAN PHYSICAL SOCIETY

